Assessment of Crash Energy – Based Side Impact Reconstruction Accuracy

Nicholas Johnson

Thesis submitted to the faculty of Virginia Polytechnic Institute and State University in partial fulfillment of the requirements for the degree of

Master of Science
In
Mechanical Engineering

Hampton C. Gabler
Stefan M. Duma
Warren N. Hardy

May 3rd, 2011
Blacksburg, Virginia

Keywords: side impact, delta V, crash reconstruction

Assessment of Crash Energy – Based Side Impact Reconstruction Accuracy

Nicholas Johnson

Abstract

One of the most important data elements recorded in the National Automotive Sampling System / Crashworthiness Data System (NASS/CDS) is the vehicle change in velocity, or ΔV. ΔV is the vector change in velocity experienced by a vehicle during a collision, and is widely used as a measure of collision severity in crash safety research. The ΔV information in NASS/CDS is used by the U.S. National Highway Traffic Safety Administration (NHTSA) to determine research needs, regulatory priorities, design crash test procedures (e.g., test speed), and to determine countermeasure effectiveness.

The WinSMASH crash reconstruction code is used to compute the ΔV estimates in the NASS/CDS. However, the reconstruction accuracy of the current WinSMASH version has not previously been examined for side impacts. Given the importance of side impact crash modes and the widespread use of NASS/CDS data, an assessment of the program's reconstruction accuracy is warranted.

The goal of this thesis is to quantify the accuracy of WinSMASH ΔV estimations for side impact crashes, and to suggest possible means of improving side impact reconstruction accuracy. Crash tests provide a wealth of controlled crash response data against which to evaluate WinSMASH. Knowing the accuracy of WinSMASH in reconstructing crash tests, we can infer WinSMASH accuracy in reconstructing real-world side crashes. In this study, WinSMASH was compared to 70 NHTSA Moving Deformable Barrier (MDB) – to – vehicle side crash tests. Tested vehicles were primarily cars (as opposed to Light Trucks and Vans, or LTVs) from model years 1997 – 2001. For each test, the actual ΔV was determined from test instrumentation and this ΔV was compared to the WinSMASH-reconstructed ΔV of the same test.

WinSMASH was found to systemically over-predict struck vehicle resultant ΔV by 12% at time of vehicle separation, and by 22% at time of maximum crush. A similar pattern was observed for the MDB ΔV; WinSMASH over-predicted resultant MDB ΔV by 6.6% at separation, and by 23% at maximum crush. Error in user-estimated reconstruction parameters, namely Principal Direction Of Force (PDOF) error and damage offset, was controlled for in this analysis. Analysis of the results indicates that this over-prediction of ΔV is caused by over-estimation of the energy absorbed by struck vehicle damage. In turn, this ultimately stems from the vehicle stiffness parameters used by WinSMASH for this purpose. When WinSMASH was forced to use the correct amount of absorbed energy to reconstruct the crash tests, systemic over-prediction of ΔV disappeared.

WinSMASH accuracy when reconstructing side crash tests may be improved in two ways. First, providing WinSMASH with side stiffness parameters that are correlated to the correct amount of absorbed energy will correct the systemic over-prediction of absorbed energy when reconstructing NHTSA side crash tests. Second, providing some treatment of restitution in the reconstruction process will correct the under-prediction of ΔV due to WinSMASH's assumption of zero restitution. At present, this under-prediction partially masks the over-prediction of ΔV caused by over-prediction of absorbed energy. If the over-prediction of absorbed energy is corrected, proper treatment of restitution will correct much of the remaining error observed in WinSMASH reconstructions of NHTSA side crash tests.

Acknowledgements

This thesis would not have been possible without the continual input and guidance of my advisor Dr. H. Clay Gabler and the support of my committee, Dr. Warren Hardy and Dr. Stefan Duma.

I would also like to thank the National Highway Traffic Safety Administration for sponsoring this work, and in particular Mr. Dinesh Sharma for his direction and assistance.

My thanks also go to fellow student Carolyn Hampton for first introducing me to WinSMASH and C#, and for providing keen insight into data analysis techniques and crash reconstruction thereafter. Finally, recognition is also in order for intern Lauren Lemieux for collecting and entering most of the data which made this thesis possible.

TABLE OF CONTENTS

1 INTRODUCTION

In 2008, a total of 23,888 individuals lost their lives in passenger vehicles involved in traffic crashes in the United States (FARS 2008). Of these, 5,265, or just over 22%, died in vehicles which were struck in the side. Research aimed at understanding side impact crashes and mitigating their toll on society relies heavily on data provided by the National Automotive Sampling System / Crashworthiness Data System (NASS/CDS), an in-depth crash investigation program sponsored by the U.S. National Highway Traffic Safety Administration (NHTSA).

One of the most important data elements recorded in the NASS/CDS is the vehicle change in velocity, or ΔV. ΔV is the vector change in velocity experienced by a vehicle during a collision, and is widely used as a measure of collision severity in crash safety research (Bahouth et al., 2004; Gabauer and Gabler, 2008). The ΔV information in NASS/CDS is used by NHTSA to determine research needs, regulatory priorities, design crash test procedures (e.g., test speed), and to determine countermeasure effectiveness.

The WinSMASH crash reconstruction code is used to compute the ΔV estimates in the NASS/CDS. However, the reconstruction accuracy of the current WinSMASH version has not previously been examined for side impacts. Given the importance of side impact crash modes and the widespread use of NASS/CDS data, an assessment of the program's reconstruction accuracy is warranted.

A basic WinSMASH reconstruction has two stages: estimation of absorbed energy, and application of momentum conservation. WinSMASH first estimates the amount of energy absorbed in a collision using a) measurements of residual vehicle crush on each vehicle, and b) a correlation between this residual crush and the amount of energy absorbed by the vehicles in the collision (Campbell, 1974; Prasad, 1990; Sharma, 2007). For simplicity, this correlation is called

a “vehicle stiffness”, or simply a “stiffness”, and is the key parameter which allows WinSMASH to estimate energy absorbed in a collision. Once the total absorbed energy is estimated, WinSMASH uses it along with an estimate of the direction of the average crash impulse, called Principal Direction of Force (PDOF) to estimate the ΔV for the collision based on a momentum conservation model (NHTSA, 1986; Sharma, 2007).

1.1 OBJECTIVE

The goal of this work is to quantify the accuracy of WinSMASH ΔV estimations for side impact crashes, and to suggest possible means of improving the program.

1.2 PRIOR RESEARCH: CRASH3, SMASH

Most existing research pertinent to the accuracy of WinSMASH has actually been done with its predecessors, CRASH3 and SMASH. CRASH, which is short for Calspan Reconstruction of Accident Speeds on the Highway, was originally developed for the NHTSA in the mid-1970s by Calspan Corporation. The original purpose of the program was to provide an initial ΔV estimate for SMAC (Simulation Model of Automobile Collisions), which was used at the time to estimate impact speeds for NASS/CDS cases. Starting in 1979, the NASS/CDS began coding ΔV estimated with CRASH as a standardized estimate of vehicle collision severity (Sharma, 2007). During the 1980s, CRASH was updated a number of times and became CRASH3. CRASH3 was designed for use on the mainframe computers of the time. When DOS-based PCs became available in the late 1980s, CRASH3 was ported to DOS to create the algorithmically identical version called CRASHPC (Sharma, 2007).

In the early 1990s, CRASH3/PC was updated again with stiffness data for 1987-1992 vehicles (Prasad and Monk, 1990; Willke and Monk, 1987) and ported to the Microsoft Windows environment to create SMASH, or Simulation of Motor vehicle Accident Speeds on

the Highway (Sharma, 2007). A number of key algorithm changes were made at this time, the details of which are discussed in Appendix A. Then, in 1995 SMASH was modified to integrate the program with the NASS/CDS data entry software and to improve the user interface: the program then became known as WinSMASH (Sharma, 2007). Versions of WinSMASH up to and including WinSMASH 2007 used the same categorical vehicle stiffness data (see Chapter 2) as SMASH. WinSMASH 2008 was the first version to use vehicle-specific stiffness data, but was otherwise algorithmically identical to prior versions of WinSMASH and to SMASH. WinSMASH versions subsequent to 2008 have used the same algorithm as WinSMASH 2008, while fixing programming bugs and stiffness information errors, and implementing improvements to the user interface.

Prior work on the accuracy of CRASH3 and SMASH tended to focus on frontal collisions. Of the studies that were conducted for side impact accuracy in these programs (Arbelaez et al, 2005; Lenard et al, 1998; Prasad and Monk 1990; Willke and Monk, 1987; Smith and Noga, 1982a, 1982b), all used CRASH3/SMASH to reconstruct crash tests or staged collisions. Many of these studies used a limited number of crashes, which were frequently only of a single configuration/impact mode. Also, with the exception of Arbelaez et al. (2005) and Lenard et al. (1998), the vehicles tested are now invariably quite old (predating model year 1990) due to the age of the studies. All these findings apply to CRASH3 or SMASH and not necessarily to the current version of WinSMASH. Table 1 summarizes the findings from each of these studies, along with important characteristics of each. Where the result data itself was reported, the mean signed percent error and standard deviation in this mean were calculated for all tests to give a common basis for comparison between studies.

Table 1. Prior studies of CRASH3/SMASH side impact accuracy.

Study, Program	Test Set	Observed ΔV Accuracy	Notes
Smith and Noga (1982 a, b), CRASH3	15 staged side crashes, 8 oblique and 7 direct, late 1970's vehicles.	1.5% high on average, error stdev 28%	Values calculated for struck vehicles only from data given in Appendix C. Authors noted dependence on collision type – oblique collisions over-predicted.
Willke and Monk (1987), CRASH3	8 staged crashes, 4 models (presumably late 1980's), non-crabbed moving rigid barrier	2.9% low on average, 2.1% stdev	Stiffness parameters used were derived from the reconstructed tests, compared to 1-D momentum conservation.
Prasad and Monk (1990), CRASH3, SMASH	12 staged crashes of varying configurations: NHTSA, Calspan and RICSAC tests	CRASH3: 18% high on average, 14% stdev SMASH: 6.0% high on average, 13% stdev	Vehicle to vehicle collisions, standard CRASH3 reconstructions for CRASH3. SMASH used vehicle-specific stiffness coefficients with the SMASH algorithm. ΔVs compared to take into account non-central nature of most collisions, verified with instrumentation.
Lenard et al. (1998), CRASH3	26 EuroNCAP side crash tests, model years 1996-1998	Centered 1 [kph] low, "scatter" of ±5 [kph]	Use special procedures to account for energy absorbed by deformable barrier, compared CRASH3 to 1-D momentum conservation.
Arbelaez et al. (2005), SMASH	42 IIHS side crash tests, model years 2002 - 2005	<1 [kph] low on average, error stdev 2.94 [kph]	Also used special procedure to account for energy absorbed by deformable barrier, 1-D momentum conservation used as check on instrumentation ΔV.

The fact that most of these studies found reasonably good systemic agreement is not terribly surprising. With the exception of the oblique side tests examined by Smith and Noga (1982b) and most of the tests examined by Prasad and Monk (1990), the collisions examined in these studies consist of one vehicle impacting the side of another at a right angle, usually near the center of the wheelbase. Because both vehicle Centers of Gravity (CGs) typically lie very close to the line of the net crash impulse in such collisions, they can be modeled well by one-dimensional momentum conservation. For such collisions, the calculations performed by WinSMASH essentially reduce to one-dimensional momentum conservation as well. The results of the above studies therefore primarily reflect on the validity (in the specific crash modes examined) of the vehicle stiffness coefficients used by the program to characterize the vehicle structures' energy absorption properties; this is discussed in further detail in Chapter 2.

1.3 PRIOR RESEARCH: WINSMASH

The only other studies relevant to WinSMASH accuracy that were actually done with some version of WinSMASH itself are the study by Niehoff and Gabler (2006), a study by Johnson (2009) and one by Hampton and Gabler (2010). Niehoff and Gabler (2006) focused only on frontal collisions and compared WinSMASH-reconstructed ΔV to EDR ΔV for NASS-CDS crashes spanning the years 2000-2003. This study used a version of WinSMASH which still used SMASH categorical stiffness coefficients as the primary source of vehicle stiffness information. Niehoff found that WinSMASH under-predicted ΔV by 23% in frontal collisions on average. It must be noted that EDR ΔV includes the effects of restitution, whereas WinSMASH ΔV estimates explicitly ignore it. The Niehoff and Gabler (2006) study also examined the effect of several parameters on frontal crash reconstruction accuracy, including crash mode, body type and vehicle stiffness. Niehoff concluded that the error was a function of vehicle body type: ΔV for front-wheel drive cars was under-predicted by 30%, while pickup trucks were under-predicted by only 3%.

A re-visitation of the Niehoff and Gabler (2006) study was conducted by Hampton and Gabler (2010) using WinSMASH 2010. This study found that WinSMASH 2010 systemically under-predicts frontal collisions by only 13% as compared to 23%. As with the Niehoff study, this is before restitution; Hampton and Gabler made no attempt to examine the effects of restitution in their results.

Johnson (2009) reconstructed the same IIHS side crash tests as Arbelaez (2005) using WinSMASH 2008 instead of SMASH. WinSMASH 2008 used vehicle-specific stiffness coefficients as opposed to categorical ones, but the WinSMASH vehicle stiffness database has since been updated. The study compared the WinSMASH-estimated ΔV to the ΔV recorded by test accelerometers at common velocity and, unlike the Niehoff and Gabler (2006) study, thereby

avoided the issue of restitution entirely. He found that WinSMASH over-predicted common-velocity ΔV (prior to restitution) by 45.4% on average for IIHS tests. This result was quite different from the findings of Arbelaez (2005); the discrepancy was attributed to the fact that WinSMASH side stiffnesses are generated from tests using an MDB geometry distinctly different than the IIHS MDB, and so did not model the IIHS side tests accurately, while the SMASH stiffnesses used by Arbelaez came from tests much more similar to IIHS side crash tests. The parameters used to characterize the energy absorption of the IIHS MDB face may also have contributed to the discrepancy. Johnson computed a WinSMASH vehicle stiffness for the IIHS MDB face based on the only available crash test data for this MDB face. This resulted in a stiffness value higher than that used for many large vehicles, and may have given overly high energy predictions at the small crush values seen in the examined side crash tests. By contrast, Arbelaez integrated the quasi-static crush strength of the MDB aluminum honeycomb material over the crushed volume. Little is known about the energy absorption properties of aluminum honeycomb under the dynamic loads characteristic of IIHS side crash tests. Quasi-static crush strength may also not characterize the energy absorption of the IIHS MDB face well.

1.4 APPROACH

Crash tests provide a wealth of controlled crash response data against which to evaluate WinSMASH. Knowing the accuracy of WinSMASH in reconstructing crash tests, we can infer WinSMASH accuracy in reconstructing real-world side crashes. For this study, WinSMASH was compared to two side impact crash test types: FMVSS 214D compliance tests and Side NCAP tests. FMVSS 214D stands for Federal Motor Vehicle Safety Standard no. 214 “Dynamic” and is the Federally mandated side impact test protocol which all new cars must pass. NCAP stands for New Car Assessment Program, and is the source of the familiar star-ratings given by the NHTSA

to new vehicles in the United States. Both test types are administered by the NHTSA, and both are identical except for the nominal impact speed: FMVSS 214D tests are run at 33.5 mph, and Side NCAP tests are run at 38.5 mph. In this analysis, for each test the actual ΔV was determined from test instrumentation, and this ΔV was compared to the WinSMASH-reconstructed ΔV of the same test.

1.5 OUTLINE OF THESIS

Chapter 2 of this study provides an in-depth introduction to WinSMASH. Historical background is presented to orient the reader, and the mathematical core of the WinSMASH crash reconstruction algorithm is presented and explained. Where appropriate, NHTSA procedures for using WinSMASH are discussed as well. This includes a thorough treatment of how crash reconstruction parameters are obtained for use with WinSMASH.

Chapter 3 is an in-depth examination of the side crash dataset used in this study. Seventy-three (73) FMVSS 214D and Side NCAP side crash tests run by the NHTSA were selected for analysis in this study. Briefly, in these tests a stationary vehicle is struck in the side by a Moving Deformable Barrier (MDB), which is a vehicle surrogate equipped with a deformable face as the name suggests. The reader will be introduced to the details of the FMVSS 214D / Side NCAP crash test in general (hereafter referred to as the NHTSA side crash test), and then provided with a breakdown of pertinent characteristics specific to the set of tests used in this analysis, such as test vehicle demographics and observed ΔV ranges.

Chapter 4 provides a study of the energy absorption properties of the FMVSS 214D Moving Deformable Barrier (MDB) face. Because WinSMASH estimates the total energy absorbed in collisions using residual crush, it is important that the energy absorption properties of the MDB face be as well understood as possible.

Chapter 5 uses the staged side crash tests presented in Chapter 3 to evaluate WinSMASH side crash reconstruction accuracy. Staged crash tests are a useful basis for comparison because they are both well documented and highly controlled. WinSMASH 2010 is used to reconstruct a number of side crash tests, and the program's ΔV estimations are compared to the ΔV determined from the crash test data in each case.

Chapter 6 presents the conclusions drawn from Chapter 5, and gives recommendations as to how WinSMASH may be improved in the future.

2 WinSMASH Fundamentals

This chapter will provide an introduction to the method by which WinSMASH reconstructs ΔV. Specifically, the discussion which follows will:

- Provide a summary of how a WinSMASH damage-only crash reconstruction works,
- Lay out the core equations used in WinSMASH reconstructions,
- Familiarize the reader with the purpose of WinSMASH vehicle "stiffnesses" and the means by which they are generated
- Discuss potential sources of error in WinSMASH crash reconstructions

2.1 WinSMASH Damage-Only Reconstructions

WinSMASH is capable of performing crash reconstructions using vehicle trajectory information recorded at the accident scene, or using only information collected from the vehicles themselves. The former is commonly referred to at a Trajectory reconstruction, while the latter is called a Damage-Only reconstruction. Most WinSMASH reconstructions use the damage-only option to compute ΔV.

The WinSMASH damage-only reconstruction algorithm estimates the ΔV experienced by the vehicles in a collision based only on the vehicle damage, an estimate of the direction of the net crash impulse and relevant vehicle specifications such as mass and wheelbase. It has the advantage of requiring very little input information (compared to a Trajectory reconstruction), but this is concomitant with the disadvantage of often having substantial ΔV errors for individual reconstructions. This set of characteristics makes the WinSMASH damage-only reconstruction algorithm a poor forensic analysis tool, but well suited to the needs of the NASS/CDS (for whose use it was originally designed). Since most NASS/CDS cases are selected for investigation weeks after they occur, NASS/CDS crash investigators rarely have access to scene evidence. Moreover, the NASS/CDS is meant to provide statistically accurate data, not to document

individual cases in extreme detail. Thus, the vast majority of NASS/CDS ΔV estimates – more than 99% - are generated using the WinSMASH damage-only algorithm. A damage-only WinSMASH crash reconstruction has two general steps: estimation of the amount of kinetic energy dissipated in the collision, and calculation of ΔV from this estimate of absorbed energy.

2.1.1 ESTIMATION OF ABSORBED ENERGY

For each vehicle involved in a collision, NASS/CDS investigators measure and record a planar crush profile. This consists of 2, 4, or most often, 6 equally spaced crush measurements taken over the entire damaged area of the vehicle, at a height "representative" of the entire, three-dimensional damaged area. Crush depth is calculated as the difference between the crushed surface and the undeformed outline of the vehicle, and is measured normal to the vehicle axis along which the damage lies. The "representative" height is determined in large part by the judgment of the individual crash investigator, taking into account that some vehicle structures are more substantial than others (e.g. window-level crush does not absorb as much energy as door sill-level crush). These raw crush measurements are adjusted under certain conditions, such as bowing of the vehicle centerline or separation of major structural components like the door sill (NHTSA, 1998).

Figure 1 shows the apparatus used by field investigators to take crush profile measurements, and illustrates the procedure just described for measuring a crush profile. The six red and yellow rods are located along the damaged length at the points where the crush measurements are taken, and the string provides a reference line for comparison to the undeformed side profile.

Figure 1. Measurement of a WinSMASH crush profile. NASS/CDS case 761011139, vehicle 1.

Using the crush profile provided for a vehicle, WinSMASH estimates the amount of energy absorbed by that vehicle's structure in the collision. This is done by applying a "vehicle stiffness", which is a linear relationship between the energy absorbed by the vehicle at the time of *max dynamic crush*, and the depth of the residual damage left on the vehicle *after the collision*.

2.1.2 CALCULATION OF ΔV USING ENERGY ESTIMATE

The total amount of energy dissipated in a given collision is estimated by summing the contributions from the damage to each vehicle involved. By applying momentum conservation principles, it is then possible to estimate the ΔV experienced by the vehicles involved based on the total energy loss. The key parameter in this calculation is the Principal Direction of Force, or PDOF. As shown in Figure 2, the PDOF is the line along which the net inter-vehicular crash impulse acts; its direction relative to a vehicle and the point at which it acts must both be

estimated by the reconstructionist based on the damage to the vehicle and/or any other relevant evidence. Other vehicle specifications, such as mass, are supplied by the reconstructionist as well. If necessary, certain vehicle specifications can be, and in practice, are frequently, estimated by WinSMASH itself.

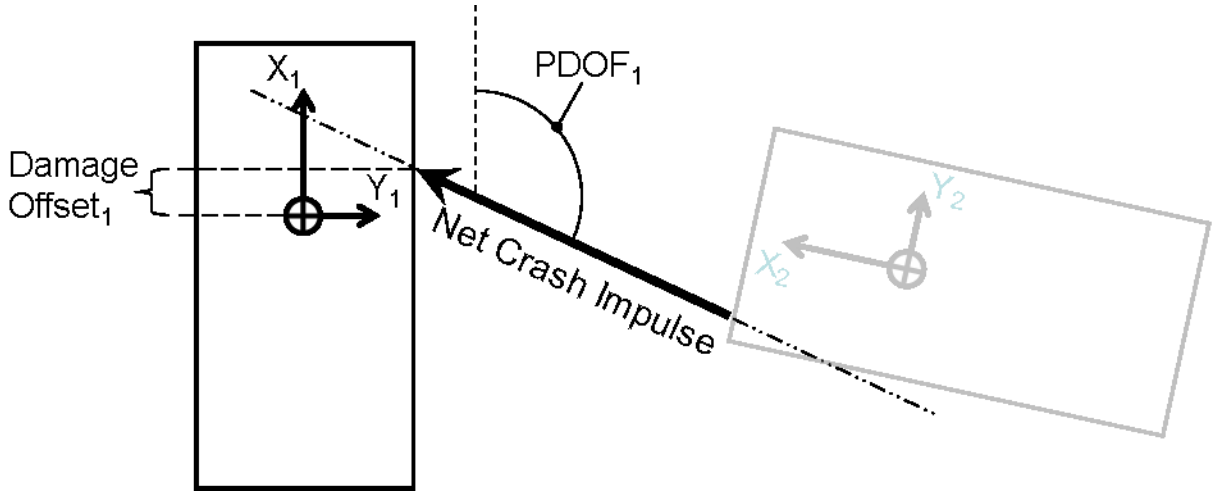

Figure 2. Diagram illustrating the PDOF and Damage Offset as used in WinSMASH reconstructions.

A key assumption made by WinSMASH is that restitution is negligible in all crashes. In effect, WinSMASH therefore only calculates ΔV up to the point of common interface velocity or maximum crush, where some point on each vehicle on the common crush interface between them has a common velocity. The difference between this "maximum crush" ΔV estimated by WinSMASH and the total ΔV at separation of the vehicles is therefore dependent upon the amount of restitution that actually occurs in the test.

2.2 CORE WINSMASH CALCULATIONS

2.2.1 CALCULATION OF ABSORBED ENERGY FROM DAMAGE

As stated earlier, a WinSMASH stiffness takes the form of a linearized relationship between static vehicle crush and energy absorbed at max dynamic crush. This relationship, given

by Equation 1, is defined in WinSMASH by two parameters, d_0 and d_1, which respectively correspond to the slope and the intercept of the crush-energy relationship.

$$\sqrt{\frac{2\,E_a}{w}} = d_0 + d_1\,C \qquad \text{Equation 1}$$

E_a represents the amount of absorbed energy, and w represents the width of the damaged region. While this is

$$\sqrt{\frac{2\,E_a}{w}}$$

the essential relationship between vehicle crush and absorbed energy in WinSMASH, in practice crush depth is rarely uniform across the width of a damaged area. A much more useful formulation is achieved by integrating Equation 1 over the damaged area to yield Equation 2:

$$E_a = \int_0^w \tfrac{1}{2}\left(d_0 + d_1\,C(x)\right)^2 dx \qquad \text{Equation 2}$$

Within WinSMASH itself, this integration is performed numerically via trapezoidal integration using the 2-, 4-, or most often, 6-point damage profile recorded by NASS/CDS investigators. The end result of such an integration, is given by Equation 3:

$$E_a = K_1\,{d_0}^2 + K_2\,d_0\,d_1 + K_3\,{d_1}^2 \qquad \text{Equation 3}$$

The terms K_1, K_2 and K_3 depend on the number of points used in the integration. For a 6-point crush profile, they are given by Equation 4:

$$K_1 = \frac{w}{2} \quad ,$$

$$K_2 = \frac{w}{10}\left(C_1 + 2\left(C_2 + C_3 + C_4 + C_5\right) + C_6\right) \quad ,$$

$$K_3 = \frac{w}{30}\left(C_1^{\,2} + 2\left(C_2^{\,2} + C_3^{\,2} + C_4^{\,2} + C_5^{\,2}\right) + C_6^{\,2} + C_1 C_2 + C_2 C_3 + C_3 C_4 + C_4 C_5 + C_5 C_6\right)$$

Equation 4

2.2.2 CALCULATION OF ΔV FROM ABSORBED ENERGY

The total energy absorbed in a collision is estimated by using Equation 3 for all involved vehicles (there can be one or two) and summing the results. Using this estimate of the total absorbed energy, the ΔV at the CG of each vehicle is calculated using Equation 5. Equation 5 is derived from linear momentum conservation principles, and assumes zero restitution, an instantaneous collision and a single point of contact between vehicles through which the net crash impulse acts.

$$\Delta V_1 = \sqrt{\frac{2\,E_T\,\gamma_1}{m_1\left(1 + \frac{\gamma_1\,m_1}{\gamma_2\,m_2}\right)}} \quad , \quad \Delta V_2 = \sqrt{\frac{2\,E_T\,\gamma_2}{m_2\left(1 + \frac{\gamma_2\,m_2}{\gamma_1\,m_1}\right)}}$$

Equation 5

In the interest of brevity, the full derivation of these equations is not presented here; the interested reader is instead directed to NHTSA (1986). E_T is the sum of the E_a calculated for each involved vehicle, m_1 and m_2 are the respective vehicle masses, and γ_1 and γ_2 are terms called "effective mass multipliers". Equation 5 was initially developed assuming that the line of the net crash impulse passed through both vehicle CGs. The effective mass multipliers are then used to expand the model to account for collisions where this is not the case. When the vehicle CGs are not collinear with the PDOF, the points of contact on the respective vehicles will reach a common velocity (again, restitution is assumed to be zero), but the CGs will in general not.

Instead, the CG ΔV will necessarily be less than that at the common contact point. Effective mass multipliers are calculated using Equation 6:

$$\gamma_1 = \frac{k_1^{\,2}}{k_1^{\,2} + h_1^{\,2}} \quad , \quad \gamma_2 = \frac{k_2^{\,2}}{k_2^{\,2} + h_2^{\,2}} \qquad \text{Equation 6}$$

k is the vehicle radius of gyration and h is the moment arm of the crash impulse about the vehicle CG. Observe that the effective mass multiplier is less than unity for all nonzero moment arms, and becomes equal to unity when the moment arm is zero.

Because Equation 5 and Equation 6 assume an instantaneous collision, the physics of this model is somewhat incomplete – centripetal acceleration and thus the change in moment arm during the collision is ignored. This has previously been cited as a shortcoming of the WinSMASH model in the literature, but a study by Rose et al (2004) concluded that it worked well for collisions without extreme rotation velocities during the contact phase.

Equation 5 gives the net ΔV for a vehicle, which is oriented parallel to the line of the net crash impulse. After calculating this, WinSMASH partitions this net ΔV into vehicle-fixed longitudinal and lateral components using Equation 7:

$$\begin{aligned} \Delta V_{long} &= -\Delta V_{net} \cos(PDOF) \quad , \\ \Delta V_{lat} &= -\Delta V_{net} \sin(PDOF) \end{aligned} \qquad \text{Equation 7}$$

The negative signs arise because the PDOF is defined pointing into the vehicle CG, rather than out from it (Figure 2). It is important to understand that PDOF affects both the partitioning of the net ΔV via Equation 7 and the magnitude of the net ΔV by partly determining the moment arm of the crash impulse used in Equation 6.

2.3 THE WINSMASH VEHICLE STIFFNESS MODEL

2.3.1 HISTORY

WinSMASH vehicle stiffnesses are central to the WinSMASH crash reconstruction process, and bear separate discussion. Campbell (1974) first observed that, for frontal barrier crashes the quantity $\sqrt{\frac{2\,E_a}{w}}$ is linear with residual crush up to 35 inches. McHenry et al. (1974) (in Prasad, 1990) then used this relationship to model the vehicle structure as a linear spring, with impact force per unit width related to residual crush. This is the relationship used by CRASH3; it has the form:

$$\frac{F}{w} = B\,C + A \qquad \text{Equation 8}$$

where $\frac{F}{w}$ is the crash force per unit damage width, A is the minimum force per width required to create residual crush, B is the slope of the force-crush relationship and C is the residual crush depth. Absorbed energy was calculated integrating this crush force over the depth of crush to obtain the work done in crushing the vehicle. Like the relationship in Equation 1 used by WinSMASH, this was integrated over a 6-point crush profile to obtain the energy absorbed by non-uniform crush profiles.

Prasad (1990) next developed the equivalent, but more conceptually direct relationship given in Equation 1 and used by both SMASH and WinSMASH. Instead of assuming linear force-deflection behavior for all modeled vehicle structures and then integrating twice to obtain absorbed energy, the Prasad relationship is a direct correlation between absorbed energy and residual crush depth. Because the McHenry model is ultimately used to compute the same thing as the Prasad model, the A and B parameters of the McHenry model can be directly related to the d_0 and d_1 of Prasad. The conversions are given by Equation 9.

$$A = d_0\, d_1 \quad , \quad B = {d_1}^2 \qquad \text{Equation 9}$$

2.3.2 CALCULATION OF VEHICLE STIFFNESS PARAMETERS

WinSMASH includes a database of vehicle stiffnesses for a large number of vehicle makes and models. These stiffnesses are overwhelmingly calculated from FMVSS-Compliance (Federal Motor Vehicle Safety Standard) and NCAP (New Car Assessment Program) crash tests run by the NHTSA (Sharma, 2007). Stiffness parameters are stored for the front, side and rear of each vehicle, assuming that at least one crash test involving each side is available. When a particular side of a particular vehicle has no test data available, the stiffness for that side from a structurally equivalent vehicle will be substituted if one can be found; most often, the surrogate vehicle is a corporate twin or the same vehicle model from a different year (within the same model generation). When multiple tests are available for a side of a particular vehicle, stiffnesses are calculated with all of them and the results are averaged.

The general procedure for stiffness calculation is essentially to apply Equation 2 through Equation 4 in reverse order to solve for d_0 and d_1. Absorbed energy is first calculated in whatever way is convenient for the particular test configuration being used. Next, for frontal and rear crash tests, crush is typically fairly uniform across the entire width of the vehicle, so crush measurements are averaged and used to solve Equation 1 for d_0 and d_1. Side crash tests typically have non-uniform crush profiles, so for side tests the measured vehicle crush is used to compute the K terms given by Equation 4. Equation 3 is then solved for d_0 and d_1, keeping only the non-negative solution. In NHTSA crash tests, crush is typically measured using the same protocol used by NASS/CDS crash investigators.

Each of these procedures produces one equation in two unknowns (d_0 and d_1) that must be solved. Even when more than one test is available for a particular vehicle on a particular side,

most of the tests available are Compliance or NCAP tests, which are all run at one or two fixed speeds, making them minimally different from other tests of the same configuration. Thus, a damage-intercept (d_0 value) is assumed when computing vehicle stiffnesses from crash tests. Prasad (1990, 1991a) originally provided the values which are used today (Sharma et al. 2007). For frontal impact tests (mostly frontal NCAP and FMVSS 208 compliance tests), d_0 is calculated assuming that the threshold for residual damage is 12 kph, specifically by setting C in Equation 1 to 0, substituting in the nominal test vehicle width and a value of E_a calculated using the vehicle mass and the assumed "damage onset speed". Rear impact tests follow the same formula, but use an impact speed of 16 kph. Rear impact tests are typically FMVSS 301 compliance tests, which use a rigid moving barrier to impact the rear of the test vehicle; 1-D momentum conservation is used to calculate the resulting ΔV for an impact speed of 16 kph, and this in turn gives the absorbed energy.

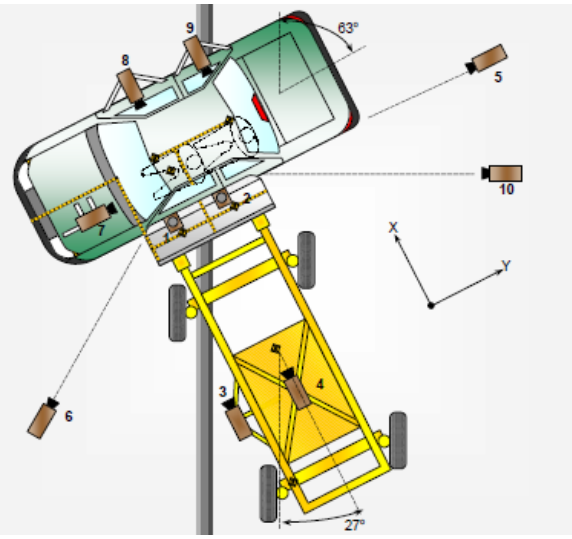

Figure 3. Vehicle configuration used in FMVSS 214D and Side NCAP tests. Reproduced from NHTSA (2006).

FMVSS 214D compliance tests and Side NCAP tests comprise the vast majority of the tests used to compute side impact stiffnesses. These tests have the same configuration, shown in

Figure 3, but slightly different nominal impact speeds. Side impact stiffnesses in WinSMASH do not assume a particular damage onset speed, but rather simply assume a constant value of 63.3 $\sqrt{N}$ for the value of d_0. According to Prasad (1991a) (cited in Sharma et al., 2007), this is equivalent to a 16 kph impact between a vehicle and an MDB (Moving Deformable Barrier) each weighing 1360 kg. When using this test configuration to compute side impact stiffnesses, there are two important considerations which must be made that do not apply to frontal and rear tests: the vehicle damage accounts for only a portion of the total absorbed energy, and the inter-vehicular crash impulse generally does not act through both vehicle CGs. The former is due to the fact that damage to the MDB used in these tests also accounts for some of the absorbed energy. The latter means the vehicles do not act as point masses, so the system does not strictly conform to a 1-dimensional momentum conservation model. Energy absorption by MDB damage is accounted for by simply assuming that the MDB absorbs 5% of the total, and that the vehicle absorbs the remaining 95%. Prasad (1991a) originally made this assumption out of necessity, as at the time little was known about the dynamic crush-energy relationship of the NHTSA MDB face. Absorbed energy is still calculated using 1-D momentum conservation as if the vehicles were colliding point masses, although in reality they deviate from this model.

2.3.3 VEHICLE-SPECIFIC STIFFNESSES AND CATEGORICAL STIFFNESSES

WinSMASH uses two distinct groups of stiffness parameters: vehicle-specific stiffnesses, and categorical stiffnesses. Vehicle specific stiffnesses are, as the name suggests, specific to a particular vehicle model. They are derived from crash tests of only that vehicle model (or structural equivalents), and in principle should give the best possible absorbed energy estimations for that vehicle. When permitted to choose vehicle stiffnesses automatically, WinSMASH preferentially uses vehicle-specific stiffnesses in its reconstructions.

However, vehicle-specific stiffnesses are not always available for every vehicle. In these instances, categorical stiffness coefficients are applied (SMASH and CRASH3 both used categorical stiffnesses exclusively). Historically, categorical stiffnesses were calculated by taking as many vehicle-specific stiffnesses as could be had, separating them into categories based on vehicle wheelbase and bodystyle, and then averaging the stiffness coefficients within each category (Prasad, 1990; Sharma et al., 2007). The current categorical stiffness coefficients used by WinSMASH are derived from an assessment of the Canadian fleet by Siddall and Day (1996).

2.4 POTENTIAL SOURCES OF ERROR

When discussing WinSMASH ΔV reconstruction error, it is important to define what is meant by "error". WinSMASH, like its antecedents CRASH3 and SMASH, is not suited to generating extremely precise reconstructions of individual cases (Sharma et al., 2007). The WinSMASH collision model is far too simplified, and many real-world crashes involve elements that WinSMASH simply cannot account for. Because WinSMASH is designed and used to generate *statistically* accurate and, more importantly from a regulatory perspective, consistent data, the *statistical* accuracy of the program is of more interest to the NHTSA than is its accuracy when reconstructing individual cases. Understanding this, when "accuracy" and "error" are mentioned in this study, unless stated otherwise they should be taken to refer to systemic bias in ΔV predictions, rather than the average difference between a particular case's actual ΔV and the ΔV predicted for it by WinSMASH.

Smith and Noga (1982a) organized sources of CRASH3 error in to three general categories, and their scheme applies equally well to WinSMASH. Error in WinSMASH reconstructions can come from:

- Error in the reconstruction inputs measured at the scene or estimated by the reconstructionist
- Problems with the stiffness parameters used to estimate the energy absorbed by vehicle damage
- Problems with the WinSMASH calculations themselves

2.4.1 RECONSTRUCTION INPUTS

The first category includes error in the damage measurements and in the vehicle specifications supplied to WinSMASH. Smith and Noga (1982a) found the 95% confidence limits on crush measurements taken by field investigators to be +/- 3.0 inches. They also found the 95% confidence limits on damage length to be +/- 6.0 inches. In many crashes, the boundaries of the damaged area are not abruptly defined, so damage length is necessarily influenced by investigator judgment; see the crush measurement in Figure 1 for an example. Crush measurements and damage length both affect the first stage of a WinSMASH reconstruction, estimation of absorbed energy. Vehicle radius of gyration is a parameter required by WinSMASH, but it is seldom known in real-world crashes. WinSMASH allows the user to specify a radius of gyration, but in most reconstructions WinSMASH approximates the parameter as $0.3 * (vehicle\ length)$. According to Sharma et al. (2007), this approximation is based on a study done at the NHTSA's Vehicle Research and Test Center (VRTC) as part of a study of vehicle inertial parameters for crash avoidance applications. Smith and Noga (1982a) also examined the confidence limits on PDOF as estimated by crash investigators; they found 95% confidence limits of +/- 20 degrees. Smith and Noga (1982a) also performed a sensitivity analysis on CRASH3 to determine the relative influence of each input, and they found that PDOF alone was responsible for 85% - 98% of the error in CRASH3 ΔV estimates of two-vehicle side impacts. While the differences between WinSMASH and CRASH3 prevent direct

application of the Smith and Noga (1982a) study to WinSMASH, PDOF is certainly still among the most influential parameters on WinSMASH-reconstructed ΔV.

2.4.2 *STIFFNESS PARAMETERS*

The second general source of WinSMASH error are the stiffness coefficients used to estimate absorbed energy from vehicle crush. Like crush measurements and damage length, vehicle stiffness parameters affect the prediction of absorbed energy. Unlike crush measurements and damage length, vehicle stiffness parameters affect every reconstruction involving the particular vehicle which they are applied to. This gives stiffness parameters a much greater potential to cause systemic errors than errors in vehicle specifications or damage measurements. Because crush is measured normally to the damaged plane of the vehicle (e.g. front, side, rear), WinSMASH stiffnesses treat all crush as if it were made that way, i.e. normal to the damaged plane. However, vehicle crush dissipates energy by both deformation of structure, and by inter-vehicular sliding which does not contribute to normal crush depth (Brach and Brach, 2005).

WinSMASH vehicle stiffnesses are thus most accurate for the exact collision configuration from which they are derived. Since they only correlate to depth of normal crush as measured in one damage plane, they implicitly include the contribution of whatever degree of inter-vehicular sliding occurred during the source test: this amount will be different in collisions of different configurations. One must also consider that crush is a 3-dimensional phenomenon, but that WinSMASH stiffnesses treat it as 2-dimensional. Differently shaped impactors or impacts at different heights can give similar 2-dimesional crush profiles, but cause vastly different patterns of crush in reality. The extent of damage must also be considered, especially given that in practice all WinSMASH vehicle stiffnesses assume a value for d_0. At low amounts of crush, the energy estimation is dominated by the assumed value of d_0 rather than the

experimentally derived value of d_1. Location of the damage on the damaged vehicle is also important, as different vehicle structures absorb different amounts of energy for a given depth of crush: for example, consider window sills versus wheel wells.

Damage location is particularly important in reconstruction of side crashes, where vehicle structure is highly inhomogeneous (Willke and Monk, 1987). The great advantage of the Prasad (1990) stiffness formulation over that of McHenry (1974) is that being a correlation and not a material model, such complexities do not need to be explicitly modeled, but can simply be "rolled into" a stiffness. However, this comes with the caveat that the reconstructionist must be very careful to use stiffness coefficients which truly represent the collision mode in a particular crash. Because the vehicle stiffness parameters provided in the WinSMASH database are primarily derived from compliance tests, there is effectively only one crash configuration represented for front, side and rear impacts.

2.4.3 WinSMASH Calculations

The third category of WinSMASH error is failure of the WinSMASH calculations themselves to effectively model and reconstruct crashes. Since the WinSMASH collision model is so highly simplified, there are many crash modes which WinSMASH simply cannot model (Sharma et al., 2007). WinSMASH reconstructs collisions in two dimensions, so any collision where there is significant motion in three dimensions cannot be reconstructed (e.g. rollovers). WinSMASH also assumes that some point on the common crush interface between vehicles (or between the vehicle and fixed object as the case may be) reaches a common velocity at some point during the collision. This requirement excludes sideswipes. It is not always obvious how closely a crash obeys these assumptions of planar behavior and common interface velocity, so it

is possible that WinSMASH may be inadvertently used to reconstruct crashes to which it is not applicable.

Even when WinSMASH is used for crashes for which it was designed, there are potential problems. The effective mass concept used by WinSMASH to model non-central collisions has in the past been questioned (Woolley et al., 1985). However, Rose et al. (2004) found that the assumption of negligible centripetal acceleration on which the effective mass concept is predicated is acceptable for crashes with all but the highest rotation rates. WinSMASH also neglects energy dissipation by tire scrub: in collisions where tire scrub is a significant influence, this may result in unacceptable error. Brach and Brach (2005) indicate that in most collisions, tire scrub accounts for a very small amount of the dissipated energy.

3 CHARACTERIZATION OF SIDE IMPACT TESTS

3.1 NHTSA SIDE IMPACT CRASH TESTS

This analysis examines a set of 70 Side NCAP and FMVSS 214D side impact crash tests run by the NHTSA, hereafter referred to collectively as NHTSA side crash tests. Figure 4 shows the collision configuration used by both of these test protocols (NHTSA 2006; 2008). A Moving Deformable Barrier (MDB) is towed into a stationary test vehicle at 33.5 mph in FMVSS 214D tests and at 38.5 mph in Side NCAP tests. The MDB is in a "crabbed" configuration, which means that the MDB wheels are all angled at 27 degrees with respect to the MDB body. This gives the MDB face a lateral velocity with respect to the struck vehicle at impact and simulates a collision wherein the striking vehicle is moving twice as fast as the struck vehicle. The impact location on the struck vehicle is such that the MDB collides with the occupant compartment and does not interact with the front wheel well.

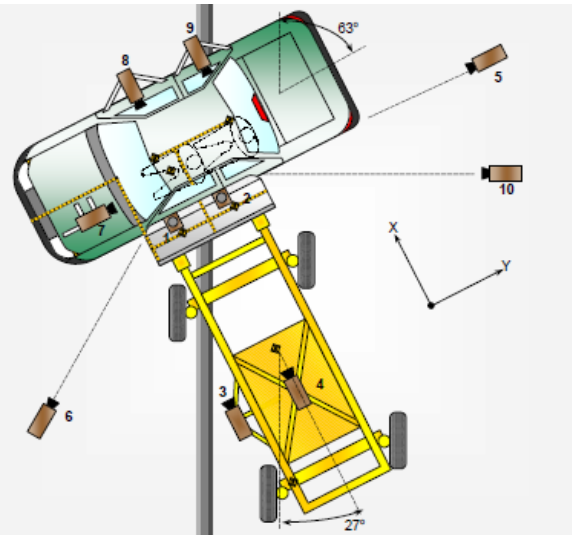

Figure 4. Crash configuration used in NHTSA side tests. Reproduced from NHTSA (2006).

In NHTSA side tests, the MDB is typically instrumented with one biaxial and one triaxial accelerometer. The triaxial accelerometer is mounted near the MDB center of gravity. The

biaxial accelerometer is mounted on the left rear frame rail as shown by labels **1** and **2** in Figure 5.

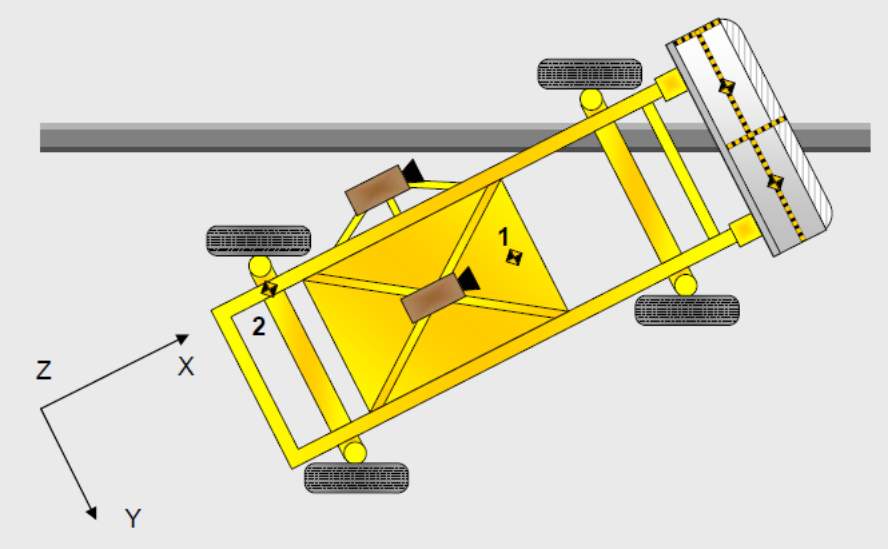

Figure 5. Overhead schematic of the NHTSA MDB showing accelerometer locations. 1 **is typcially a triaxial accelerometer, while** 2 **is typically biaxial. Reproduced from test report for NHTSA test number 5849.**

Test vehicles in NHTSA side crash tests are instrumented with a variable number of accelerometers intended for a number of purposes. Biaxial accelerometers suitable for reconstructing vehicle kinematics are typically attached to the right front door sill, right rear door sill, near the center of gravity and to the floorpan over the rear axle (typically on the trunk floor). Accelerometers may not be present at all of these locations in a given test. Figure 6 shows accelerometer locations for a typical NHTSA side test: 1, 2, 3 and 13 correspond to the right front sill, right rear sill, trunk floor and CG accelerometers, respectively.

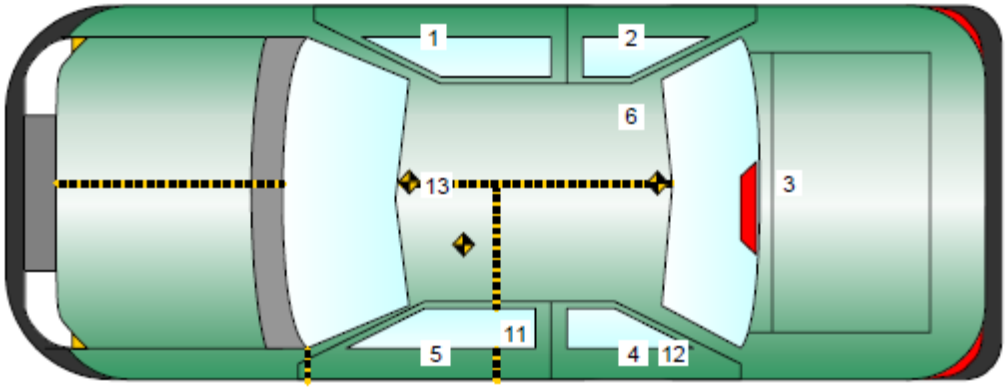

Figure 6. Overhead schematic of a typical test vehicle, showing accelerometer locations typical of NHTSA side crash tests. Reproduced from test report for NHTSA test number 5849.

3.2 DATASET COMPOSITION

Appendix B identifies each of the NHTSA side crash tests examined in this analysis. Each of these tests has passed stringent validation criteria in order to be considered in this analysis. The details of the validation performed on all tests are discussed in Chapter 5. Of 111 tests initially considered, 70 successfully passed all validation tests.

Table 2 gives a frequency table for vehicle model year, and Table 3 gives a frequency table for vehicle bodystyle. The majority of examined vehicles are late 1990s / early 2000's 4-door sedans (4S). Table 4 shows the proportion of NCAP tests versus FMVSS 214D tests.

Table 2. Frequency table for vehicle model year.

Year	Frequency	Percent
1994	1	1.43
1995	3	4.29
1996	2	2.86
1997	11	15.71
1998	9	12.86
1999	9	12.86
2000	8	11.43
2001	10	14.29
2002	4	5.71
2003	5	7.14
2004	4	5.71
2005	3	4.29
2006	1	1.43

Table 3. Frequency table for vehicle bodystyle.

Bodystyle	Frequency	Percent
2 door sedan	6	8.57
3 door hatchback	2	2.86
4 door sedan	56	80.0
Pickup	2	2.86
SUV	1	1.43
Van	3	4.29

Table 4. Frequency table for test type.

Test Type	Frequency	Percent
FMVSS	28	40
NCAP	42	60

3.3 METHOD

NHTSA side crash tests involve measureable amounts of vehicle yaw. In order to ensure that the ΔVs calculated from test instrumentation were not distorted by potentially significant centripetal acceleration, accelerometer data was processed using a technique described by Marine and Werner (1998). Briefly, this technique applies rigid body dynamics to compute the true vehicle CG acceleration using two biaxial accelerometers at different, known positions on a vehicle. Equation 10 through Equation 13 gives the calculation which Marine and Werner derived to achieve this. Subscripts a and b denote two different accelerometers, the variable a represents acceleration and r represents distance from the vehicle CG location.

$$a_{cg_x} = \frac{1}{2}\left(a_{a_x} + a_{b_x} + \frac{d\omega}{dt}\left(r_{a_y} + r_{b_y}\right) + \omega^2\left(r_{a_x} + r_{b_x}\right)\right) \quad \text{Equation 10}$$

$$a_{cg_y} = \frac{1}{2}\left(a_{a_y} + a_{b_y} - \frac{d\omega}{dt}\left(r_{a_x} + r_{b_x}\right) + \omega^2\left(r_{a_y} + r_{b_y}\right)\right) \quad \text{Equation 11}$$

$$\frac{d\omega}{dt} = \left[\frac{\left(a_{a_x} - a_{b_x}\right)\left(r_{b_y} - r_{a_y}\right) - \left(a_{a_y} - a_{b_y}\right)\left(r_{b_x} - r_{a_x}\right)}{\left(r_{b_x} - r_{a_x}\right)^2 + \left(r_{b_y} - r_{a_y}\right)^2}\right] \quad \text{Equation 12}$$

$$\omega^2 = \left[\frac{\left(a_{a_x} - a_{b_x}\right)\left(r_{b_x} - r_{a_x}\right) + \left(a_{a_y} - a_{b_y}\right)\left(r_{b_y} - r_{a_y}\right)}{\left(r_{b_x} - r_{a_x}\right)^2 + \left(r_{b_y} - r_{a_y}\right)^2}\right] \quad \text{Equation 13}$$

This gives the vehicle CG acceleration in vehicle-fixed coordinates: because it is not a fixed reference frame, directly integrating this acceleration will yield incorrect velocities. To overcome this, Equation 10 and Equation 11 were transformed to ground-fixed coordinates using the angle obtained by integrating Equation 12 before integrating. After ΔV was calculated from the velocity histories thusly obtained, it was transformed back to vehicle-fixed coordinates for reporting and analysis. Note that direct integration of Equation 12 gives yaw velocity, and a second integration gives yaw angle.

ΔV may be calculated in this way for any time during the collision event. For purposes of this analysis, there are two times that are of interest: maximum crush and separation. Maximum crush occurs just before the colliding vehicles begin to push apart. ΔV calculated at this time is equivalent to the ΔV if the coefficient of restitution was zero, and is thus equivalent to the ΔV calculated by WinSMASH. The time of maximum crush was determined in this analysis using the relative positions and orientations of the vehicle and MDB. As Figure 7 shows, maximum crush was determined when the area of overlap between the MDB perimeter and vehicle perimeter was at a maximum.

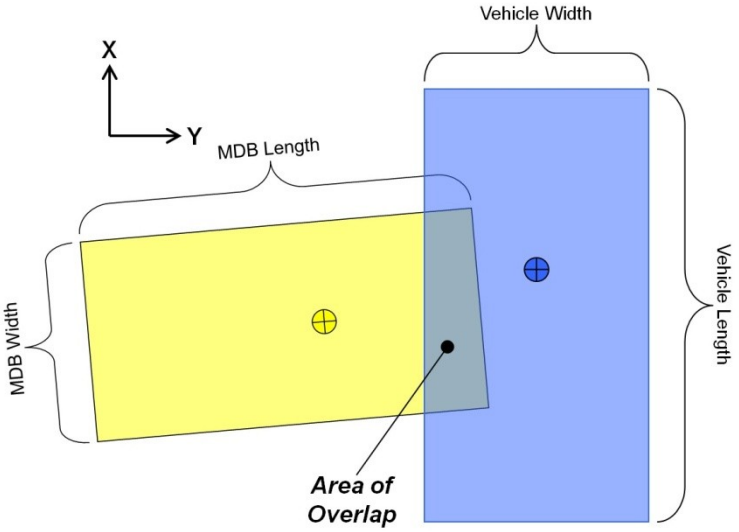

Figure 7. Time of maximum crush was determined by finding the maximal overlap between the vehicle and MDB perimeters.

Separation occurs at the instant when the colliding vehicles are no longer in contact. It includes the contribution of restitution and is thus the maximal ΔV attained in any collision. In this analysis separation was taken to occur at the time of maximum struck vehicle velocity.

3.4 RESULTS

Figure 8 is a histogram depicting the distribution of analyzed vehicle masses. All masses represent the as-tested vehicle mass recorded in the test report. Mean vehicle mass was 1601.5 kg, standard deviation in vehicle mass was 208.2 kg.

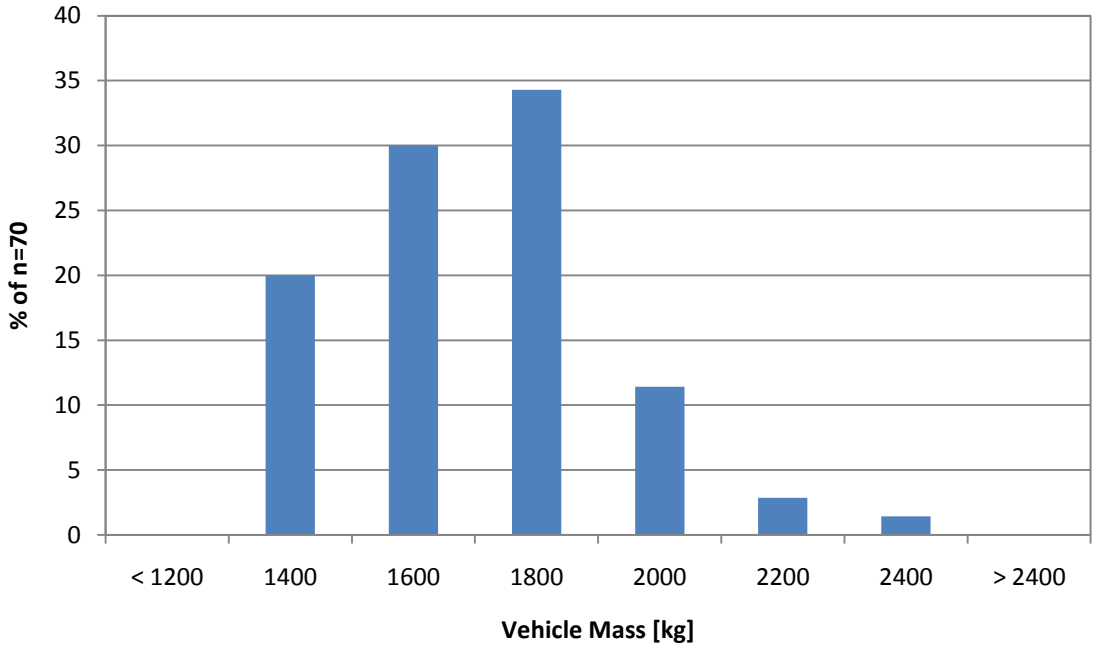

Figure 8. Histogram depicting vehicle mass distribution. Mean = 1601.5 kg, standard deviation = 208.2 kg.

Figure 9 is a histogram depicting the distribution of struck vehicle and MDB ΔV (at time of separation) in the examined tests. ΔV was determined from test instrumentation via the methods described in Chapter 5. Mean vehicle ΔV was 25.4 kph with a standard deviation of 2.98 kph. Mean MDB ΔV was 31.4 kph with a standard deviation of 3.48 kph.

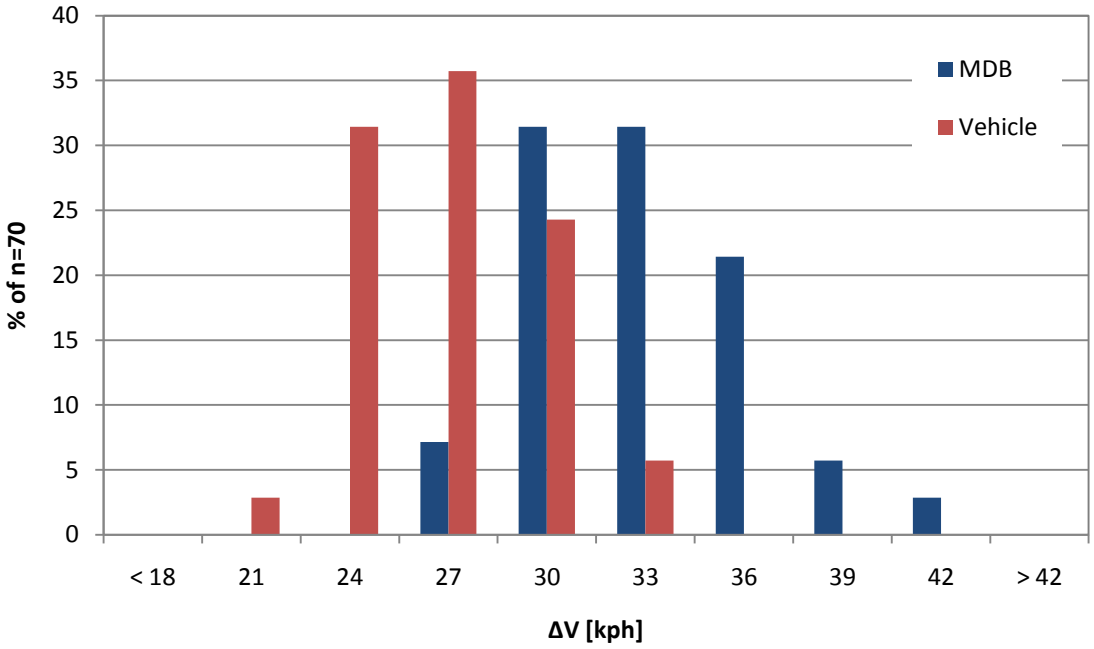

Figure 9. Histogram depicting ΔV distribution for struck vehicle and MDB. ΔV is measured from test instrumentation at time of vehicle separation. Vehicle: mean = 25.4 kph, standard deviation = 2.98 kph. MDB: mean = 31.4 kph, standard deviation = 3.48 kph.

Figure 10 depicts histograms of the measured yaw rate at separation for the vehicle and MDB. Yaw rate was calculated from test data using techniques discussed in Chapter 5. Mean vehicle yaw rate was 87.2 deg/s with standard deviation of 36.3 deg/s. Mean MDB yaw rate was 105.8 deg/s with standard deviation of 39.7 deg/s.

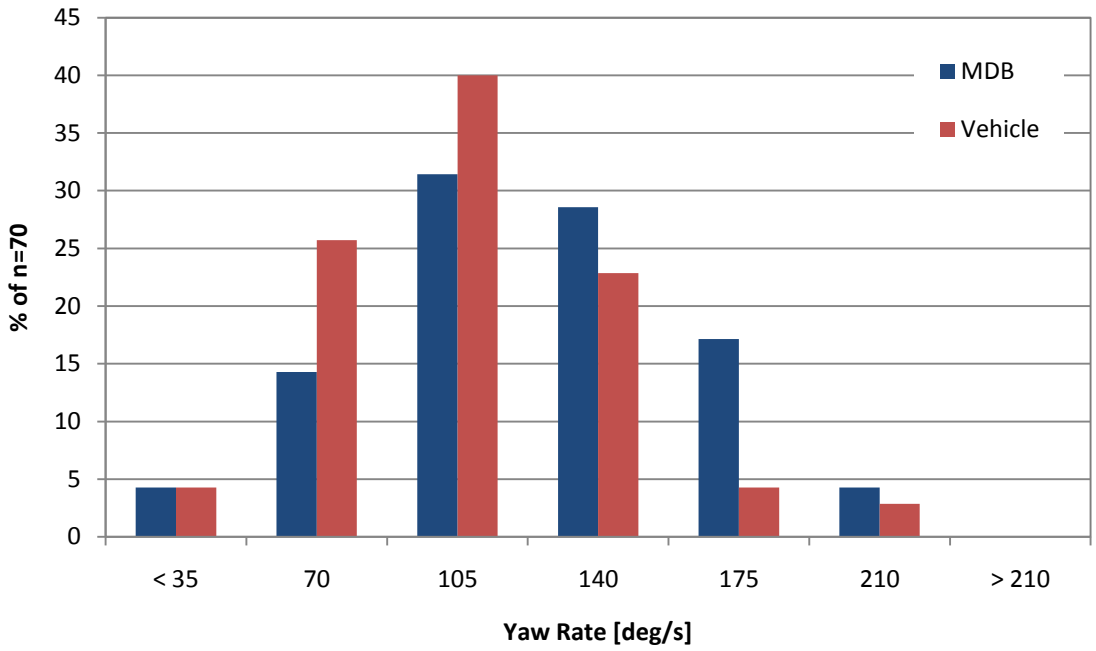

Figure 10. Histogram depicting vehicle and MDB yaw rate measured at separation. Vehicle: mean = 87.2 deg/s, standard deviation = 36.3 deg/s. MDB: mean = 105.8 deg/s, standard deviation = 39.7 deg/s.

Figure 11 compares the distribution of average crush levels for the MDB and struck vehicle. Average crush was computed as the mean of all six values in the WinSMASH crush profile for an individual vehicle/MDB. Mean average crush for the struck vehicle was 15.2 cm with standard deviation of 3.69 cm. Mean average MDB crush was 8.10 cm with standard deviation of 3.62 cm.

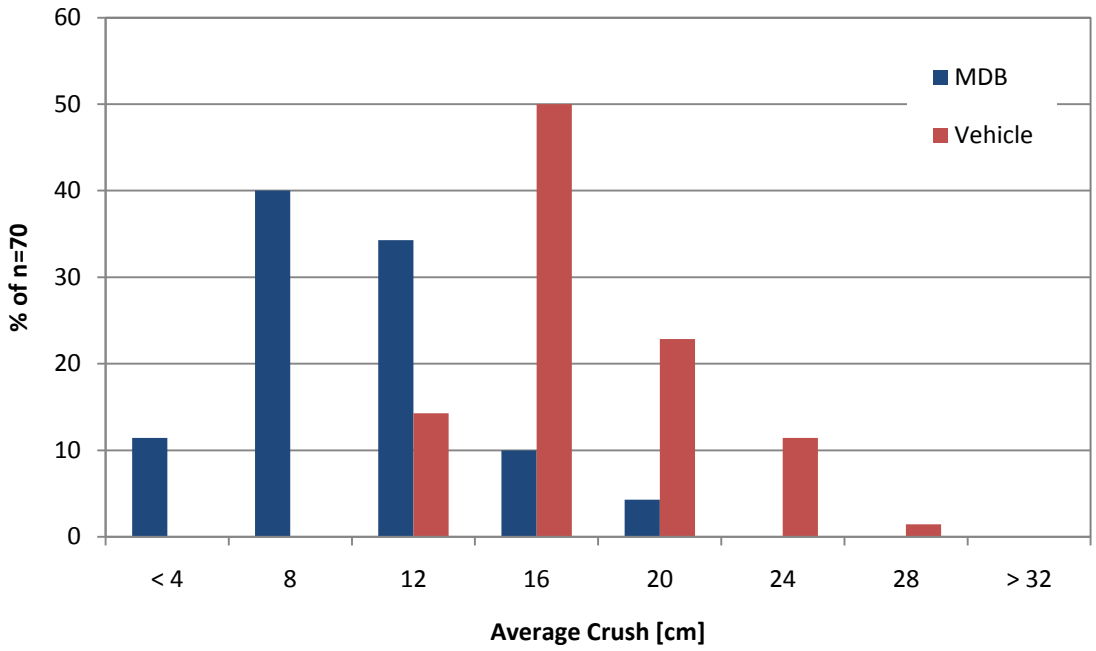

Figure 11. Histogram depicting average crush depth for struck vehicles and MDBs. Vehicle: mean = 15.4 cm, standard deviation = 3.53 cm. MDB: mean = 8.20 cm, standard deviation = 3.64 cm.

3.5 SUMMARY

The dataset consists of 70 passenger vehicles (primarily cars) from model years 1994-2006, with a roughly even mix of lower-speed FMVSS 214D compliance tests and higher-speed Side NCAP tests. Observed struck vehicle ΔVs (at separation) were typically on the order of 25 kph, while MDB ΔVs at the same time were typically closer to 30 kph. This is unsurprising, considering that the NHTSA MDB has a nominal mass of 1361 kg (3000 lbs), which is somewhat less than a typical passenger automobile. Observed yaw velocities at vehicle separation were typically on the order of 100 deg/s for both vehicles and MDBs.

4 ANALYSIS OF ENERGY ABSORPTION PROPERTIES OF THE NHTSA MOVING DEFORMABLE BARRIER FACE

The goal of this thesis is to reconstruct staged NHTSA side crash tests with WinSMASH and then to infer conclusions about WinSMASH's performance when reconstructing real-world crashes. In order to do this, we must account for the fact that real-world crashes do not involve MDBs, while NHTSA side crash tests do. The MDB change in velocity must be reconstructed as accurately as possible in the examined side crash tests, in order to avoid introducing systemic error into the results.

Between the FMVSS 214D test specification (NHTSA, 2006) and the test documentation for each examined crash test, basic dimensions, inertial properties, mass and residual crush are all extremely well documented for the NHTSA MDB. However, the crash test reports do not record the amount of energy absorbed by damage to the MDB. WinSMASH reconstructs crashes by summing the energy absorbed by both involved vehicles, so it is necessary to provide some estimate of this value for the MDB.

WinSMASH vehicle side stiffnesses are calculated from the residual vehicle crush and the amount of energy absorbed by the vehicle structure in side crash tests. In practice, virtually all current WinSMASH side stiffnesses are generated from FMVSS 214 compliance and Side NCAP crash tests run by the NHTSA – the same tests being reconstructed in this work. As discussed in Chapter 2, the MDB itself absorbs some energy in these tests, so some portion of the total absorbed energy must be attributed to it.

4.1 PREVIOUS RESEARCH

Determination of the amount of energy absorbed by the NHTSA MDB face has previously been a topic of research interest by other investigators. Recognizing the need to

quantify MDB energy absorption, but lacking any better means to do so, Prasad (1991a) simply assumed that the NHTSA MDB absorbed 5% of the total E_a in the original side stiffness calculation procedure. The rationale was that even though the amount of energy absorbed by the MDB would not be constant between collisions, the MDB was believed to be quite rigid when compared to most vehicle side structures. Thus, it was a reasonable assumption that the vehicle would absorb most of the energy, and a 95%-5% division was chosen as an educated guess.

Arbelaez (2005) went a step further in his work using SMASH to reconstruct IIHS side crash tests. Instead of assuming the IIHS MDB absorbed a constant percentage of the total crash energy, he estimated the amount of energy absorbed by integrating the quasi-static crush strength of the aluminum honeycomb from which the IIHS MDB face is made over the total volume of measured crush. In quasi-static deformation, aluminum honeycomb is characterized by a constant crushing force, so the integration is quite simple to perform. However, Trella et al. (2000) noted in tests of the NHTSA MDB that there appears to be some form of rate sensitivity in the crush strength, as the force-crush profiles he observed were decidedly not constant. NHTSA MDB faces are not pre-crushed, and pre-crushing can affect the force-deflection behavior of aluminum honeycomb, so this is one possible explanation of this behavior. IIHS MDB faces are by specification constructed of the same honeycomb material as NHTSA MDB faces. Trella's finding is thus applicable to IIHS MDB faces as well as NHTSA faces.

The approach taken by Struble et al. (2001) was somewhat simpler than that of Arbelaez (2005), and has the bonus of accounting for any rate effects that may or may not occur. Struble calculated a WinSMASH stiffness for the NHTSA MDB face based on two fixed, frontal barrier tests performed with the MDB. The portion of E_a absorbed by MDB deformation in NHTSA side crash tests was then determined by using this MDB stiffness and applying it to the crush

measured for the MDB face. When calculating a struck vehicle stiffness, this energy can then be subtracted from total absorbed energy to get the energy absorbed by only the vehicle crush. This MDB face stiffness can also be used along with measured MDB crush to reconstruct a side crash test in WinSMASH without resorting to program modification or post-processing of results.

Note that Struble et al. (2001) presented two MDB face stiffnesses: one using a constant-stiffness model, and another using a constant stiffness model adjusted to account for force saturation (recall that constant-stiffness coefficients A and B can be converted to the WinSMASH coefficients d_0 and d_1 via Equation 9 in Chapter 2). Since the WinSMASH stiffness model does not use force saturation, the stiffness which is not adjusted for force saturation is used for comparison here in Figure 21 and Table 7.

However, the approach used by Struble et al. (2001) to compute MDB stiffness has three drawbacks. First, this stiffness was generated by correlating static MDB crush to the energy absorbed at separation of the MDB from the fixed barrier, not at common interface velocity. Because WinSMASH does not account for restitution, the stiffness calculation would be improved by correlating to the common velocity. The amount of energy returned via restitution however is typically quite small (Prasad 1991b; Rose et al. 2006). Given the inherently approximate nature of crush-energy reconstruction methods, restitution probably makes little difference in absorbed energy prediction. Second, the crush measurements used by Struble et al. were those directly recorded in the crash test reports, which are not recorded according to NASS protocol. Crash test crush measurements are far more detailed than the 6-point profiles recorded by NASS investigators and used by WinSMASH, so by using this crush Struble et al. correlated to a technically different measurement of vehicle damage than is used in practice. Finally, only two tests were examined: tests 2819 and 2910. This is the bare theoretical minimum required to

generate the two parameters that comprise a WinSMASH stiffness, and thus cannot account for any experimental variability.

4.2 OBJECTIVE

The goal of this chapter is to ascertain the energy absorption behavior of the NHTSA MDB face under loading conditions similar to the NHTSA side impact test. This will facilitate partitioning of E_a in side impact crash tests and enable WinSMASH reconstruction of those same tests. In order to facilitate reconstruction of NHTSA side crash tests with WinSMASH later in this thesis, as well as comparison with prior findings, this analysis will attempt to characterize the MDB face using a WinSMASH vehicle stiffness.

4.3 METHODS

The approach used follows that of Struble (2001), but with several notable differences. First, MDB crush will be correlated to the energy absorbed at common interface velocity and not separation. Second, the stiffness will be calculated using the larger number of tests shown in Table 5 in order to help account for experimental variability. In each test, the collision partner for the MDB is rigid and absorbs no energy by deformation. Finally, in each test MDB crush will be measured using NASS standard protocol in order to be consistent with the computation of other WinSMASH stiffnesses.

Table 5. General information for tests used in generating NHTSA MDB stiffness.

NHTSA Test #	MDB Type	Closing Speed [kph]	Crab Angle [deg]	MDB Mass [kg]	Collision Partner
1068	NHTSA	40.2	26	1364.0	Fixed Barrier
2819	NHTSA	41.5	26	1358.9	Fixed Barrier
2910	NHTSA	54.7	27	1358.9	Fixed Barrier

4.3.1 CALCULATION OF TEST ΔV

Characterization of the NHTSA MDB was performed using three tests run by the NHTSA: tests 1068, 2819 and 2910. These tests were selected because the MDB impact configuration is the same as in NHTSA side crash tests – barrier face normal to the impacted surface with wheels crabbed at 26° or 27°. Unlike NHTSA side crash tests, the impact partner in these collisions was a fixed, rigid barrier and not a moveable, deformable vehicle. All energy was absorbed by the MDB face. Since these tests were planar in nature and not linear, 1-D momentum conservation would have introduced some degree of error if used to calculate MDB CG velocity at max crush. To avoid making assumptions about how well the tests agreed with 1-D momentum conservation, accelerometer data was used to determine the true ΔV in the tests. Accelerometer data on the MDB was first processed according to Marine and Werner (1998) to account for MDB yaw and then integrated to yield both velocity and position of the MDB. Figure 14 and Figure 17 show that the calculated yaw angles stay quite small while the MDB is in contact with the impact surface. More importantly, Figure 15 and Figure 18 show that the yaw velocity achieved during this period is far less negligible.

Determination of true CG ΔV from accelerometer data in tests with rotation requires that the positions of at least two biaxial accelerometers be known (Marine and Werner, 1998). Accelerometer locations were reported for test 1068, but not for tests 2819 and 2910. However, both of these tests were run by MGA Research Corporation, and nearly every side test examined in Chapter 3 which was conducted by MGA Research Corporation reported the same MDB accelerometer locations. Since the accelerometer layout used in these two tests was identical to that used in regular NHTSA side crash tests, the MGA accelerometer locations reported for every MGA test in Chapter 3 were used for tests 2819 and 2910 in this analysis as well. For reference, Table 6 lists the exact locations used.

Table 6. Accelerometer positions used in tests 2891 and 2910. X is forward of front axle centerline, and Y is right of longitudinal cart centerline.

CG	
X	-1092 [mm]
Y	0 [mm]
Left Rear Frame Member	
X	-2951 [mm]
Y	-625 [mm]

The time of maximum relative longitudinal displacement of the cart with respect to the fixed, rigid barrier was taken to be the time of common interface velocity. Since significant yawing of the cart did not occur in any test until later in the collision, this time could be determined accurately based only on the X-component of the motion despite the vehicle rotation in the test. This approach was also used by Struble et al. (2001). The resultant MDB CG velocity at this time was then taken to be the max crush velocity. The observed max crush velocity was not used in the analysis for test 2910 however, because of complications stemming from the severe crush in this test which are discussed shortly.

In these tests, crush measurements were essentially recorded using NASS protocol, but were sometimes taken at many more points than the 6 required. Thus, a 6-point crush profile was linearly interpolated (when required) from the bumper level crush data on the MDB face in each test (Figure 12). For tests 2910 and 2819, crush was recorded at the top and bottom of the bumper; these crush profiles were averaged to get a profile representative of the bumper center.

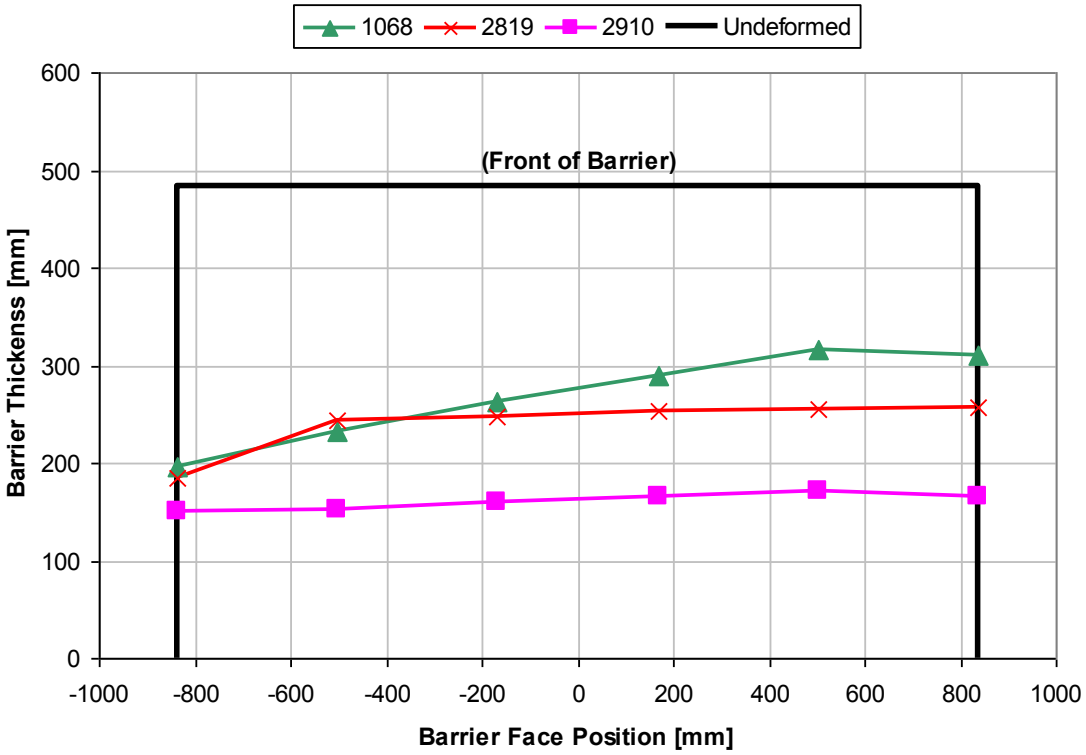

Figure 12. NHTSA MDB mid-bumper crush profiles, measured.

4.3.2 FORCE-DISPLACEMENT CHARACTERISTICS AND "BOTTOMING OUT"

Due to the higher impact speed of the MDB in test 2910, the barrier face had very severe amounts of crush (Figure 12). In fact, the crush was so severe that the deformable barrier face crushed completely and "bottomed out" against the backing plate in this test. Figure 13, a force-deflection plot for test 2910, confirms this; observe the spike in force at maximal MDB deflection. This bottoming-out was also noted by Trella et al. (2000) in the original report for test 2910.

The force data in Figure 13 required no time shifting, and was collected from load cells placed behind the MDB face (Trella et al., 2000), so an impulse correction factor (Appendix C) was not attempted as the momentum of the barrier face itself did not contribute to the impulse seen there. The center of gravity longitudinal acceleration channel did however contain a small time offset which was corrected by shifting -0.0015 [s]. Bias correction was performed on all

channels by subtracting the mean of all points before time zero. The deflection data used in this plot is actually ground-fixed displacement normal to the impact surface – although this test involved a lateral impact velocity component and thus rotation, Figure 14 shows that the yaw angle of the cart remains quite tiny during contact, so the ground-fixed normal displacement is for practical purposes the same as cart-fixed longitudinal displacement.

For comparison, Figure 16 shows force-displacement for test 1068. This test did not bottom out and thus does not exhibit the pronounced force spike at peak crush. CG-longitudinal acceleration was time-shifted by -0.002 [s], CG-lateral by -0.00325 [s], rear-longitudinal by -0.0025 [s] and rear-Y by -0.002 [s]. As with test 2910, the longitudinal displacement given is actually ground-fixed displacement normal to the barrier, which is again practically equivalent to vehicle-fixed longitudinal displacement (Figure 17). Since this test did not bottom out, this force-displacement relationship was not used anywhere in the analysis of test 1068 – it is provided for comparison to test 2910 only.

Figure 19 compares the force-deflection curves for tests 2910, 2819 and 1068 with the theoretical force-deflection curve for normal, quasi-static crush of a NHTSA MDB face. The force levels in tests 2910 and 2819 appear lower than those in test 1068 because in these tests, the load cells were mounted behind the MDB face on the cart itself, so the deceleration of the MDB face is not measured in these tests. The vertical lines in Figure 19 mark the average bumper-level crush measured after each test. The average difference between max dynamic crush (as determined by CG displacement normal to the rigid barrier) and the average bumper-level static crush (measured post-test) is 21.1%. If it is assumed that the force-deflection curves for tests 2819 and 2910 generate force levels similar to test 1068 when measured at the rigid barrier and not behind the MDB face, then it is clear that the quasi-static crush strength under-

predicts the actual level of crush force. This finding is consistent with the increase in crush strength of aluminum honeycomb under dynamic loading observed by other authors (Hong et al., 2008). Note that the stepped profile of the quasi-static force-deflection curve arises because initially only the MDB bumper element is loaded. The body of the MDB is softer than the bumper, so in practice the bumper is pushed into the main block (NHTSA 2006, Struble et al. 2001).

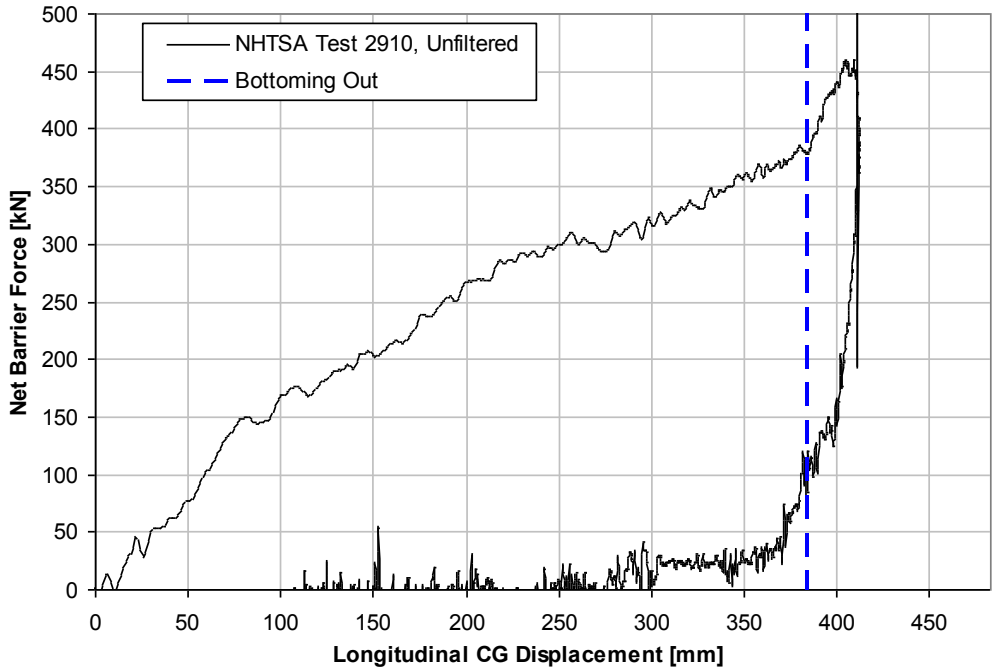

Figure 13. Force-deflection, NHTSA test 2910. X-axis length equals MDB depth.

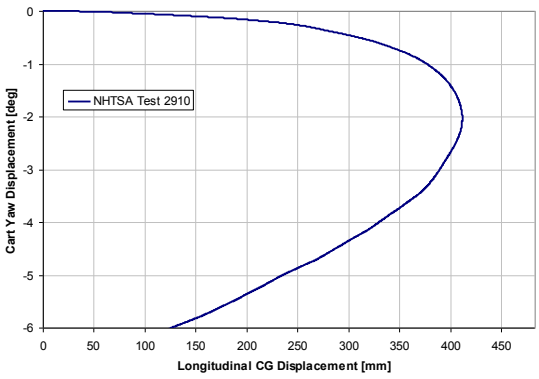

Figure 14. NHTSA test 2910, cart yaw angle (calculated) versus displacement.

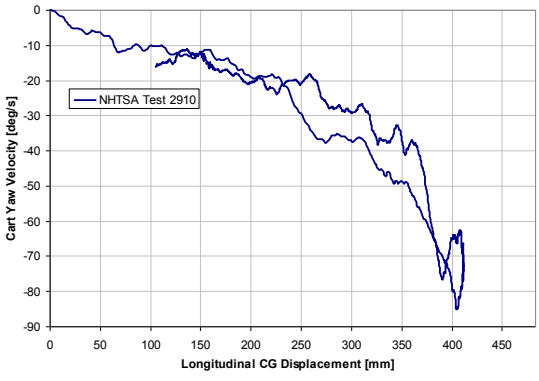

Figure 15. NHTSA test 2910, cart yaw velocity (calculated) versus displacement.

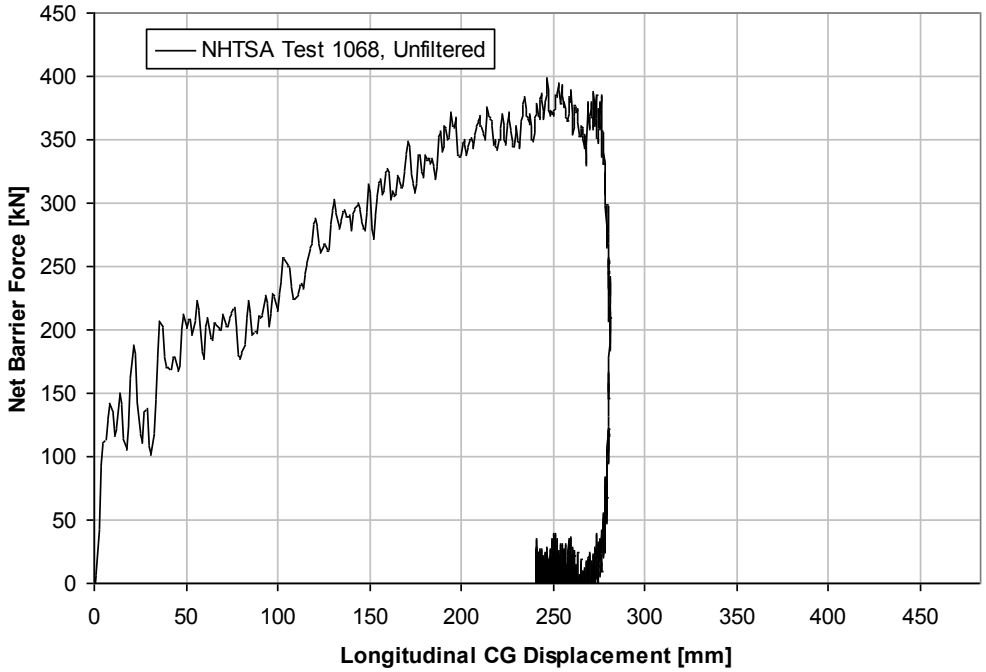

Figure 16. Force-displacement for NHTSA test 1068. This test did not bottom out the MDB face and is provided for comparison. X-axis length equals MDB depth. We have no explanation for the abrupt rise in barrier force at the onset of contact.

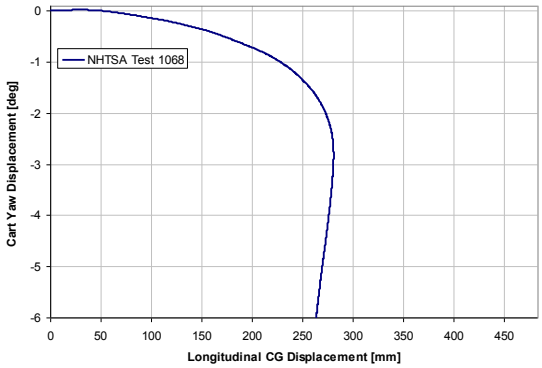

Figure 17. NHTSA test 1068, cart yaw angle (calculated) versus displacement.

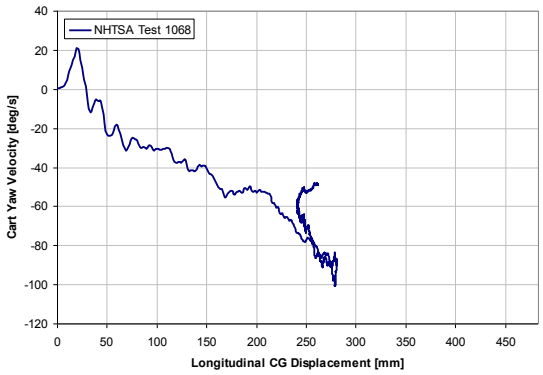

Figure 18. NHTSA test 1068, cart yaw velocity (calculated) versus displacement.

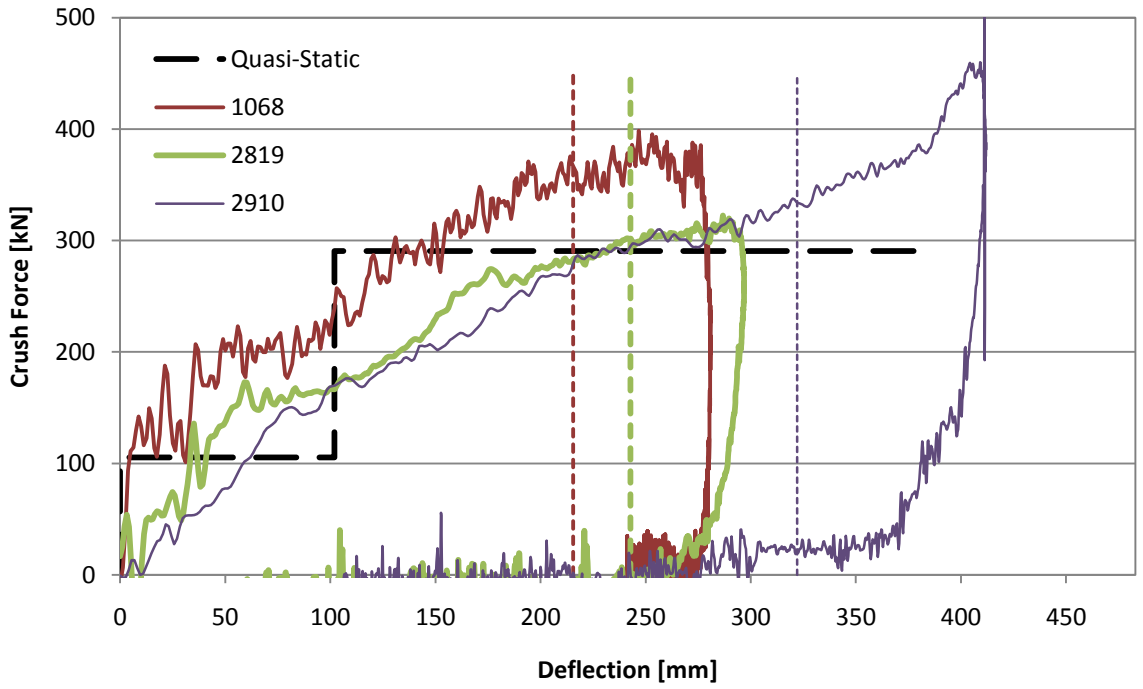

Figure 19. Force-deflection plots for tests 2910, 2819, 1068 and for quasi-static deflection normal to the barrier surface. The vertical, dashed lines indicate the average static crush measured in each test. Note that in tests 2910 and 2819, the load cells were positioned behind the MDB face on the cart, and so do not measures the full crush force.

Once the MDB face has been completely crushed, it is no longer an effective energy absorber (Hong et al., 2008). The remaining kinetic energy of the cart must then be dissipated in other ways which are not characteristic of the much lower crush levels typically seen in normal use. Thus, in order to obtain any relevant barrier characteristics, bottoming out of the MDB face must be accounted for where it occurs, or the test must not be used.

Before bottoming out, aluminum honeycomb primarily deforms via the folding of the cell walls, whereas after bottoming out, it behaves much more like a solid mass (Hong et al., 2008). If it is assumed that MDB compression before bottoming out is much less elastic than compression past the bottoming out point, and that the amount of pre-bottoming-out crush is large in comparison to the amount of post-bottoming-out crush, it can then be assumed that any compression of the MDB face past its bottoming out point will have relatively little effect on the

resulting static crush depth of the barrier. More succinctly, if this behavior can be assumed then once an MDB face has absorbed enough energy to reach its bottoming out point, any further energy it absorbs should not significantly increase the amount of static crush measured after the test.

Thus, the bottoming out in test 2910 was accounted for by using the measured static crush data as described earlier, but correlating this to the amount of kinetic energy dissipated only up to the point where the MDB was observed to bottom out. The bottoming out point was chosen by manual inspection of the force-deflection plot in Figure 13. The MDB face appeared to bottom out at 384 mm of crush. Hexcel (2005) suggests 70% crush (along the cell axis) as a rule of thumb for the minimum bottoming-out point of aluminum honeycomb material, and Trella et al. (2000) states that 80% is an accepted bottoming-out threshold (this statement is not attributed to a reference in the text, but Trella et al. (2000) does list an earlier version of Hexcel (2005) among his references). The bottoming-out point in test 2910, which was quite clearly defined, corresponds to 79.5% crush.

4.3.3 STIFFNESS CALCULATION

With ΔV at max crush calculated for each crash test in Table 5, the amount of energy absorbed by the MDB face was calculated as the difference in MDB kinetic energy between max crush and the start of impact (Equation 14).

$$E_a = KE_{initial} - KE_{final}$$

$$KE_{initial} = \frac{1}{2} m {V_0}^2 \qquad \text{Equation 14}$$

$$KE_{final} = \frac{1}{2} m {V_{max\ crush}}^2 + \frac{1}{2} I {\omega_{max\ crush}}^2$$

m is the mass of the MDB, I is the yaw-axis moment of inertia, V is the velocity of the MDB CG, ω is the yaw velocity and E_a is the energy absorbed by the MDB face at max dynamic crush.

Struble et al. (2001) used exactly two tests in his analysis. By simultaneously solving Equation 2 (Chapter 2) for both the lower and higher energy tests, he solved algebraically for d_0 and d_1. In our analysis, the dataset consists of three tests which will require the use of linear least-squares regression instead. In order to facilitate the use of linear least-squares regression to fit d_0 and d_1 for more than two cases, Equation 2 was rearranged and was integrated over $\sqrt{w}$ as shown in Equation 15:

$$\sqrt{2 \cdot E_{av}} = \int_0^{\sqrt{w}} \left(d_0 + d_1 \cdot C(x)\right) dx \qquad \text{Equation 15}$$

Applying the same trapezoidal integration procedure for $C(x)$ as in the WinSMASH integration, the result is as follows:

$$\sqrt{2 \cdot E_{av}} = \left(d_0 \cdot \sqrt{w}\right) + \left(d_1 \cdot \frac{\sqrt{w}}{10}\right) \cdot \left(C_1 + 2 \cdot \left(C_2 + C_3 + C_4 + C_5\right) + C_6\right) \qquad \text{Equation 16}$$

Since $\sqrt{w}$ is constant across all the tests examined ($\sqrt{1.676}$ m, or the width of the NHTSA MDB face), d_0 and d_1 can be calculated from the coefficients of a linear least-squares regression of a plot of the energy term of Equation 16 (left side) versus the crush term (right side).

4.4 RESULTS

Figure 20 shows the raw regression analysis for the NHTSA MDB. There are only three tests in this analysis, and two of them have very similar amounts of crush and absorbed energy, so the high R-squared value is not terribly surprising.

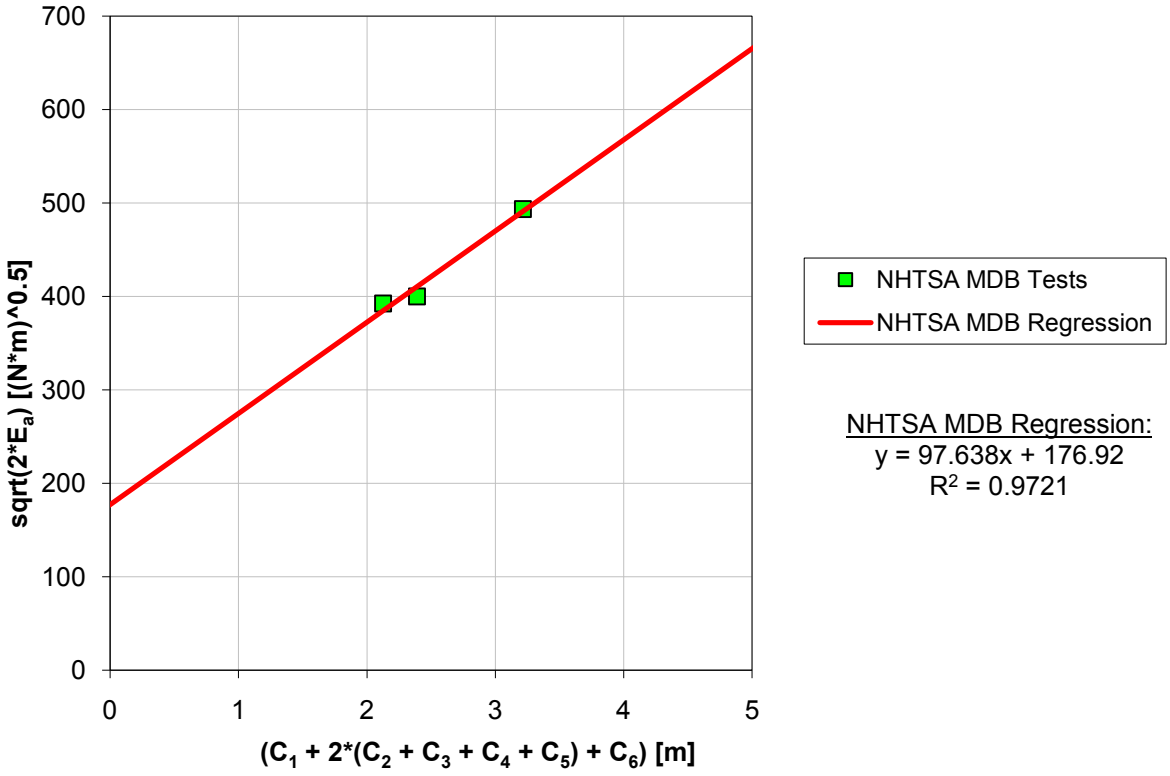

Figure 20. Crash test regression analysis of the NHTSA MDB face stiffness.

Table 7 gives the d_0 and d_1 stiffness coefficients calculated from the regression parameters of Figure 20, as well as those which result when bottoming out is not accounted for, and those found in the analysis of Struble et al. (2001) for comparison.

Table 7. NHTSA MDB stiffness coefficients plotted in Figure 21.

	$d_0 \left[\sqrt{N}\right]$	$d_1 \left[\sqrt{N}/cm\right]$
Corrected	136.66	7.5420
Non - Corrected	85.107	9.8223
Struble et al. (2001)	44.555	11.285

The effects of bottoming out of the MDB face are best illustrated in Figure 21. The regression analysis shown in Figure 20 is over-plotted with the regression line using the uncorrected test data. If the bottoming out in test 2910 is not accounted for, the calculated stiffness ends up having a lower intercept (d_0) and a higher slope (d_1) (Table 7). The MDB stiffness given by Struble et al. (2001) is also plotted in Figure 21 for comparison. This stiffness was calculated using only tests 2910 and 2819, and bottoming out in test 2910 was accounted for by slightly increasing one of the crush measurements.

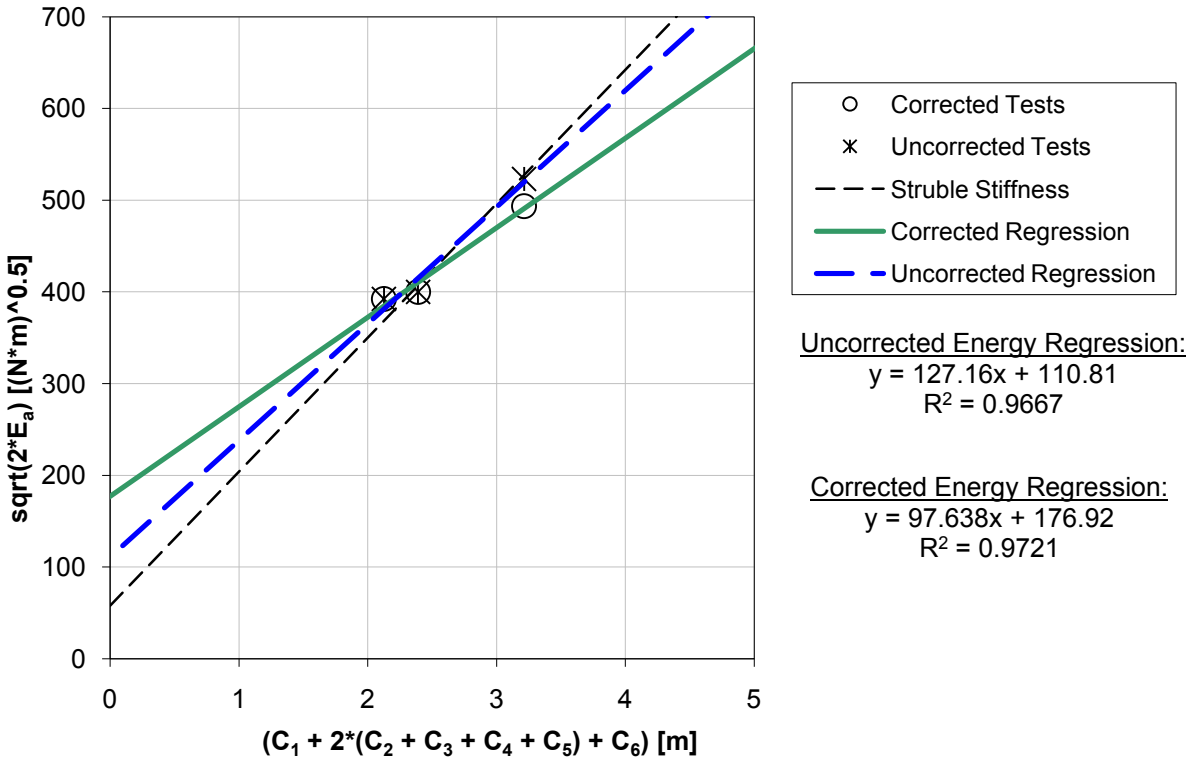

Figure 21. Comparison of NHTSA MDB stiffnesses showing the effects of bottoming out of the MDB face.

The exact 6-point crush profiles used in the stiffness calculations for each test are given in Table 8. There was a great deal of variation in the crush recording format between each test report. The different ways in which crush was extracted are explained in Methods.

Table 8. Crush profile data, all crash tests.

Test #	C1 [m]	C2 [m]	C3 [m]	C4 [m]	C5 [m]	C6 [m]
1068	0.333	0.330	0.323	0.316	0.312	0.317
2819	0.298	0.240	0.236	0.230	0.227	0.226
2910	0.287	0.251	0.221	0.193	0.168	0.173

Finally, the CG velocities in Table 9 are given in ground-fixed coordinates, where the coordinate axes are coincident with the MDB-local axes at the moment of impact.

Table 9. Calculated crash test parameters. *Velocities at bottoming out, not max crush.

Test #	CG Vel. @ Max Crush (long., lat.) [km/h]		Angular Vel. @ Max Crush [deg/s]	Absorbed Energy [J]
1068	-0.0108	9.637	-88.87	77204
2819	-0.0216	12.10	-73.57	80124
2910	17.05*	19.21*	-56.73*	137524

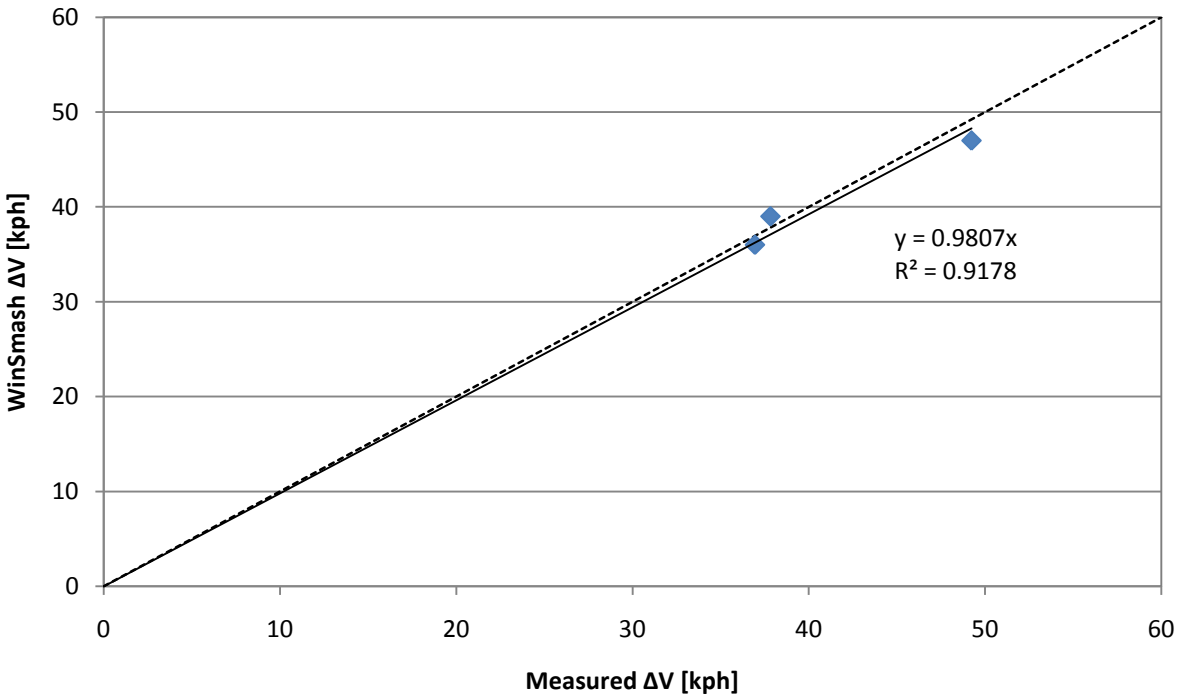

Figure 22. WinSMASH estimated ΔV vs. measured max crush ΔV, tests 2910, 2819 and 1068 using corrected stiffness.

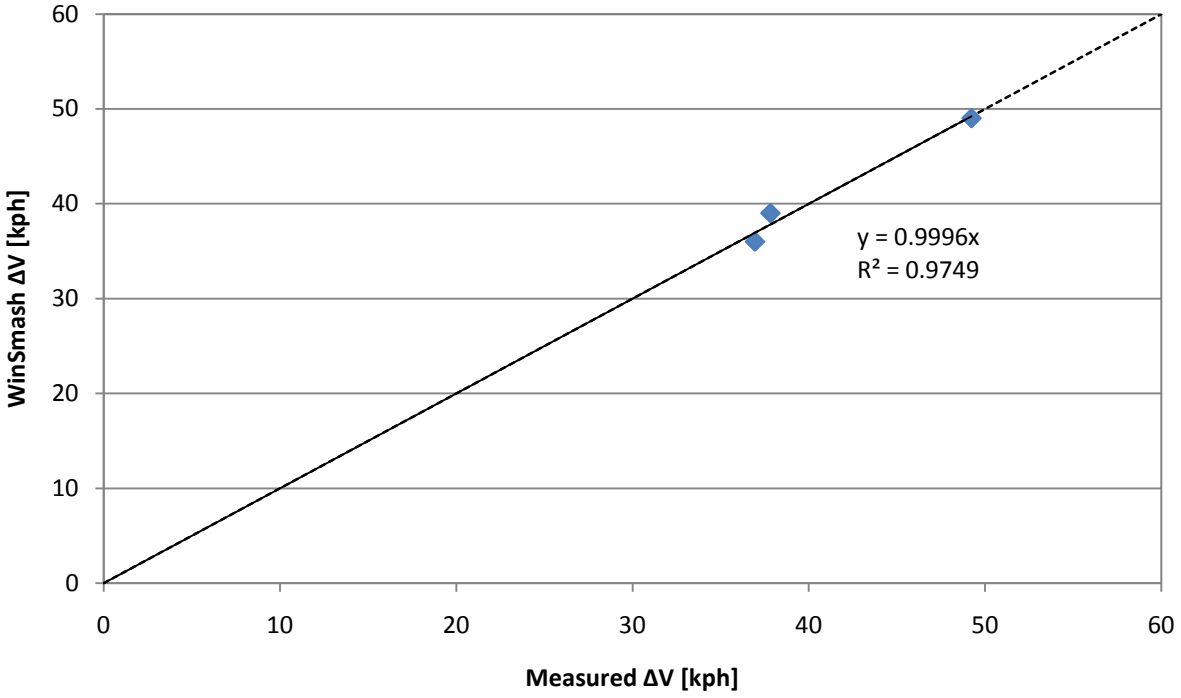

Figure 23. WinSMASH estimated ΔV vs. measured max crush ΔV, tests 2910, 2819 and 1068 using uncorrected stiffness.

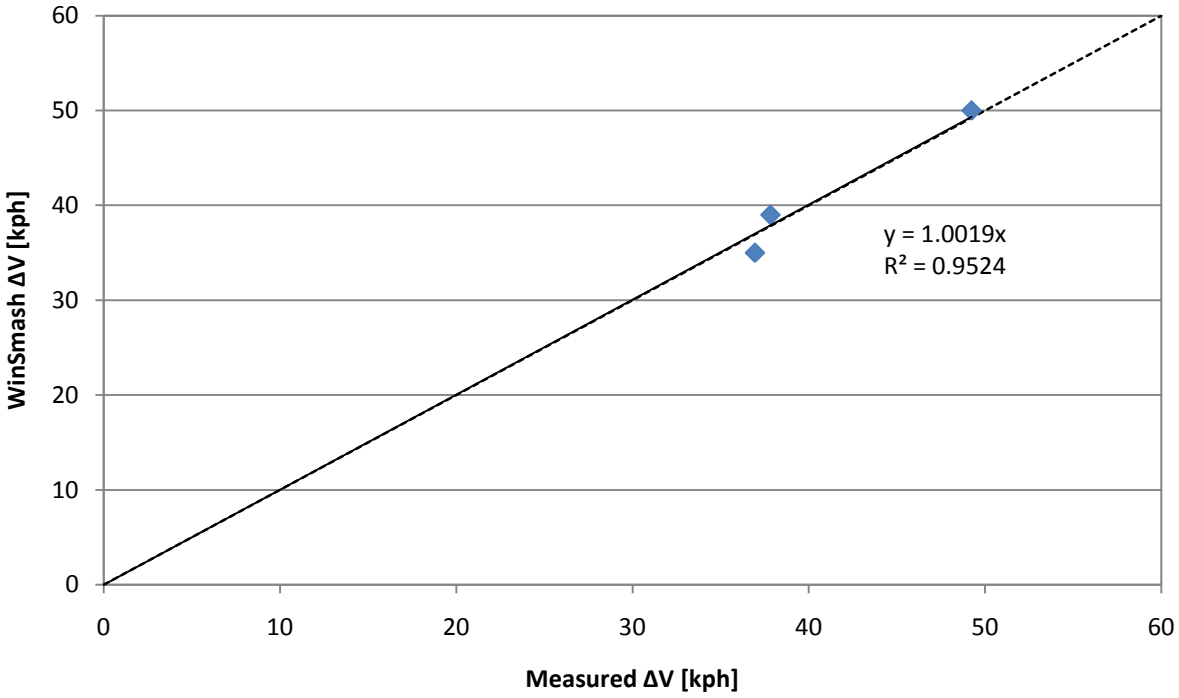

Figure 24. WinSMASH estimated ΔV vs. measured max crush ΔV, tests 2910, 2819 and 1068 using stiffness calculated by Struble et al. (2001).

4.5 DISCUSSION

The corrections made for bottoming out and the inclusion of test 1068 in this analysis account for virtually all of the difference between the NHTSA MDB stiffness calculated here and that calculated by Struble et al. (2001). Compare the Struble stiffness to the stiffness calculated here without bottoming-out corrections in Figure 21 and Table 7. If the uncorrected regression is recalculated using only tests 2910 and 2819 (as was done by Struble et al. (2001)), the calculated stiffness is $d_0 = 32.815 \left[\sqrt{N}\right]$, $d_1 = 11.550 \left[\sqrt{N}/cm\right]$, which is practically identical to the stiffness computed by Struble et al. (2001).

Although the energy was recorded at separation and not common interface velocity in Struble et al. (2001), there does not appear to be a great deal of difference between the energies at these two times. This is consistent with the findings of Prasad (1991b) and Rose et al. (2006),

who states that this is generally the case. Careful consideration of the MDB restitution coefficients reported in Struble et al. (2001) supports this further. The restitution coefficients reported in Struble (2001) were in the range of 0.19. This means that the MDB rebound velocity was 0.19 that of the impact velocity. While this would have a substantial effect on an analysis of ΔV, the energy returned by this amount of restitution would be 0.19*0.19 = 0.0361 times the kinetic energy at impact (in these tests, also the absorbed energy), or just under 4%. It also seems that the differences in crush measurement protocol between that study and this one makes almost no appreciable difference. Of course, the bowing constant and sill – averaging features of the NHTSA protocol (NHTSA, 1998) which Struble and many others have objected to never came into use in any of the MDB tests used here. In the NASS crush measurement protocol, the bowing constant is a multiplier applied to all crush values in the event that the central vehicle axis is bent. Sill-averaging refers to a procedure used in the NASS measurement protocol to modify measured crush values in the event the B-pillar separates from the door sill.

Figure 22, Figure 23 and Figure 24 compare WinSMASH reconstructions of NHTSA tests 2910, 2819 and 1068 made using the stiffness coefficients in Table 7 to the actual test ΔVs measured at max crush. As expected, all three stiffnesses do an excellent job of predicting the max crush ΔV from which they were calculated. Also as expected, the predictions given by the stiffness corrected for bottoming out in test 2910 under-predict test ΔV very slightly (based on regression line slope). This is because the stiffness does not account for the energy dissipated after bottoming out, but the test ΔV is affected by it nonetheless.

However, the objective of this analysis is to attempt to develop an improved MDB stiffness for use in NHTSA side crash tests. The typical average MDB crush seen in NHTSA side crash tests is on the order of 10 cm, which is far below the crush seen in tests 2910, 2819

and 1068, which had average crush values of 32.2 cm, 24.3 cm and 21.5 cm respectively. Ideally, the energy predictions of each stiffness in Table 7 would be tested by application to low-crush MDB tests of the same configuration which were not used to generate the stiffness coefficients. Regrettably, the three tests used in this analysis are, to the author's knowledge, the only existing tests of the NHTSA MDB face in a 27 degree crabbed impact mode. Thus, some other metric is required to judge the relative merit of the MDB stiffness coefficients examined here.

Prior authors, most notably Prasad (1990, 1991a) and Struble et al. (2001), have used the concept of a "damage onset speed" to help intuitively understand the low-crush behavior predicted by vehicle stiffnesses. The d_0 parameter of the WinSMASH stiffness corresponds to the absorbed energy per unit damage width at which residual crush is first observed. Squaring this and multiplying by the damage width (1.676 m in the case of the NHTSA MDB face) gives the minimum energy required to cause residual crush using the stiffness in question. Now consider an MDB cart of a given mass crashed in a non-crabbed configuration into a rigid barrier. The energy absorbed at max crush is the initial kinetic energy, which is solely a function of the mass and initial velocity. The damage onset speed may thus be intuitively understood as the minimum impact speed into a rigid barrier required to generate residual crush, given a vehicle of a particular mass. Table 10 gives the damage onset speeds calculated for each of the stiffness coefficients listed in Table 7, for a 3000 lb (1361 kg) NHTSA MDB.

Table 10. Damage onset speeds for different stiffness coefficients, calculated for a 3000 lb (1361 kg) MDB impacting a rigid barrier.

Stiffness	Damage Onset Speed [mph]
Corrected for bottoming out	15.2
Uncorrected for bottoming out	9.45
Struble et al. (2001), no force saturation	4.95

Another perspective is to consider the d_0 in the context of what it implies about the difference between max dynamic crush and static crush. Figure 25 shows the amount of energy

absorbed in each of the three tests examined here plotted against displacement of the MDB relative to the rigid crash barrier. Recall that yaw angle changes are minimal over the duration of each test. For test 1068, the measured crush force was integrated over the displacement calculated from accelerometers to yield the crush energy curve. In tests 2819 and 2910, the load cells were mounted between the MDB cart and the crushable MDB face, so the amount of energy loss was calculated from kinematic data instead. The black, dashed line represents the theoretical energy loss due to quasi-static, normal crush of a NHTSA MDB face. It is readily apparent that the quasi-static crush strength gives a reasonable approximation to the observed energy absorption behavior, especially at the low crush values which are of interest in this thesis.

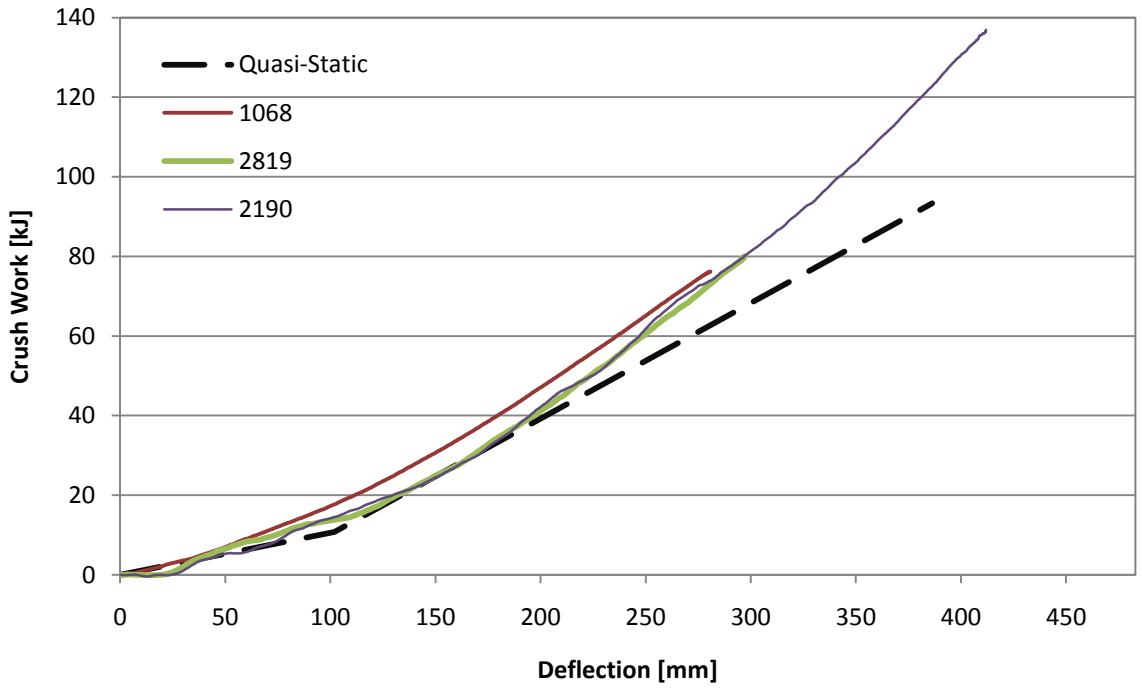

Figure 25. Energy absorbed versus dynamic crush, NHTSA tests 2910, 2819 and 1068 and theoretical quasi-static deflection.

This naturally suggests using Equation 1 to over-plot the energies predicted by each of the stiffnesses in Table 7 and the dynamic MDB behavior in Figure 25. However, the deflections

used in Figure 25 are dynamic deflections, and not static crush values. Equation 1 is valid for average static crush, and Figure 19 makes it very apparent that there is a substantial difference between average static crush and the maximum dynamic crush achieved in these MDB tests. By using Equation 1 to calculate the average "crush" at which zero energy is absorbed we can estimate the amount of dynamic deflection necessary to initiate static damage, giving us a kind of "damage-onset crush". Figure 26 shows the average crush – absorbed energy curves for each of the stiffnesses in Table 7, as well as all the curves displayed in Figure 25.

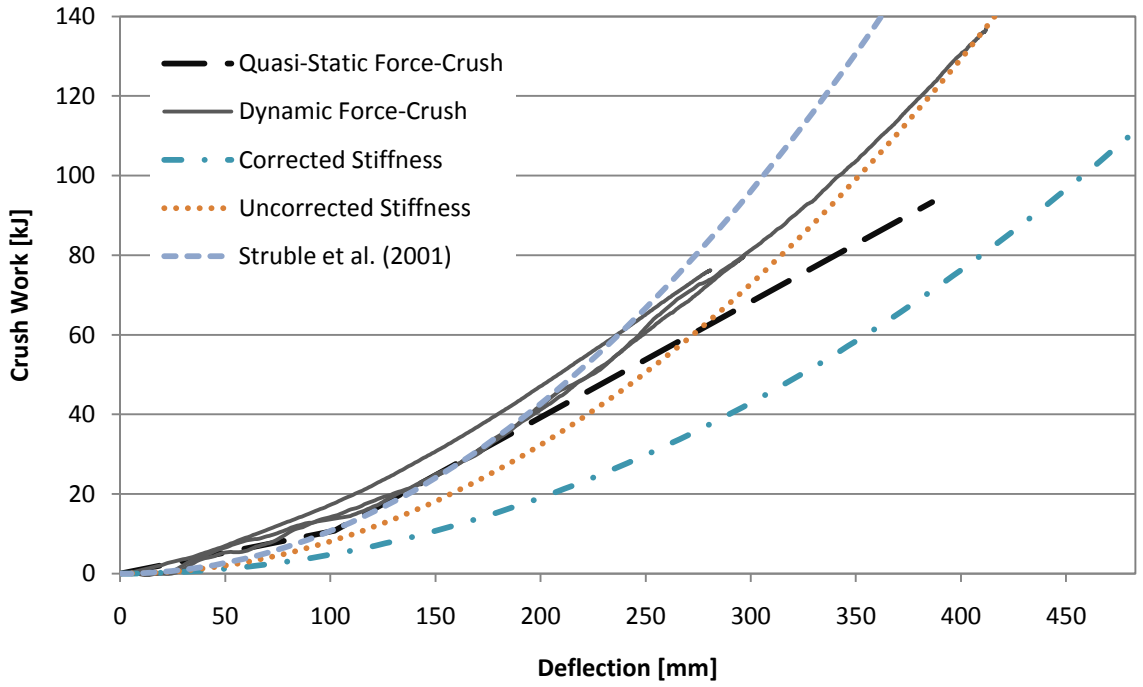

Figure 26. Energy absorption versus crush for each of the stiffnesses in Table 7. Each curve has been shifted forward by the "damage-onset crush" described in the text. The curves shown in Figure 25 are given for comparison.

Of the three stiffnesses examined, the stiffness reported by Struble et al. (2001) agrees the most closely with the observed dynamic force-crush behavior and the theoretical quasi-static force-crush relationship, particularly at low and intermediate levels of crush.

4.5.1 LIMITATIONS

There were only three tests used for the NHTSA MDB. Given inevitable inter-test variability, this study would benefit from use of a larger number of tests. The degree of variability between tests is likely exacerbated by the fact that the NHTSA MDB face is not pre-crushed (NHTSA, 2006, 2008). The crush behavior of aluminum honeycomb is highly dependent on the way in which crush in initiated. Since this is effectively uncontrolled for the NHTSA MDB face, the inter-test variability is not surprising.

Another limitation was that all the crush-energy data was obtained at relatively high energies. All of the tests used in this analysis involved crush depths and E_as far more severe than those normally seen in side impact tests. We are unaware of any tests of the NHTSA MDB face that fall within the E_a/crush regime typical of NHTSA side crash tests. We do not know how the stiffnesses calculated in this analysis generalize to the lower ΔVs typical of MDB – side crash tests.

The fact that all tests examined here used rigid barrier walls as the impact partner allowed the energy absorbed by the MDB faces to be calculated. However, different crush patterns typically result when the impact partner is a deformable object such as a vehicle side. In vehicle impacts, much of the crush occurs as the bumper element is pushed into the main block. In rigid barrier impacts, this would also be the pattern at lower severity impacts, but at the high severities at which all the examined tests were run, there is substantial crush over the entire main block. How much difference this would potentially make is not certain, but if it were found to be significant, it would have implications not only for this analysis of MDB behavior, but also for every WinSMASH reconstruction using a frontal vehicle stiffness from the WinSMASH database as well.

4.6 CONCLUSIONS

This study has computed WinSMASH stiffness coefficients for the NHTSA MDB in impact configurations representative of NHTSA side crash tests, and compared them with other means of estimating energy absorbed by damage to the NHTSA MDB. Integration of damaged volume using the quasi-static crush force of the NHTSA MDB, as done by Arbelaez (2005), appears to reasonably approximate the energy-crush curves observed in NHTSA tests 1068, 2819 and 2910. However, the observed difference between average static crush and max dynamic crush (Figure 25) indicates that this method may under-estimate absorbed energy when used with static crush. Thus, based on the limited crash test data available for the NHTSA MDB face, the stiffness computed by Struble et al. (2001) seems to be the most reasonable choice for reconstructing NHTSA side crash tests with their characteristically low levels of MDB crush.

5 EVALUATION OF WINSMASH ACCURACY IN SIDE CRASH TESTS

For this study, WinSMASH was used to reconstruct 70 FMVSS 214D and Side NCAP side crash tests. For each test, the ΔV determined from test instrumentation was compared to the ΔV estimated by WinSMASH.

5.1 WINSMASH RECONSTRUCTIONS

All WinSMASH reconstructions performed in this study were damage-only reconstructions of the "standard" type. A standard reconstruction reconstructs a collision between two vehicles, where the full set of WinSMASH input parameters are known for each vehicle. This includes a damage profile and a PDOF. For NHTSA side crash tests such as those examined here, 6-point damage profiles are generated for the struck vehicle and recorded in the test documentation. Detailed crush measurements are also made for the MDB face, but a 6-point damage profile is not recorded. For the reconstructions in this study, a 6-point damage profile was generated for the MDB damage profile by linearly interpolating from the MDB crush measurements recorded at mid-bumper height.

When reconstructing a crash, WinSMASH requires that the investigator estimate Principal Direction of Force (PDOF) and damage offset. PDOF is the direction of the crash impulse relative to the vehicle and damage offset describes the location of the point of application of the crash impulse relative to the vehicle center of gravity (CG). Errors in estimations of these parameters, which are largely unavoidable since they are reconstructionist estimates, will introduce some amount of error into all WinSMASH reconstructions. In order to eliminate this confounding effect from the analysis, the PDOF and damage offset used here were both calculated from the crash test data itself. PDOF was simply calculated as the direction of the vehicle's ΔV at maximum crush.

Damage offset was determined by calculating the crash impulse moment arm required to generate the observed vehicle yaw rate at maximum crush, assuming the estimated value of radius of gyration (Equation 17). Net crash impulse was calculated from the vehicle mass and the observed ΔV at max crush.

$$(moment\ arm) = {}^{(I\ \omega_{max\ crush})}\Big/_{(net\ crash\ impulse)} \qquad \text{Equation 17}$$

$$I = (mass)\ (0.3 * length)^2$$

Using the calculated PDOF, the longitudinal position of the point of impulse application was then calculated, assuming some lateral depth for the application point. In this analysis, the lateral depth of the damage profile centroid was chosen for this purpose, based on the work of Ishikawa (1994).

Most vehicle specifications and contact configuration parameters used in WinSMASH reconstructions were obtained from the crash test records and/or testing protocols. The vehicle radius of gyration is specified by the NHTSA testing protocols for the MDB, however this parameter is seldom known for actual vehicles, in crash tests or in real-world crashes. All reconstructions in this study used the WinSMASH default method of estimation (Sharma et al. 2007) shown in Equation 18 to estimate the struck vehicle radius of gyration.

$$radius\ of\ gyration = 0.3 * (length) \qquad \text{Equation 18}$$

This approximation is surprisingly good according to the NHTSA's Vehicle Inertial Parameter Measurement Database. Examining only cars for which a yaw moment of inertia and a length are listed (87 vehicles total), the radius if gyration is on average 29.1 % of the length with a standard deviation of only 1.07 %. Radius of gyration may be calculated as $\sqrt{yaw\ moment\ /\ mass}$.

Vehicle Center of Gravity (CG) location was not recorded directly in the test reports, but was calculated from the recorded wheelbase and front/rear tire weight distribution and assumed to lie on the vehicle centerline.

In order to separate the effect of the restitution assumption from other effects, WinSMASH ΔV was compared to the crash test ΔV recorded at both the time of common velocity and the time of separation. ΔV at separation is the quantity of interest to crash researchers, as it represents the whole ΔV experienced during a collision. But by treating all collisions as plastic, WinSMASH actually predicts ΔV at maximum crush, in effect ignoring the portion of the ΔV that occurs after maximum crush. The purpose of using reconstruction parameters (PDOF, damage offset) calculated at max crush as opposed to separation is to give WinSMASH the most precise inputs possible, corresponding to precisely the ΔV that WinSMASH estimates. In other words, since WinSMASH actually reconstructs ΔV at max crush, crash tests are reconstructed using PDOF and damage offset at max crush as opposed to separation. This, in turn, allows the effects of WinSMASH's assumption of zero restitution to be considered completely separately of the reconstruction parameters used.

Because the MDB face in side crash tests absorbs some energy, its deformation must be accounted for in WinSMASH reconstructions of crash tests. Based on the findings of Chapter 4, this analysis used a stiffness value computed by Struble et al. (2001) from frontal barrier tests of the NHTSA MDB face (Table 11), since it matches the observed crush-energy behavior of the NHTSA MDB the most closely of all the stiffnesses in Chapter 4. Struble originally presented this stiffness in a format used by CRASH3, the predecessor to WinSMASH. The second value in Table 11 was converted using the relationships $A = d_0 * d_1$ and $B = {d_1}^2$ developed by Prasad (1990) and presented by Sharma et al. (2007).

Table 11. MDB face stiffness reported by Struble et al. (2001), used in WinSMASH reconstructions.

CRASH3 Format (original)		WinSMASH Format (used here)	
$A\ [N/cm]$	$B\ [N/cm^2]$	$d_0\ [\sqrt{N}]$	$d_1\ [\sqrt{N}/cm]$
502.8	127.4	44.555	11.285

Stiffness parameters for the struck vehicle were selected by WinSMASH automatically, based on the year, make, model, bodystyle and damaged side (front/side/rear). WinSMASH first attempts to find a vehicle-specific stiffness coefficient in its integrated library for the exact vehicle specified. If an exact match cannot be found, WinSMASH applies a categorical stiffness coefficient instead.

5.2 PROCESSING OF CRASH TEST DATA

NHTSA side crash tests, being crabbed, can involve substantial rotation. To capture both rotational and translational motion, NHTSA tests record bi-axial acceleration for both vehicles (MDB and test vehicle) at multiple locations. Using a technique presented by Marine and Werner (1998), the full planar motion history of both the MDB and the struck vehicle was first calculated. By determining the time at which the MDB protruded the farthest into the struck vehicle, the time of maximum crush could be determined and the maximum crush ΔV at that time recorded. Separation ΔV was then simply taken at the time when the struck vehicle achieved its maximum velocity. Total absorbed energy was calculated by subtracting the rotational and linear kinetic energy for each vehicle at maximum crush from the kinetic energy of the MDB at the start of the test (the vehicle is initially stationary) (Equation 19).

$$\boldsymbol{E_{abs\ total} = KE_{MDB-0} - (KE_{MDB\ max\ crush} + KE_{Veh\ max\ crush})} \qquad \text{Equation 19}$$

$$\boldsymbol{KE_{MDB-0} = \frac{1}{2} * m_{MDB} * V_{0\_MDB}{}^2}$$

$$\boldsymbol{KE_{MDB\ max\ crush} = \left(\frac{1}{2} * m_{MDB} * V_{MDB\ max\ crush}{}^2\right) + \left(\frac{1}{2} * I_{MDB} * \omega_{MDB\ max\ crush}{}^2\right)}$$

$$\boldsymbol{KE_{Veh\ max\ crush} = \left(\frac{1}{2} * m_{Veh} * V_{Veh\ max\ crush}{}^2\right) + \left(\frac{1}{2} * I_{Veh} * \omega_{Veh\ max\ crush}{}^2\right)}$$

In the tests examined in this study, rotation accounted for 6.3% of the total kinetic energy of the struck vehicle at maximum crush on average, and 8.6% of the MDB kinetic energy at the same time on average.

All tests were checked for problems using multiple techniques. Any tests with problems that could not be corrected were discarded from the analysis. Data quality checks included the following:

- **Visual Inspection of Data:** Visual inspection of plots of the data for each case eliminated obvious problems such as corrupted accelerometer channels, or typographical errors in crush measurements.

- **Momentum Conservation:** From momentum conservation, the ratio of the resultant ΔV for the MDB and vehicle to the inverse ratio of their masses should be nearly equal (Equation 20):

$$\left\|\frac{\Delta V_1}{\Delta V_2}\right\| = \frac{m_2}{m_1} \qquad \text{Equation 20}$$

  Marine and Werner (1998) used two biaxial accelerometers to compute a motion history. The MDBs in NHTSA tests have exactly this number, but the struck vehicles often have more biaxial accelerometers. There is no guarantee however that all of these accelerometers recorded useful data. Thus, the vehicle ΔV was computed using each possible pairing of accelerometers. The results for the accelerometer pairing which most closely obeyed momentum conservation at common velocity were retained. If the best ratio of the resultant ΔVs differed from the inverse ratio of the masses by more than 5%, the case was excluded from further analysis.

- **Sequence of Events:** Any cases in which the time of vehicle separation occurred before the calculated time of maximum crush were discarded.

- **PDOF Colinearity:** The calculated PDOFs for the vehicle and MDB were checked for colinearity. In theory, the test vehicle and MDB should both change velocity along the same line, but in opposite directions. Knowing the velocity change of each vehicle, and its orientation at maximum crush, the agreement with theory was tested. Maximum crush was chosen since, being earlier in the collision than separation, it is less affected by cumulative errors in the velocity integration. WinSMASH itself allows for 10 degrees difference between vehicle PDOFs. Any tests in which the observed MDB PDOF and vehicle PDOF differed by more than this amount were excluded from the analysis. For purposes of the WinSMASH reconstruction, the MDB PDOF was set to be precisely collinear with the measured struck vehicle PDOF, rather than to the value calculated directly from the measured MDB ΔV. The reason for this is twofold: first, in physical reality the PDOF of the vehicle and the MDB do not deviate from colinearity (Newton's Third Law), and second, the struck vehicle data is derived from the best of several different accelerometer pairs, whereas there is only one pairing on the MDB. The magnitude of the difference between the measured MDB PDOF and the value used in WinSMASH was 3.91 degrees on average, with a minimum of 0.08 degrees and a maximum of 9.82 degrees.

5.3 STATISTICS

All comparisons between WinSMASH – predicted values and measured values were visualized using a cross plot displaying the data points and a linear regression line fit to the data using a fixed intercept of zero. This has the virtue of concisely describing both systemic error and random error about the mean. Rigorous tests on the statistical significance of all comparisons were carried out in SAS 9.2 using Student's Paired T-test ('PROC TTEST' using the 'PAIRED' keyword) or the Wilcoxon Signed Rank Sum test (part of the output of 'PROC UNIVARIATE'), which is the non-parametric equivalent of the Paired T-test (Ott and Longnecker, 2001). Whenever a significance level is stated, the test used to determine it is given as well. The test

used, Student's or Wilcoxon, is indicative of whether or not PROC UNIVARIATE found the difference to be normally distributed.

5.4 RESULTS

For an in-depth description of the dataset used in this analysis, please refer to Chapter 3. Table 12 briefly summarizes major characteristics of the data set used in this study. Test included both FMVSS 214D compliance tests (33.5 mph nominal impact speed) and Side NCAP tests (38.5 mph nominal impact speed) from 1994 to 2006. WinSMASH was able to find vehicle-specific stiffness coefficients for all but 4 of the examined tests.

Table 12. Summary of dataset composition.

Dataset Composition	
Total Tests:	70
Vehicle Type:	
Cars	64
LTVs	6
Nominal Impact Speed:	
33.5 mph (FMVSS)	28
38.5 mph (NCAP)	42
Stiffness Type:	
Vehicle Specific	66
Categorical	4

Figure 27 shows a plot of WinSMASH-estimated resultant vehicle ΔV versus the value measured from tests at separation and Figure 28 shows the analogous plot for the MDB. WinSMASH was observed to over-predict resultant vehicle ΔV by 12% systemically (see regression equation), with a great deal of case-to-case variability. The observed difference between the WinSMASH vehicle ΔV and the measured vehicle ΔV was found to be significant at 95% confidence (p-value < 0.0001) using Student's Paired T-test. MDB ΔV was over-predicted by 6.6% and exhibited a qualitatively similar amount of inter-case variability. The observed difference in MDB ΔV between WinSMASH and the measured values was also found to be significant at 95% confidence (p-value = 0.0002) using Student's Paired T-test.

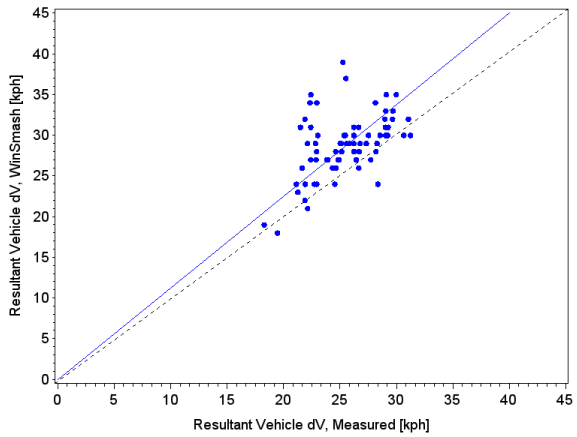

Figure 27. Resultant vehicle ΔV at separation, WinSMASH predictions versus measured values. Regression equation: y = 1.125x

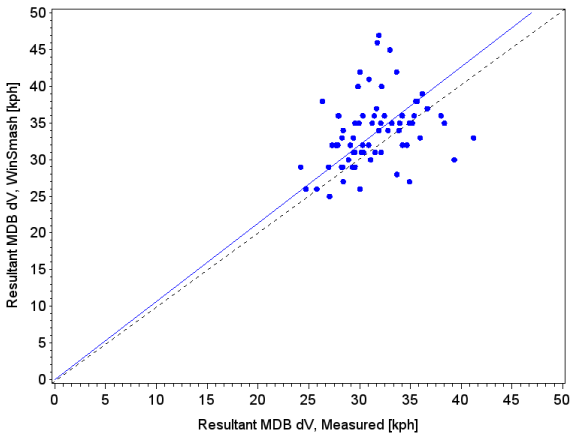

Figure 28. Resultant MDB ΔV at separation, WinSMASH predictions versus measured values. Regression equation: y = 1.066x

Figure 29 compares vehicle ΔV measured at separation to vehicle ΔV measured at maximum crush, and demonstrates the effect of restitution on the measured ΔV. When comparing vehicle ΔV at max crush and separation, NHTSA side tests appear to exhibit about 8% restitution on average. When MDB ΔV is examined in Figure 30, ΔV is observed to increase by 14% on average, with a slight qualitative increase in variance. For both the vehicle and MDB, the observed difference in ΔV was found to be significant at 95% confidence (p-value <0.0001) using the Wilcoxon Signed Rank Sum test.

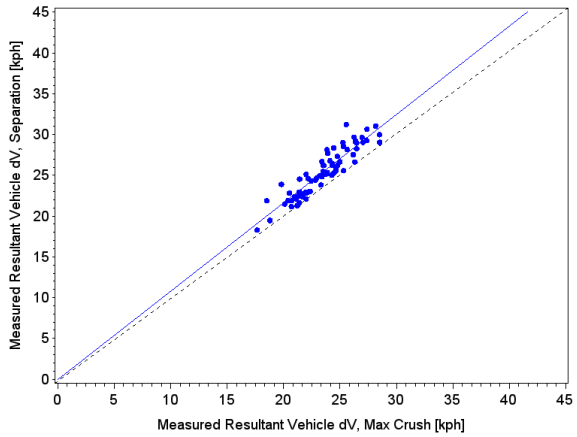

Figure 29. Vehicle ΔV measured at separation versus ΔV measured at maximum crush. Regression equation: y = 1.081x

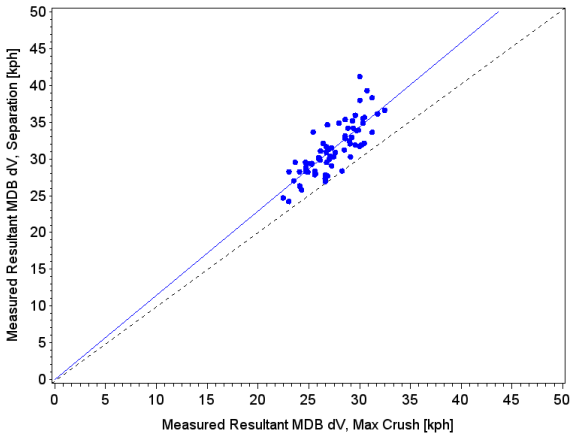

Figure 30. MDB ΔV measured at separation versus ΔV measured at maximum crush. Regression equation: y = 1.145x

Figure 31 and Figure 32 compare WinSMASH ΔV to the ΔV measured at maximum crush, for the vehicle and MDB respectively. This comparison is not affected by WinSMASH's assumption of zero restitution as are Figure 27 and Figure 28. Notice that the difference between WinSMASH ΔV and the measured ΔV has increased to 22% - 23%, and that both the vehicle and MDB are now over-predicted by virtually the same amount. For both the MDB and the struck vehicle, the observed difference was found to be significant at the 95% confidence level (p-value < 0.0001) using Student's Paired T-test.

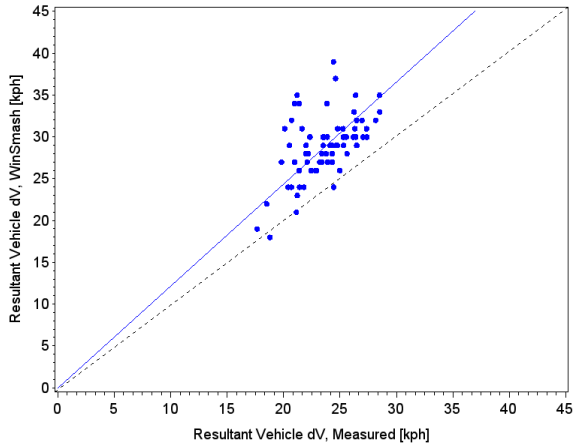

Figure 31. Resultant vehicle ΔV at maximum crush, WinSMASH predictions versus measured values. Regression equation: y = 1.218x

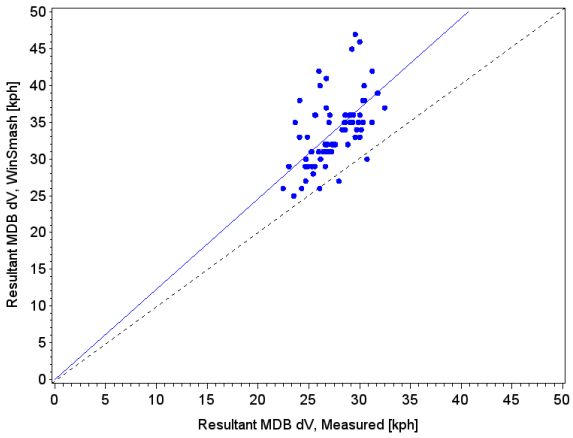

Figure 32. Resultant MDB ΔV at maximum crush, WinSMASH predictions versus measured values. Regression equation: y = 1.229x

Figure 33 compares WinSMASH's estimate of the total amount of energy absorbed in the collision (the sum of energy absorbed by both the vehicle and MDB) to the actual value calculated from the test data at maximum crush. This is a key comparison, as the WinSMASH stiffness model predicts energy absorbed specifically at maximum crush and not at separation. The observed difference is consistent with over-prediction of ΔV, and was found to be significant at 95% confidence (p-value < 0.0001) using Student's Paired T-test.

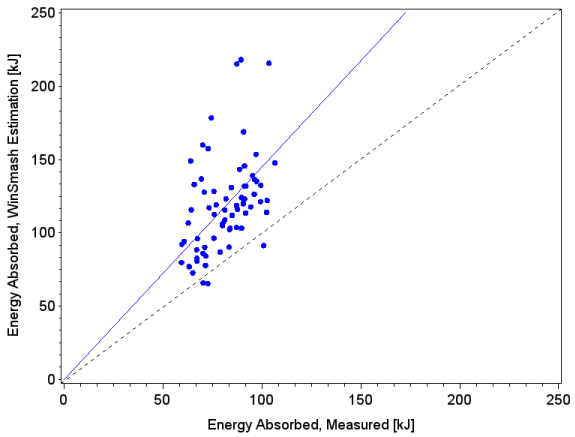

Figure 33. Total energy absorbed in test, WinSMASH estimation versus measured value at maximum crush. Regression equation: $y = 1.449x$

Figure 34 (vehicle) and Figure 35 (MDB) compare the ΔV measured at maximum crush and the ΔV estimated by WinSMASH when WinSMASH is forced to use precisely the energy calculated from the test data at maximum crush. This comparison is not affected by either error due to restitution or inaccurate energy estimations. In each case WinSMASH ΔV was still found to be significantly different from the measured ΔV at 95% confidence (p-value = 0.0002 for vehicle using Wilcoxon Signed-Rank Sum test, p-value < 0.0001 for MDB using Student's Paired T-test). However, the mean difference for the vehicle was only 0.42 km/h, or about 2% on average as shown in the regression equation; for the MDB the mean difference was a mere 0.79 km/h, or roughly 3% by the regression line. Note also the drastic reduction in case-to-case variability in both plots.

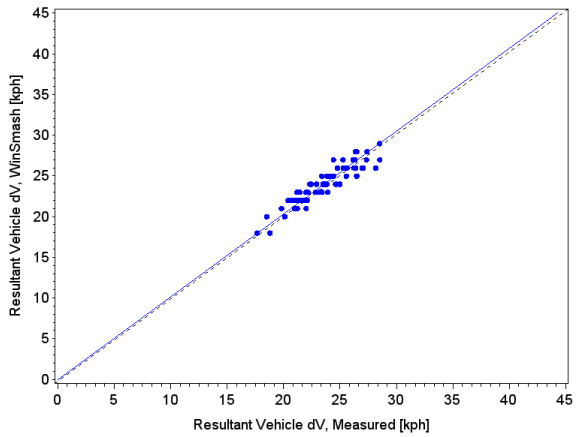

Figure 34. Resultant vehicle ΔV at maximum crush, WinSMASH predictions using measured energy versus measured ΔV values. Regression equation: y = 1.016x

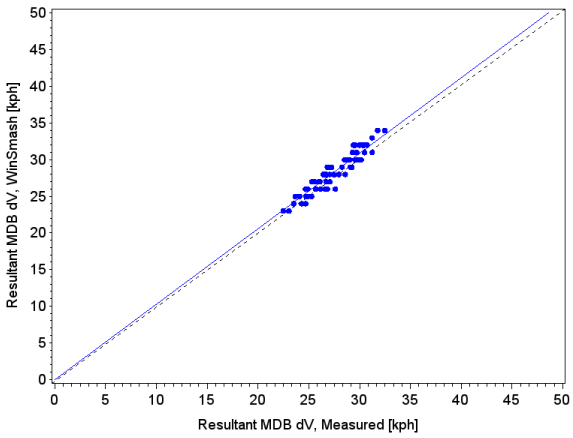

Figure 35. Resultant MDB ΔV at maximum crush, WinSMASH predictions using measured energy versus measured ΔV values. Regression equation: y = 1.029x

5.5 DISCUSSION

Figure 27 and Figure 28 indicate that WinSMASH over-predicts struck vehicle ΔV in NHTSA side crash tests by 12%, and MDB ΔV by 6.6%. The accuracy of the WinSMASH reconstruction model is strongly affected by investigator estimates of PDOF (Brach and Brach, 2005), but PDOF (and damage offset) error has been controlled for in this analysis. Vehicle specifications are all known with a high degree of certainty from the test documentation, except for the struck vehicle radius of gyration. However, the damage offset parameter used in the WinSMASH reconstructions was calculated using the estimated radius of gyration (Equation 17), so this is controlled for as well. This leaves WinSMASH's restitution assumptions and estimations of absorbed energy as the most probable sources of error.

Figure 29 and Figure 30 indicate that restitution in NHTSA side crashes is between about 8% and 14% on average (considering the more stringent validation allowed by the vehicle ΔV data, the figure is probably closer to 8%). If WinSMASH were reconstructing the crash tests otherwise perfectly, an under-prediction of about 8% average would be expected due to ignoring restitution (ΔV always being higher at separation than at maximum crush). Figure 27 and Figure

28 clearly demonstrate that the opposite is happening, which implies some other effect is present in these reconstructions. Figure 31 and Figure 32 bear this out further. By comparing the WinSMASH – reconstructed ΔV to the ΔV measured at maximum crush, restitution no longer factors into the comparison. The observed over-prediction of crash test ΔV then increases from 12% to 22% for the vehicle, and from 6.6% to 23% for the MDB. The WinSMASH assumption of zero restitution appears to partly mask the error due to some other influence.

This other influence is the accuracy of WinSMASH's estimation of the amount of energy absorbed in collisions. Estimation of absorbed energy is central to the WinSMASH crash reconstruction algorithm (Campbell, 1974; Sharma et al., 2007). As previously discussed in Chapter 2, WinSMASH first estimates the energy absorbed in a collision, at the time of maximum crush, based on the residual vehicle crush and a vehicle stiffness. WinSMASH then calculates ΔV from this energy estimate using momentum conservation principles (NHTSA, 1986; Prasad, 1990; Sharma et al., 2007). Recall that for side crashes, this stiffness is derived from NHTSA side crash tests using two important assumptions, both of which affect the accuracy of WinSMASH. First, WinSMASH side stiffnesses are computed using an absorbed energy value calculated by applying 1-D momentum conservation. Second, the computation of WinSMASH side stiffness assumes that MDB damage accounts for only 5% of the total energy absorption.

1-D momentum conservation is the theoretical upper limit on absorbed energy in a collision between two bodies. By treating all colliding bodies as point masses, it constrains the crash impulse to act through both vehicle CGs, resulting in the maximum potential ΔV for any given impact speed (Brach and Brach, 2005). For a fixed impact speed, collisions between two bodies where the crash impulse is not collinear with one or more CGs will result in a smaller ΔV,

and thus a smaller change in kinetic energy. The vehicle CGs in NHTSA crash tests – and in many real-world crashes – are not in general collinear with the crash impulse, so the absorbed energy in such tests will invariably be less than what is predicted by 1-D momentum conservation. Figure 36, which compares the energy absorption predicted by 1-D momentum conservation to the value actually measured from the test data at maximum crush, confirms this for the tests used in this study.

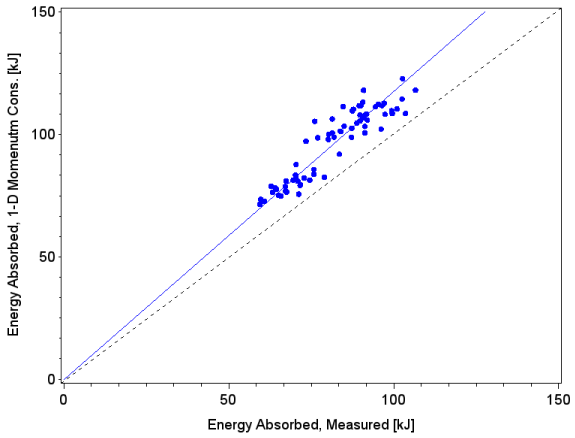

Figure 36. Total absorbed energy, 1-D momentum conservation versus measured at maximum crush. Regression equation: y = 1.175x

Additionally, WinSMASH side stiffness computation assumes that the MDB accounts for 5% of the total absorbed energy. Prasad (1991a) made this assumption out of necessity, as at the time little was known about the dynamic crush-energy relationship of the NHTSA MDB face. Since the Prasad (1991a) paper, the NHTSA has conducted several frontal-barrier tests of the NHTSA MDB. Struble et al. (2001) used these tests to compute the MDB stiffness values used in this study. WinSMASH continues to use side stiffness values computed assuming 5% energy absorption in the MDB. This may not be the case for the NHTSA side crash tests examined here. On average, WinSMASH computes that the MDB absorbs 13.6% of the total absorbed energy, with a minimum of 2.49% and a maximum of 49.1%. Even compared with the WinSMASH

prediction of total absorbed energy which are likely high, the fraction of the energy absorbed by the MDB (using the MDB stiffness reported by Struble) is still almost three times the 5% assumed when calculating WinSMASH side stiffnesses.

Because of these two effects, it is likely that the vehicle stiffnesses used by WinSMASH correlate an artificially high amount of energy to a given amount of crush. Figure 33 confirms that WinSMASH is over-estimating the total amount of energy absorbed in the studied crash tests. For the tests examined, WinSMASH over-predicts the amount of energy absorbed in the collision by 43% on average. By itself, Figure 33 could be attributed equally well to high vehicle stiffness or to high MDB stiffness, since the energies predicted by both are summed to obtain the total absorbed energy. However, when the same WinSMASH reconstructions are run with the MDB energy specified as 5% of the total, or 0.05/0.95 of the WinSMASH-predicted vehicle energy, the observed over-prediction of ΔV still persists. Figure 37 and Figure 38 compare the vehicle and MDB ΔV predicted by WinSMASH to the ΔV measured at separation, and Figure 39 and Figure 40 show analogous plots comparing to ΔV measured at max crush.

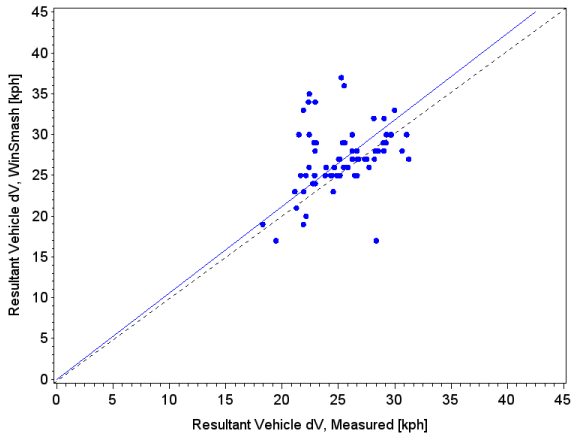

Figure 37. WinSMASH vehicle ΔV versus measured ΔV at separation, with MDB energy as 5% of total. Regression equation: y = 1.059x

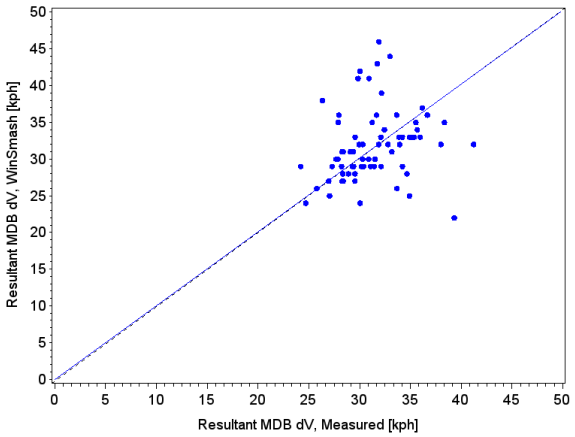

Figure 38. WinSMASH MDB ΔV versus measured ΔV at separation, with MDB energy as 5% of total. Regression equation: y = 1.004x

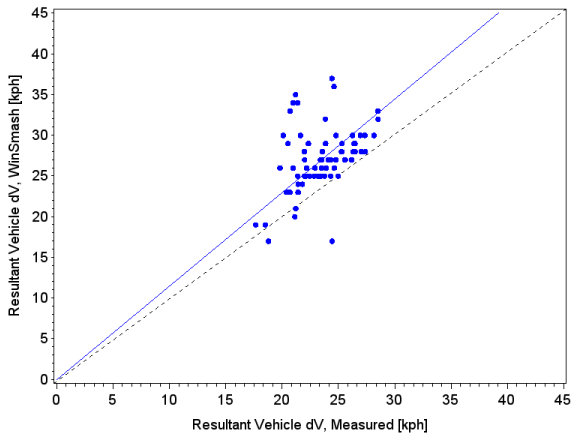

Figure 39. WinSMASH vehicle ΔV versus measured ΔV at max crush, with MDB energy as 5% of total. Regression equation: $y = 1.148x$

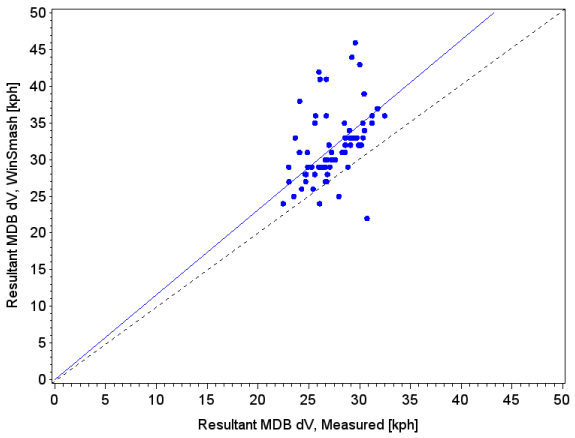

Figure 40. WinSMASH MDB ΔV versus measured ΔV at max crush, with MDB energy as 5% of total. Regression equation: $y = 1.158x$

Given that the observed effect of restitution in the examined tests is 8% for vehicles and 14% for MDBs, WinSMASH should under-predict vehicle ΔV and MDB ΔV by these amounts at separation since it does not account for restitution. However, even when cases are reconstructed assuming that MDB damage contributes 5% of the total absorbed energy, which is the same assumption used when calculating vehicle stiffnesses, this is not the case. Vehicle ΔV at separation is over-predicted by 5.9% instead of under-predicted by 8%, and MDB ΔV shows no under-prediction at all, instead of 15% under-prediction. Comparing the WinSMASH-reconstructed ΔV to the measured ΔV at max crush, the masking effect of restitution is removed. Vehicle ΔV is over-predicted by 15% on average, and MDB ΔV is over-predicted by 16% on average when there should be no systemic discrepancy at all. Thus, the energy predicted by the vehicle stiffness alone is sufficient to cause WinSMASH to over-predict ΔV in side crash test reconstructions.

These results suggest that during the computation of WinSMASH side stiffness values, both the total amount of energy absorbed in the crash, and the fraction absorbed by the struck vehicle are over-estimated. Careful comparison of Figure 33 and Figure 36 reinforces the notion that both effects are at work. Consider that the systemic difference between the energies

predicted by 1-D momentum conservation and those calculated from test data is only 17% (Figure 36), while Figure 33 indicates that the net over-prediction of energy by WinSMASH is 45%. If the MDB did indeed absorb 5% of the total crash energy, then the only energy over-prediction would be a result of correlating stiffnesses to 1-D momentum conservation. Figure 33 would then show roughly 18% over-prediction of energy, as opposed to the 45% which it actually indicates.

The vehicle crush measurements used in reconstructions also affect WinSMASH's absorbed energy estimations, but it is far less likely that they would cause the observed systemic error. Errors in crush measurement would have to be systemically high. Any errors in post-test crush measurements would be more likely to randomly distributed given that they are recorded at different times and by different test houses. More convincingly, many of the crush profiles for the crash tests in this study were used to calculate the very stiffnesses which WinSMASH used to reconstruct these selfsame tests, in which case it would be highly unlikely for these measurements to be systemically high.

Whichever the cause, Figure 34 and Figure 35 show that much of the observed error in the WinSMASH-reconstructed ΔV is eliminated when the correct value for absorbed energy is used to reconstruct the test. The WinSMASH ΔVs in Figure 34 and Figure 35 were generated using a specially modified version of WinSMASH which bypasses the crush/stiffness model and accepts a value for absorbed energy directly. Using this version of WinSMASH, the tests were reconstructed with the amount of absorbed energy calculated from the crash test data at maximum crush. Not only does this eliminate almost all of the systemic over-prediction of ΔV, but the case-to-case variation is drastically reduced as well. Taken together, the results of Figure 27 through Figure 35 indicate that, excluding other confounding factors such as PDOF, damage

offset and restitution, WinSMASH's ability to accurately reconstruct ΔV in NHTSA side crash tests is highly dependent on its ability to accurately estimate the amount of energy absorbed in the collision.

5.5.1 LIMITATIONS

The dataset examined in this study consists overwhelmingly of car body types, e.g. 2-door and 4-door sedans and hatchbacks. Other authors (Hampton and Gabler, 2010; Niehoff and Gabler, 2006) have found substantial differences in WinSMASH accuracy between different vehicle body types. In light of this, without adding substantially more tests of LTVs (Light Trucks and Vans) no conclusions can reasonably be drawn regarding WinSMASH accuracy in crash tests involving different body styles.

This study also assumes that MDB absorbed energy is well described by the Struble et al. (2001) stiffness. Struble's calculations used the only source of crash test data available for the NHTSA MDB – rigid barrier tests. The MDB ΔVs in these tests were 44.9 km/h and 59.1 km/h (separation) and the average crush depths (across the entire MDB face at bumper level) were 24.3 cm and 32.2 cm respectively. These crush and ΔV values are substantially more severe than the values in the NHTSA side crash tests examined in this study. Mean MDB ΔV at separation was 31.4 km/h (minimum 24.2 km/h, maximum 41.2 km/h), and mean average crush depth was 8.23 cm (min 1.67 cm, maximum 17.8 cm). The crush patterns themselves are also radically different – the rigid barrier tests have essentially uniform crush across the entire height and depth of the barrier face, while the side crash tests produce damage almost exclusively at bumper level. There is also evidence that the MDB face may have actually crushed completely and bottomed out in the rigid barrier tests. Thus, the Struble et al. (2001) MDB stiffness may not characterize

energy absorption by the MDB face well at the lower crush values seen in NHTSA side crash tests.

Our absorbed energy estimates could be improved if lower-severity MDB tests were available. However, it is important to note that of the three stiffnesses presented in Chapter 4, the Struble et al. (2001) stiffness has the lowest d_0 value. At low crush values such as are observed for the MDBs in the tests examined here, d_0 has by far the largest influence over the energy predicted. In effect, the Struble et al. (2001) stiffness gives the lowest predictions of energy absorbed by the MDB, yet WinSMASH is still observed to over-predict ΔV and total absorbed energy. Furthermore, the analysis described in Figure 37 through Figure 40 show that the vehicle stiffness alone is sufficient to cause observable over-prediction of ΔV by WinSMASH. So, if the absorbed energy predictions for the MDB damage are in error, our observations remain qualitatively the same and are only changed in degree.

Another limitation of this study is that all comparisons were made at only two closing speeds, both of which represent the extreme of severity in real-world crashes. Whether the findings of this study are also true at lower, more representative impact speeds could not be evaluated.

Finally, there are the assumptions and approximations made to facilitate WinSMASH reconstructions of the crash tests. PDOF can be a substantial source of error in the WinSMASH reconstructions of real-world crashes (Brach and Brach, 2005; Smith and Noga, 1982a). The sensitivity of a reconstruction to PDOF error depends on the exact collision configuration, and the direction of the error. As an example, for the 70 cases examined here increasing all PDOFs by 20° causes WinSMASH to reconstruct vehicle ΔVs 11% lower on average (standard deviation

2.14%). Decreasing all PDOFs by the same amount results in vehicle ΔV estimations that are 0.557% lower on average with a standard deviation of 4.05%.

With crash tests however, PDOF can be readily computed and had no effect on our estimates of WinSMASH error. However, reliance on an approximated radius of gyration for the struck vehicles could potentially have some effect on the fidelity of reconstructions, both directly and via its use in calculating damage offset. Our reconstructions are also dependent on the crush measurements recorded in the crash test reports. In particular, the overall length of the damaged region spanned by the 6-point crush profile is difficult to define consistently at times.

6 CONCLUSIONS

WinSMASH damage-only reconstructions are the source of all ΔV estimates in the NASS/CDS. NASS/CDS ΔV estimates are the basis for much of the safety policy produced by the NHTSA, including crash test speeds, countermeasure effectiveness requirements, and the development of injury criteria. The accuracy of WinSMASH ΔV estimates therefore has a direct impact on motor vehicle safety regulation in the United States.

This thesis examined WinSMASH accuracy in side crash reconstruction. ΔVs in side crash tests were reconstructed using WinSMASH and compared to ΔVs determined from test instrumentation. This thesis used crash tests because they are highly controlled and provide ample data with which to determine ΔV. By contrast, real-world crashes recorded in databases such as the NASS/CDS as a general rule do not provide enough information to generate a reliable estimate of ΔV independent of WinSMASH.

The dataset for the study consists of 70 MDB – to – vehicle side crash tests run by the NHTSA. Exactly 40% of the tests were FMVSS 214D compliance tests (33.5 mph nominal impact speed), with the remaining 60% being Side NCAP tests (38.5 mph nominal impact speed). Tested vehicles were primarily car body styles from production years 1994-2006. Observed struck vehicle ΔVs (at separation) were typically on the order of 25 kph, while MDB ΔVs at the same time were typically closer to 30 kph. Observed yaw velocities at vehicle separation were typically on the order of 100 deg/s for both vehicles and MDBs.

Crucial to the reconstruction of side crash tests are accurate estimates of the energy absorbed by MDB damage. Chapter 4 compared two approaches for estimating this energy: integration of quasi-static crush strength over damaged volume, and the use of WinSMASH stiffnesses derived from MDB frontal barrier tests. Based on the very limited crash test data

available for the NHTSA MDB, integration of quasi-static crush strength over static crush volume may potentially under-estimate absorbed energy. Of the three NHTSA MDB WinSMASH stiffness examined, the stiffness reported by Struble et al. (2001) appears to give the best agreement with the observed crush-energy curves.

This study investigated the accuracy of WinSMASH ΔV estimates in the reconstructions of the 70 NHTSA side crash tests. WinSMASH was found to over-predict struck vehicle resultant ΔV by 12% at time of separation, and by 22% at time of maximum crush. A similar pattern was observed for the MDB ΔV; WinSMASH over-predicted resultant MDB ΔV by 6.6% at separation, and by 23% at maximum crush. Error in user-estimated reconstruction parameters, namely PDOF error and damage offset, was controlled for in this analysis.

Restitution was observed to increase struck vehicle ΔV by 8% in the examined cases and MDB ΔV by 14%. WinSMASH assumes zero restitution, and therefore actually predicts ΔV at max crush. WinSMASH should therefore under-predict struck vehicle resultant ΔV at separation by 8%, and be in agreement with the observed ΔV at max crush. MDB ΔV should be under-predicted by 14% at separation, and also in agreement at maximum crush.

The difference between the expected results and the observed results appears to stem from an overestimation of the energy absorbed by struck vehicle damage. WinSMASH was found to over-predict the total energy absorbed in NHTSA side crash tests by 45%. When the same side crash tests are reconstructed in WinSMASH using the correct amount of absorbed energy, (and PDOF and damage offset error are controlled for), there is no systemic difference between WinSMASH ΔV and measured ΔV at max crush. This indicates that over-prediction of total energy causes the over-prediction of ΔV. Additionally, when tests are reconstructed assuming that the MDB damage accounts for 5% of the total absorbed energy, which is the same

assumption used in calculating WinSMASH vehicle side stiffness coefficients, WinSMASH still over-predicts ΔV. This shows that the vehicle stiffnesses alone are capable of causing the absorbed energy to be over-predicted. These results also indicate that, if given correct reconstruction parameters, WinSMASH is capable of accurately reconstructing NHTSA side crash tests.

6.1 SUGGESTIONS FOR IMPROVEMENT OF WINSMASH

This study shows that given accurate reconstruction parameters, WinSMASH is capable of accurately reconstructing NHTSA side crash tests. However, the over-prediction of absorbed energy by the currently used vehicle side stiffnesses is resulting in over-prediction of total ΔV at separation, which is the parameter of interest to the users of WinSMASH. While error from WinSMASH's assumption of zero restitution is partly masking this effect to some extent, this is a less than ideal situation. The over-prediction of absorbed energy by WinSMASH side stiffnesses will be relatively consistent, but the degree of masking by restitution depends on the coefficient of restitution in the reconstructed collision, and this is variable.

Supplying WinSMASH with side stiffnesses that correlate the correct amount of absorbed energy to vehicle damage should correct the observed over-prediction of absorbed energy. However, by itself this improvement will result in under-prediction of ΔV at separation. One might then argue that over-prediction of absorbed energy is acceptable, provided that it balances the under-prediction of total ΔV at separation due to assuming zero restitution. While this could conceivably be done for a single collision configuration, it is unlikely to be practical for real-world collisions of varied (and, to an extent, less well known) collision configurations. In practice the difference in absorbed energy between max crush and separation is frequently not discernable via test instrumentation. Furthermore, different collision configurations also result in

different coefficients of restitution even when the same vehicles are involved, but one stiffness parameter cannot correctly compensate for more than one value of coefficient of restitution.

It is therefore suggested that, in addition to using correctly correlated side stiffnesses, WinSMASH also be modified to utilize coefficients of restitution in its ΔV calculations, if it can practicably be done. The necessary modifications to the WinSMASH calculations to incorporate restitution have been known for some time, but they have never been implemented. Restitution modeling in vehicle crashes has been studied for some time, but there remains much work to be done. However, the same NHTSA side crash tests from which WinSMASH side stiffness parameters are calculated might also be used provide empirical coefficients of restitution for use by WinSMASH. There is sufficient instrumentation in these crash tests to compute restitution coefficients, and the WinSMASH stiffness database provides a means for WinSMASH to store them and access them. This would of course only provide coefficients for a single collision configuration involving an MDB, but future work may provide ways to estimate or extrapolate coefficient of restitution for different collision types, providing better estimates.

6.2 IMPLICATIONS FOR CRASH SAFETY

If the observed over-prediction of ΔV in side crash tests involving cars can be generalized to real-world side crashes of similar configurations, then there is reason to suspect that NASS/CDS ΔVs for such side crashes are over-predicted. Any injury risk curves for side crashes based on this NASS/CDS data would then project risk onto higher ΔVs than what is actually the case. In effect, NASS/CDS data may potentially be under-predicting true injury risk in side crashes involving cars.

7 REFERENCES

Arbelaez RA, Baker BC and Nolan JM (2005), "Delta Vs for Side Impact Crash Tests and their Relationship to Real-World Crash Severity," *Proc. 19th International Technical Conference on the* Enhanced *Safety of Vehicles*, Paper No. 05-0049.

Bahouth GT, Digges KH, Bedewi NE, Kuznetsov A, Augenstein JS and Perdeck E (2004), "Development of URGENCY 2.1 for the Prediction of Crash Injury Severity," *Topics in Emerging Medicine*, Vol. 26, No. 2, pp 157-165.

Brach RM and Brach RM (2005), Vehicle Accident Analysis and Reconstruction Methods, ISBN 0-7680-0776-3, SAE International.

Campbell K (1974), "Energy Basis for Collision Severity," SAE 740565, Society of Automotive Engineers.

Gabauer DJ and Gabler HC (2008), "Comparison of Roadside Crash Injury Metrics using Event Data Recorders," *Accident Analysis and Prevention*, vol. 40, issue 2, pp 548-558.

Hampton CE and Gabler HC (2010), "Evaluation of the Accuracy of NASS/CDS Delta-V Estimates from the Enhanced WinSMASH Algorithm," *Proceedings of the 54th Annual AAAM Conference*.

Hexcel Corporation (2005), "HexWeb® Honeycomb Energy Absorption Systems," Hexcel Corporation, accessed 7/9/2010, available URL; http://www.hexcel.com/Products/Downloads/Brochures/.

Hong S, Pan J, Tyan T and Prasad P (2008), "Dynamic Crush Behaviors of Aluminum Honeycomb Specimens under Compression Dominant Inclined Loads," *International Journal of Plasticity*, Vol. 24, pp. 89-117.

Ishikawa H (1994), "Impact Center and restitution Coefficients for Accident Reconstruction," SAE 940564, Society of Automotive Engineers.

Johnson N, Hampton CE and Gabler HC (2009), "Evaluation of the Accuracy of Side Impact Crash Test Reconstructions," *Biomedical Sciences Instrumentation* 45: pp. 250-255.

Lenard J, Hurley B and Thomas P (1998), "The Accuracy of CRASH3 for Calculating Collision Severity in Modern European Cars," *Proceedings of the 16th International Technical Conference on the Enhanced Safety of Vehicles*, Paper No. 98-S6-O-08.

Marine MC and Werner SM (1998), "Delta-V Analysis from Crash Test Data for Vehicles with Post-Impact Yaw Motion," SAE 980219, Society of Automotive Engineers.

NHTSA (1986), *CRASH3 Technical Manual*, Accident Investigation Division, N.C.S.A., National Highway Traffic Safety Administration.

NHTSA (1998), *Vehicle Measurement Techniques (draft)*, National Highway Traffic Safety Administration.

NHTSA (2006), *Laboratory Test Procedure for FMVSS No. 214 "Dynamic" Side Impact Protection*, National Highway Traffic Safety Administration, Document # TP214D-08.

NHTSA (2008), *Laboratory Test Procedure for New Car Assessment Program Side Impact Moving Deformable Barrier Testing*, National Highway Traffic Safety Administration, rev. September 2008.

Niehoff P and Gabler HC (2006), "The Accuracy of WinSMASH Delta-V Estimates: The Influence of Vehicle Type, Stiffness, and Impact Mode," *Proceedings of the 50th Annual AAAM Conference*.

Ott RL and Longnecker M (2001), An Introduction to Statistical Methods and Data Analysis, 5th edition, ISBN 0-534-25122-6, section 12.7, pp. 670 to 674, Wadsworth Group.

Prasad AK and Monk MW (1990), "CRASH3 Damage Algorithm Reformulation, " Report No. VRTC-87-0053, Vol. I & II, National Highway Traffic Safety Administration.

Prasad AK (1990), "CRASH3 Damage Algorithm Reformulation for Front and Rear Collisions," SAE 900098, Society of Automotive Engineers.

Prasad AK (1991), "Energy Absorbed by Vehicle Structures in Side-Impacts," SAE 910599, Society of Automotive Engineers.

Prasad AK (1991), "Coefficient of Restitution of Vehicle Structures and its use in Estimating the Total ΔV in Automobile Collisions," AMD Vol 126/BED Vol 19, Crashworthiness and Occupant Protection in Transportation Systems, ASME, New York, NY.

Rose NA, Fenton SJ and Beauchamp G (2006), "Restitution Modeling for Crush Analysis: Theory and Validation," SAE 2006-01-0908, Society of Automotive Engineers.

Rose NA, Fenton SJ and Ziernicki RM (2004), "An Examination of the CRASH3 Effective Mass Concept," SAE 2004-01-1181, Society of Automotive Engineers.

Siddall DE and Day TD (1996), "Updating the Vehicle Class Categories," SAE 960897, Society of Automotive Engineers.

Sharma D, Stern S, Brophy J and Choi E (2007), "An Overview of NHTSA's Crash Reconstruction Software WinSMASH," *Proceedings of the 20th International Technical Conference on Enhanced Safety of Vehicles*, Paper No. 07-0211.

Smith RA and Noga JT (1982a), "Accuracy and Sensitivity of CRASH," SAE 821169, Society of Automotive Engineers.

Smith RA and Noga JT (1982b), "Accuracy and Sensitivity of CRASH," National Highway Traffic Safety Administration, report DOT-HS-806-152.

Strother CE, Kent RW and Warner CY (1998), "Estimating Vehicle Deformation Energy for Vehicles Struck in the Side," SAE 980215, Society of Automotive Engineers.

Struble DE, Walsh KJ and Struble JD (2001), "Side Impact Structural Characterization from FMVSS 214D Test Data," SAE 2001-01-0122, Society of Automotive Engineers.

Trella TJ, Samaha RR, Fleck JJ and Strassburg G (2000), "A Moving Deformable Barrier with Dynamic Force and Deflection Spatial Measurement Capabilities for Full Scale Tests," SAE 2000-01-0637, Society of Automotive Engineers.

Willke DT and Monk MW (1987), *CRASH III Model Improvements: Derivation of New Side Stiffness Parameters from Crash Tests, Volume 2*, National Highway Traffic Safety Administration.

Woolley RL, Warner CY and Tagg MD (1985), “Inaccuracies in the CRASH3 Program,” SAE 850255, Society of Automotive Engineers.

APPENDIX A: COMPARISON OF CRASH3 AND WINSMASH

While the core calculations in CRASH3 and WinSMASH are substantially the same, there are key differences that bear mention. CRASH3 used a correction factor for estimating energy dissipated by vehicle crush that was not made normal to the vehicle surface (crush being measured normal to the vehicle surface). A number of researchers (Smith and Noga, 1982a, 1982b; Woolley et al, 1985; Strother et al, 1998) have expressed contentions about this correction factor. Prasad and Monk (1990) found that the removal of this factor resulted in a substantial reduction in ΔV error. SMASH and subsequently WinSMASH therefore retained this correction factor only as an option.

The vehicle stiffness parameters used by CRASH3 and WinSMASH are also different. CRASH3 categorized vehicles into one of 9 categories based on wheelbase and body type, and then applied a vehicle stiffness derived from a test of one or possibly a handful of vehicles taken to represent that particular category. These categories were updated once when CRASH3 was fitted with a GUI to become SMASH in the early 1990s (Sharma 2007). Because these stiffnesses were based on vehicles from the 1990's and earlier, they also cannot be assumed to represent the present vehicle fleet.

By contrast, WinSMASH uses stiffness parameters specific to a given vehicle when such parameters are available in its database, and fills in any missing stiffnesses with categorical stiffnesses from one of 12 categories which are based on the current fleet. The switch to vehicle-specific stiffnesses occurred after a paper published by Niehoff and Gabler (2006) found that vehicle-specific stiffnesses reduced bias in WinSMASH results by 5%.

Additionally, the current version of WinSMASH contains many corrections for programming errors which had accumulated since over the long history of the code's development.

APPENDIX B: ANALYZED TESTS

GENERAL TEST INFORMATION

Table 13. Test protocol, test vehicle production year, make, model and bodystyle.

NHTSA Test #	Test Type	Year	Make	Model	Bodystyle
2096	FMVSS	1994	MITSUBISHI	GALANT	4S
2118	FMVSS	1995	MAZDA	MILLENIA	4S
2119	FMVSS	1995	NISSAN / DATSUN	810/MAXIMA	4S
2218	FMVSS	1995	FORD	THUNDERBIRD (ALL SIZES)	2S
2410	FMVSS	1996	HYUNDAI	SONATA	4S
2435	FMVSS	1996	KIA	SEPHIA	4S
2720	FMVSS	1998	SUBARU	LEGACY	4S
2721	FMVSS	1998	TOYOTA	COROLLA	4S
2722	FMVSS	1998	TOYOTA	CAMRY	4S
2762	FMVSS	1998	NISSAN / DATSUN	810/MAXIMA	4S
2977	FMVSS	1999	HONDA	ACCORD	4S
3000	FMVSS	1999	FORD	WINDSTAR	VN
3036	FMVSS	1999	VOLKSWAGEN	NEW BEETLE	2S
3037	FMVSS	1999	TOYOTA	SIENNA	VN
3059	FMVSS	1999	HYUNDAI	ELANTRA	4S
3200	FMVSS	2000	NISSAN / DATSUN	DATSUN/NISSAN PU/FRONTIER	PU
3201	FMVSS	2000	NISSAN / DATSUN	810/MAXIMA	4S
3202	FMVSS	2000	BUICK	LESABRE/CENTURION/WILDCAT	4S
3341	FMVSS	2000	FORD	FOCUS	3H
3559	FMVSS	2001	KIA	SPECTRA	4S
3569	FMVSS	2001	KIA	OPTIMA	4S
3572	FMVSS	2001	VOLVO	60 SERIES	4S
3744	FMVSS	2001	HYUNDAI	ACCENT	4S
4197	FMVSS	2002	FORD	F-SERIES PICKUP	PU
4221	FMVSS	2003	HYUNDAI	TIBURON	2S
4256	FMVSS	2002	MITSUBISHI	LANCER	4S
5460	FMVSS	2005	SATURN	ION	4S
5475	FMVSS	2004	HONDA	ACCORD	4S
2479	NCAP	1997	HONDA	ACCORD	4S
2480	NCAP	1997	FORD	THUNDERBIRD (ALL SIZES)	2S
2508	NCAP	1997	SUBARU	LEGACY	4S
2509	NCAP	1997	PONTIAC	GRAND AM	4S
2510	NCAP	1997	MAZDA	626	4S
2516	NCAP	1997	TOYOTA	CAMRY	4S
2519	NCAP	1997	NISSAN / DATSUN	810/MAXIMA	4S

2520	NCAP	1997	CHEVROLET	LUMINA	4S
2523	NCAP	1997	CADILLAC	DEVILLE/FLEETWOOD	4S
2525	NCAP	1997	VOLVO	850	4S
2686	NCAP	1997	FORD	MUSTANG/MUSTANG II	2S
2715	NCAP	1998	DODGE	NEON	4S
2728	NCAP	1998	TOYOTA	COROLLA	4S
2737	NCAP	1998	TOYOTA	AVALON	4S
2753	NCAP	1998	OLDSMOBILE	INTRIGUE	4S
2768	NCAP	1998	NISSAN / DATSUN	SENTRA	4S
2957	NCAP	1999	TOYOTA	COROLLA	4S
2958	NCAP	1999	TOYOTA	CAMRY	4S
2999	NCAP	1999	DODGE	INTREPID	4S
3011	NCAP	1999	TOYOTA	SIENNA	VN
3193	NCAP	2000	HONDA	ACCORD	4S
3203	NCAP	2000	DODGE	NEON	4S
3291	NCAP	2000	BUICK	LESABRE/CENTURION/WILDCAT	4S
3363	NCAP	2001	CHRYSLER	PT CRUISER	4S
3474	NCAP	2001	NISSAN / DATSUN	810/MAXIMA	4S
3478	NCAP	2000	KIA	SEPHIA	4S
3515	NCAP	2001	MITSUBISHI	GALANT	4S
3531	NCAP	2001	MAZDA	MILLENIA	4S
3550	NCAP	2001	HYUNDAI	ACCENT	4S
3795	NCAP	2001	VOLVO	60 SERIES	4S
3951	NCAP	2002	MITSUBISHI	LANCER	4S
4222	NCAP	2002	SUZUKI	X-90/VITARA	UV
4602	NCAP	2003	SATURN	ION	4S
4619	NCAP	2003	SAAB	9 - 5	4S
4658	NCAP	2003	HYUNDAI	ACCENT	4S
4728	NCAP	2003	HONDA	ACCORD	4S
4868	NCAP	2004	HYUNDAI	TIBURON	2S
4889	NCAP	2004	SUZUKI	AERIO	4S
4928	NCAP	2004	TOYOTA	CAMRY	4S
5115	NCAP	2005	FORD	FOCUS	3H
5260	NCAP	2005	SATURN	ION	4S
5849	NCAP	2006	KIA	OPTIMA	4S

STRUCK VEHICLE PARAMETERS

Table 14. Struck vehicle PDOF, mass, radius of gyration, damage length, maximum crush and average crush.

NHTSA Test #	PDOF [deg]	Mass [kg]	Radius of Gyration [cm]	Damage Offset [cm]	Damage Length [cm]	Maximum Crush [cm]	Average Crush [cm]
2096	287	1469	143	-8	216	37	21.7
2118	279	1687	144	22	427	33	19.5
2119	278	1544	142	-1	427	39	21.8
2218	279	1831	150	3	472	27	20
2410	279	1557	137	5	405	40	13.7
2435	280	1319	128	-17	360	28	9.8
2479	277	1470	140	6	405	49	18
2480	280	1814	151	-23	435	48	15
2508	281	1553	137	-17	405	42	15.7
2509	282	1570	141	-37	405	40	14.7
2510	287	1424	139	2	405	43	15.7
2516	274	1601	143	5	345	38	14.5
2519	276	1618	144	-6	420	44	16.3
2520	277	1750	152	0	450	40	14.5
2523	275	2081	159	-16	495	44	17
2525	281	1723	139	8	405	31	11.3
2686	277	1606	137	-12	405	32	12.5
2715	285	1381	130	5	375	34	15
2720	281	1520	139	-4	220	32	20.7
2721	283	1332	133	12	265	28	13.7
2722	280	1655	144	-2	285	27	12
2728	283	1303	131	-36	285	38	17
2737	285	1750	144	-6	375	36	13.3
2753	282	1803	147	-21	435	41	15
2762	274	1654	145	16	405	40	12.3
2768	281	1323	128	11	310	42	19.8
2957	290	1350	132	10	390	36	13.2
2958	277	1644	143	-4	420	37	13.5
2977	283	1534	143	-4	420	32	11.2
2999	284	1765	155	-31	420	30	10.5
3000	284	2071	150	-6	315	33	15.3
3011	284	1976	146	-26	405	33	13
3036	279	1565	122	0	220	24	13
3037	281	1957	148	-8	312	24	10.8
3059	282	1436	132	27	375	35	13.7
3193	285	1619	143	18	225	35	21
3200	276	1760	152	-6	405	34	14.8
3201	284	1686	144	4	225	40	25.5
3202	280	1853	151	-8	450	34	14.8
3203	280	1377	133	0	345	36	14.7
3291	278	1866	152	10	300	39	19.7
3341	279	1390	128	13	285	29	14.3

3363	284	1692	128	6	275	22	10.5
3474	286	1644	146	-10	345	41	18.7
3478	284	1377	133	-18	315	35	18.7
3515	278	1581	143	5	330	35	16.8
3531	284	1727	146	-37	405	36	14.3
3550	286	1294	126	10	345	36	16.8
3559	280	1408	134	6	295	27	13
3569	278	1660	142	-15	369	32	14.3
3572	287	1699	137	1	375	26	9.2
3744	284	1291	125	0	345	30	11
3795	281	1740	137	-4	245	33	18.7
3951	280	1393	134	-8	375	34	13
4197	277	2342	159	-9	275	30	14.5
4221	273	1616	131	-8	330	25	12.5
4222	285	1592	121	-26	300	35	17.2
4256	277	1394	136	-16	315	32	17.5
4602	287	1469	140	-26	195	31	20.7
4619	279	1832	145	-11	310	32	15.8
4658	277	1334	128	15	255	35	23.8
4728	280	1595	145	2	255	34	22
4868	280	1543	131	-10	240	32	18.5
4889	281	1460	145	3	270	31	16.8
4928	281	1644	144	-10	320	33	14.3
5115	285	1407	129	-9	300	33	15.8
5260	283	1448	141	-15	255	28	13
5460	283	1456	140	-8	285	24	11.2
5475	283	1615	144	-1	345	31	12.3
5849	282	1665	139	-8	375	33	12.3

STRUCK VEHICLE ΔV AT MAX CRUSH

Table 15. Observed struck vehicle ΔV and yaw angle at maximum crush.

NHTSA Test #	Resultant ΔV [kph]	Longitudinal ΔV [kph]	Lateral ΔV [kph]	Yaw Velocity [deg/s]	Yaw Angle [deg]
2096	21.7	-7.0	20.5	-81.4	3.2
2118	20.7	-3.3	20.5	-31.1	-3.3
2119	21.4	-3.3	21.1	-60.6	-4.2
2218	20.1	-3.2	19.9	-34.5	-3.7
2410	21.4	-3.7	21.1	-50.1	-3.5
2435	23.6	-5.1	23.0	-110.9	-2.2
2479	25.3	-2.8	25.2	-47.8	-5.0
2480	22.4	-4.3	21.9	-78.3	-4.2
2508	24.8	-5.4	24.2	-85.7	-3.7
2509	23.9	-6.6	23.0	-151.2	-3.8
2510	26.5	-7.6	25.4	-87.8	-3.9
2516	24.6	-2.0	24.6	-34.0	-3.5
2519	23.9	-2.8	23.7	-68.8	-4.9
2520	23.3	-3.1	23.1	-61.3	-3.9
2523	20.7	-1.9	20.6	-56.4	-5.9
2525	23.5	-4.9	23.0	-52.4	-3.3
2686	24.3	-3.3	24.1	-67.8	-2.1
2715	26.4	-7.8	25.2	-101.3	-1.3
2720	22.5	-4.4	22.0	-39.4	-3.1
2721	25.0	-5.7	24.3	-41.3	-2.1
2722	21.2	-3.8	20.8	-52.8	-2.9
2728	27.0	-7.6	25.9	-165.8	-2.1
2737	23.2	-6.4	22.3	-79.9	-2.5
2753	21.2	-5.1	20.6	-97.9	-4.9
2762	21.6	-1.2	21.6	-19.3	-1.1
2768	27.4	-5.8	26.7	-64.4	-2.7
2957	28.2	-10.4	26.2	-74.8	-4.2
2958	24.1	-3.6	23.9	-61.3	-3.7
2977	22.0	-5.7	21.3	-67.2	-3.0
2999	22.1	-6.3	21.2	-116.8	-6.1
3000	18.8	-4.7	18.2	-61.4	-4.1
3011	22.0	-6.4	21.1	-102.3	-3.9
3036	21.4	-3.9	21.1	-68.0	-1.8
3037	18.5	-3.9	18.1	-52.7	-1.6
3059	22.8	-4.3	22.4	-17.8	-2.6
3193	25.6	-6.4	24.7	-41.5	-2.2

3200	20.4	-2.1	20.3	-26.2	-1.8
3201	21.0	-5.5	20.2	-61.1	-1.4
3202	19.8	-3.6	19.5	-59.1	-1.3
3203	27.4	-5.9	26.8	-85.6	-1.3
3291	23.5	-3.5	23.3	-29.8	-0.5
3341	23.4	-4.0	23.1	-26.6	-2.1
3363	24.5	-6.1	23.7	-62.8	-2.2
3474	24.6	-8.0	23.3	-89.9	-5.2
3478	26.4	-7.6	25.3	-127.0	-0.4
3515	25.3	-3.8	25.0	-49.0	-0.3
3531	23.4	-7.0	22.4	-122.7	-5.6
3550	28.5	-8.3	27.3	-73.4	-4.2
3559	23.9	-4.2	23.5	-44.1	-1.4
3569	20.5	-2.9	20.3	-73.1	-2.7
3572	21.2	-6.6	20.2	-60.0	-3.9
3744	23.8	-6.2	22.9	-81.9	-1.5
3795	24.3	-5.2	23.7	-63.7	-3.4
3951	26.2	-5.2	25.7	-91.6	-2.8
4197	17.7	-3.6	17.3	-38.5	-1.9
4221	21.0	-1.5	20.9	-69.8	-2.5
4222	25.6	-7.3	24.6	-100.8	-3.0
4256	22.0	-3.3	21.8	-86.4	-3.9
4602	26.3	-8.7	24.8	-133.0	-2.7
4619	22.9	-3.7	22.6	-72.6	-2.7
4658	28.5	-3.5	28.3	-32.3	-0.9
4728	24.4	-4.6	24.0	-58.4	-1.3
4868	25.3	-5.1	24.8	-94.9	-3.0
4889	26.5	-5.2	26.0	-46.7	-0.6
4928	24.8	-5.4	24.2	-64.8	-2.8
5115	26.3	-7.8	25.1	-134.0	-1.0
5260	27.0	-7.0	26.1	-93.1	-3.1
5460	22.2	-5.2	21.6	-75.4	-3.4
5475	21.6	-5.1	21.0	-62.6	-3.3
5849	24.3	-5.1	23.8	-85.6	-2.9

STRUCK VEHICLE ΔV AT SEPARATION

Table 16. Observed struck vehicle ΔV and yaw angle at separation.

NHTSA Test #	Resultant ΔV [kph]	Longitudinal ΔV [kph]	Lateral ΔV [kph]	Yaw Velocity [deg/s]	Yaw Angle [deg]
2096	22.7	-7.8	21.4	-85.8	9.7
2118	21.9	-5.5	21.2	-72.2	-6.6
2119	23.0	-5.2	22.3	-86.4	-7.3
2218	21.5	-3.7	21.2	-75.5	-8.5
2410	21.7	-6.0	20.8	-69.3	-9.2
2435	26.2	-5.5	25.6	-123.2	-5.2
2479	25.6	-4.0	25.3	-74.3	-6.4
2480	23.0	-4.9	22.5	-90.9	-5.5
2508	26.2	-6.9	25.3	-115.9	-6.6
2509	27.7	-8.2	26.5	-195.9	-4.2
2510	28.3	-10.9	26.1	-102.7	-13.2
2516	25.8	-2.3	25.7	-4.8	-7.8
2519	25.4	-5.7	24.7	-106.4	-8.4
2520	23.8	-8.1	22.4	-106.1	-13.5
2523	21.2	-6.1	20.3	-85.7	-15.6
2525	25.5	-8.3	24.1	-91.6	-8.9
2686	26.5	-7.0	25.5	-88.1	-6.2
2715	29.2	-10.2	27.4	-107.8	-4.2
2720	24.3	-7.3	23.2	-57.4	-9.4
2721	26.7	-5.7	26.0	-62.8	-3.1
2722	22.1	-5.1	21.5	-50.8	-7.7
2728	29.7	-8.1	28.5	-202.0	-3.3
2737	24.9	-7.9	23.6	-93.4	-4.7
2753	22.4	-6.6	21.4	-117.4	-6.8
2762	23.0	-0.8	22.9	-36.1	-1.8
2768	29.3	-9.1	27.8	-107.5	-6.1
2957	31.1	-10.8	29.1	-92.9	-6.6
2958	26.8	-6.2	26.1	-72.8	-16.5
2977	25.1	-7.4	24.0	-62.2	-10.8
2999	22.9	-11.3	19.9	-113.8	-20.8
3000	19.5	-5.3	18.7	-71.5	-12.2
3011	22.1	-6.5	21.2	-108.7	-5.2
3036	24.6	-5.2	24.0	-74.8	-4.7
3037	21.9	-4.5	21.4	-43.8	-3.1
3059	24.4	-4.8	23.9	-23.0	-7.7
3193	31.3	-9.6	29.8	-53.5	-9.1

3200	21.9	-7.1	20.8	-56.8	-10.7
3201	22.4	-8.1	20.8	-90.9	-4.1
3202	23.9	-5.3	23.3	-47.8	-2.9
3203	30.7	-9.1	29.3	-123.9	-3.0
3291	26.2	-8.4	24.9	-80.2	-3.1
3341	26.7	-5.0	26.2	-40.0	-6.2
3363	28.4	-7.5	27.4	-86.6	-5.0
3474	25.5	-10.0	23.5	-107.6	-11.1
3478	29.1	-13.0	26.1	-170.9	-1.5
3515	29.0	-7.0	28.2	-65.7	-1.2
3531	24.9	-10.8	22.4	-122.4	-15.5
3550	29.1	-9.3	27.5	-106.2	-5.3
3559	28.2	-4.9	27.7	-42.3	-5.6
3569	22.8	-3.6	22.6	-81.5	-3.5
3572	21.3	-6.5	20.3	-59.6	-4.1
3744	25.2	-6.7	24.2	-103.7	-2.0
3795	25.0	-5.2	24.5	-51.5	-7.5
3951	27.5	-5.3	27.0	-104.9	-5.8
4197	18.3	-7.6	16.7	-81.3	-11.5
4221	22.4	-3.9	22.1	-60.7	-8.6
4222	28.2	-13.5	24.8	-120.3	-10.1
4256	22.9	-3.1	22.7	-89.0	-5.1
4602	29.7	-10.6	27.7	-158.1	-6.2
4619	24.7	-8.2	23.3	-106.0	-8.1
4658	30.0	-4.1	29.7	-23.3	-2.8
4728	25.3	-4.7	24.8	-73.8	-1.7
4868	28.6	-5.8	28.0	-125.7	-4.8
4889	29.0	-5.9	28.4	-63.0	-1.9
4928	27.3	-6.9	26.4	-81.1	-5.7
5115	26.7	-8.4	25.3	-146.7	-1.1
5260	29.1	-8.4	27.8	-88.3	-7.5
5460	24.6	-6.4	23.8	-65.9	-9.9
5475	22.4	-5.1	21.8	-71.0	-4.3
5849	26.2	-7.7	25.1	-77.8	-9.3

MDB PARAMETERS

Table 17. MDB PDOF, mass, radius of gyration, damage length, maximum crush and average crush. MDB PDOF is that used in WinSMASH reconstructions, not that measured from the test data.

NHTSA Test #	PDOF [deg]	Mass [kg]	Radius of Gyration [cm]	Damage Offset [cm]	Damage Length [cm]	Maximum Crush [cm]	Average Crush [cm]
2096	17	1356	138	18	168	10	2.3
2118	9	1356	138	-12	168	8	2.3
2119	8	1356	138	11	168	6	2.5
2218	9	1356	138	7	168	13	5.2
2410	9	1356	138	5	168	8	3.8
2435	10	1356	138	27	168	15	7.5
2479	7	1356	138	4	168	10	4.7
2480	10	1356	138	33	168	19	7.5
2508	11	1356	138	27	168	17	8.7
2509	12	1356	138	47	168	13	8.3
2510	17	1356	138	8	168	15	7.5
2516	4	1356	138	5	168	19	12.2
2519	6	1356	138	16	168	9	5.3
2520	7	1356	138	11	168	16	9.3
2523	5	1356	138	26	168	10	7.3
2525	11	1356	138	2	168	18	14
2686	7	1356	138	22	168	18	10.5
2715	15	1356	138	5	168	12	6.5
2720	11	1356	138	15	168	10	5
2721	13	1356	138	-2	168	8	4.7
2722	10	1356	138	12	168	14	6.5
2728	13	1356	138	46	168	12	8.3
2737	15	1356	138	17	168	13	9.8
2753	12	1356	138	32	168	12	6.2
2762	4	1356	138	-6	168	6	1.7
2768	11	1356	138	-1	168	14	7.5
2957	20	1356	138	0	168	13	9.2
2958	7	1356	138	14	168	16	10.3
2977	13	1356	138	14	168	17	9.2
2999	14	1356	138	41	168	14	10.7
3000	14	1356	138	25	168	6	4.2
3011	14	1356	138	36	168	20	16.3
3036	9	1356	138	10	168	11	5.7
3037	11	1356	138	16	168	13	11.3
3059	12	1356	138	-17	168	9	6.2
3193	15	1356	138	-7	168	23	13.8
3200	6	1356	138	19	168	8	5.3
3201	14	1356	138	7	168	9	2.5
3202	10	1356	138	18	168	11	6.2
3203	10	1356	138	10	168	15	9
3291	8	1356	138	-9	168	21	12.3
3341	9	1356	138	-2	168	10	7.2

3363	14	1356	138	5	168	19	16.5
3474	16	1356	138	20	168	12	7.7
3478	14	1356	138	25	168	26	17.8
3515	8	1356	138	5	168	24	12.5
3531	14	1356	138	47	168	20	6.2
3550	16	1356	138	2	168	12	8.3
3559	10	1356	138	4	168	17	9.8
3569	8	1356	138	26	168	8	4.5
3572	17	1356	138	9	168	12	7.5
3744	14	1356	138	10	168	11	7.7
3795	11	1356	138	18	168	18	10.8
3951	10	1356	138	15	168	17	11
4197	7	1356	138	27	168	3	2
4221	3	1356	138	17	168	11	8.5
4222	15	1356	138	37	168	10	6
4256	7	1356	138	26	168	12	3.2
4602	17	1356	138	34	168	19	11.2
4619	9	1356	138	22	168	20	11
4658	7	1356	138	-8	168	17	12.2
4728	10	1356	138	9	168	23	14.3
4868	10	1356	138	19	168	17	11
4889	11	1356	138	9	168	21	13
4928	11	1356	138	21	168	14	9.2
5115	15	1356	138	21	168	17	11
5260	13	1356	138	25	168	14	9.7
5460	13	1356	138	18	168	13	6.7
5475	13	1356	138	10	168	11	6
5849	12	1356	138	18	168	12	6.3

MDB ΔV AT MAX CRUSH

Table 18. Observed MDB ΔV and yaw angle at maximum crush.

NHTSA Test #	Resultant ΔV [kph]	Longitudinal ΔV [kph]	Lateral ΔV [kph]	Yaw Velocity [deg/s]	Yaw Angle [deg]
2096	23.3	-22.7	-5.1	119.2	-2.1
2118	26.1	-25.2	-6.7	-93.5	-0.4
2119	24.1	-23.4	-6.0	-107.1	-1.0
2218	26.7	-25.0	-9.5	-145.1	0.2
2410	24.9	-23.8	-7.4	-128.5	-1.3
2435	23.1	-21.6	-8.0	-119.7	-2.7
2479	27.3	-26.2	-7.7	-137.1	0.4
2480	30.5	-29.1	-9.0	-117.4	-1.0
2508	29.0	-27.6	-8.8	-122.9	-1.2
2509	26.8	-25.9	-6.9	-126.6	-3.8
2510	27.1	-25.9	-7.8	-133.4	0.6
2516	28.3	-28.2	-2.7	-89.8	-0.7
2519	28.5	-27.4	-7.9	-128.9	-0.9
2520	29.1	-28.1	-7.3	-137.5	-0.4
2523	32.5	-31.1	-9.5	-149.7	-0.6
2525	30.5	-29.7	-7.0	-133.6	-0.7
2686	28.9	-28.3	-5.4	-86.0	-0.6
2715	26.2	-25.9	-4.1	-77.2	-2.5
2720	25.6	-24.5	-7.5	-103.1	-0.2
2721	23.5	-22.3	-7.4	-98.6	-0.6
2722	26.1	-24.9	-7.8	-105.6	-0.7
2728	25.3	-24.7	-5.4	-91.7	-3.1
2737	29.9	-29.6	-4.3	-86.3	-1.3
2753	29.6	-29.1	-5.2	-97.7	-2.3
2762	25.5	-25.1	-4.3	-44.0	0.6
2768	26.0	-25.5	-5.1	-99.3	-1.5
2957	27.6	-25.6	-10.3	-168.2	-1.3
2958	29.3	-27.7	-9.6	-159.1	-1.1
2977	24.9	-23.5	-8.2	-142.7	-1.7
2999	29.1	-27.6	-9.2	-162.8	-2.8
3000	28.0	-25.9	-10.5	-162.8	-0.7
3011	31.3	-30.0	-8.7	-159.9	-2.5
3036	25.4	-24.3	-7.7	-104.6	-1.0
3037	26.8	-26.0	-6.8	-83.0	-1.1
3059	24.7	-24.1	-5.3	-105.5	0.7
3193	30.0	-28.5	-9.6	-110.1	0.5

3200	27.3	-26.0	-8.3	-69.3	0.3
3201	26.0	-25.0	-7.3	-46.8	-1.0
3202	26.7	-25.7	-7.3	-45.2	0.0
3203	26.4	-25.0	-8.4	-55.8	-2.0
3291	31.8	-31.2	-6.3	-12.5	-0.4
3341	24.7	-23.5	-7.7	-89.8	-0.7
3363	30.8	-29.3	-9.2	-95.0	-0.7
3474	29.3	-27.8	-9.1	-152.2	-3.2
3478	27.1	-26.3	-6.6	-29.9	-2.6
3515	29.4	-28.7	-6.3	-7.7	-0.5
3531	30.2	-28.6	-9.5	-137.9	-3.4
3550	26.6	-24.8	-9.7	-193.4	-0.8
3559	23.7	-22.5	-7.2	-80.2	-0.5
3569	25.6	-24.6	-7.2	-95.4	-0.3
3572	26.6	-25.2	-8.6	-133.8	-0.9
3744	22.5	-22.2	-3.7	-68.2	-0.8
3795	30.3	-28.9	-9.3	-116.3	-1.4
3951	26.8	-25.8	-7.0	-130.8	-1.2
4197	29.6	-28.0	-9.4	-70.0	-4.8
4221	24.1	-23.6	-4.8	-98.4	-0.7
4222	30.0	-29.2	-6.8	-94.0	-1.9
4256	23.1	-22.0	-6.8	-135.4	-1.7
4602	28.6	-26.9	-9.7	-111.2	-2.4
4619	31.2	-29.8	-9.5	-101.0	-0.8
4658	27.0	-26.1	-7.1	-33.5	-0.3
4728	30.0	-29.0	-7.9	-42.3	-1.0
4868	28.6	-27.2	-8.8	-125.8	-1.8
4889	28.6	-27.6	-7.5	-28.1	-0.3
4928	30.4	-28.7	-9.8	-109.2	-1.4
5115	26.6	-25.7	-7.0	-36.3	-2.5
5260	27.5	-26.3	-7.9	-104.1	-1.9
5460	24.7	-23.3	-8.2	-121.4	-0.3
5475	25.7	-24.2	-8.7	-127.7	-0.7
5849	29.7	-28.7	-7.9	-116.6	-0.5

MDB ΔV AT SEPARATION

Table 19. Observed MDB ΔV and yaw angle at separation.

NHTSA Test #	Resultant ΔV [kph]	Longitudinal ΔV [kph]	Lateral ΔV [kph]	Yaw Velocity [deg/s]	Yaw Angle [deg]
2096	26.0	-25.9	-2.4	148.7	-6.1
2118	29.9	-28.4	-9.3	-95.2	-2.6
2119	26.4	-25.2	-7.8	-102.1	-3.5
2218	30.9	-28.9	-11.1	-129.7	-2.2
2410	28.2	-25.8	-11.4	-147.7	-4.0
2435	28.3	-26.6	-9.6	-142.3	-5.4
2479	29.1	-27.9	-8.3	-133.7	-0.3
2480	32.2	-30.7	-9.7	-116.4	-2.0
2508	32.5	-30.8	-10.3	-110.2	-3.8
2509	27.7	-26.8	-6.9	-125.9	-4.3
2510	30.4	-27.3	-13.4	-146.7	-8.0
2516	28.4	-28.0	-4.8	-89.9	-1.9
2519	31.3	-29.7	-9.7	-121.6	-3.6
2520	32.1	-29.4	-13.0	-149.6	-7.4
2523	36.7	-32.7	-16.6	-154.8	-6.3
2525	35.7	-34.3	-10.0	-129.5	-4.6
2686	34.2	-33.3	-7.8	-79.3	-5.4
2715	31.1	-30.7	-4.8	-75.3	-7.5
2720	28.4	-26.0	-11.4	-103.2	-4.0
2721	27.1	-26.0	-7.5	-89.6	-1.2
2722	30.1	-28.1	-10.8	-98.7	-3.9
2728	29.4	-29.0	-4.9	-76.7	-5.7
2737	34.0	-33.6	-5.2	-72.5	-3.9
2753	31.9	-31.3	-6.5	-100.2	-4.4
2762	29.4	-29.1	-4.0	-35.8	0.0
2768	30.2	-29.6	-5.8	-88.4	-5.2
2957	30.9	-28.7	-11.4	-164.3	-2.5
2958	35.2	-29.4	-19.3	-189.2	-6.7
2977	29.4	-26.3	-13.1	-152.3	-5.6
2999	30.3	-24.5	-17.8	-181.6	-13.6
3000	34.9	-30.9	-16.3	-165.2	-4.7
3011	33.7	-32.2	-9.9	-167.5	-3.3
3036	33.7	-32.3	-9.4	-109.0	-2.7
3037	34.7	-33.3	-9.8	-109.9	-1.9
3059	28.4	-27.4	-7.6	-100.3	-0.8
3193	38.0	-34.4	-16.2	-118.2	-3.5

3200	31.5	-27.4	-15.5	-110.6	-6.5
3201	30.0	-28.6	-9.3	-59.1	-6.0
3202	31.7	-30.3	-9.2	-55.6	-2.4
3203	32.1	-30.9	-8.9	-47.8	-6.1
3291	36.2	-34.4	-11.2	-56.1	-6.3
3341	29.6	-27.8	-10.0	-85.0	-3.0
3363	39.3	-37.3	-12.5	-91.7	-3.0
3474	33.0	-30.3	-13.1	-154.1	-7.3
3478	31.5	-30.7	-7.0	-27.1	-11.1
3515	34.2	-33.2	-8.4	-31.5	-5.3
3531	31.9	-27.0	-17.1	-145.9	-12.1
3550	27.9	-26.1	-9.7	-187.5	-1.3
3559	29.6	-28.2	-9.0	-72.4	-3.4
3569	27.9	-26.9	-7.3	-88.6	-0.9
3572	27.0	-25.5	-8.8	-134.2	-1.0
3744	24.7	-24.4	-3.7	-68.0	-1.5
3795	35.6	-32.9	-13.6	-119.7	-3.4
3951	29.6	-28.4	-8.1	-123.4	-3.7
4197	36.0	-30.6	-18.9	-125.9	-8.6
4221	28.3	-27.0	-8.6	-99.8	-6.1
4222	41.2	-39.0	-13.4	-61.8	-14.1
4256	24.2	-23.3	-6.8	-131.3	-2.5
4602	35.4	-33.6	-11.1	-92.2	-7.4
4619	38.4	-35.7	-14.0	-81.0	-8.0
4658	30.0	-28.7	-8.5	-37.9	-3.1
4728	31.8	-30.7	-8.0	-43.4	-1.7
4868	32.8	-31.6	-8.7	-111.6	-3.5
4889	33.2	-32.0	-8.7	-41.6	-2.8
4928	34.9	-32.8	-12.1	-102.1	-3.6
5115	27.3	-26.5	-6.6	-34.2	-2.8
5260	30.3	-28.5	-10.4	-103.6	-6.0
5460	28.9	-26.2	-12.2	-124.0	-5.0
5475	28.0	-26.5	-9.0	-122.6	-1.2
5849	33.9	-31.2	-13.2	-116.1	-6.3

APPENDIX C: IMPULSE CORRECTION FACTOR

When analyzing crash tests into a fixed barrier, it is often desirable to know how the net force between the barrier and impactor changes with time. To get this, the normal force data for each load cell on the barrier can simply be summed. However, when dealing with so many channels it is inevitable that some of them will have problems that will skew their output in some way.

A technique to correct for this is called the "impulse correction factor". Knowing the change in impactor velocity during the test and the mass of the impactor, it can be determined what the impulse acting on the impactor must have been to generate that velocity change. The impulse acting on the impactor is then calculated by integrating the net force data over the time of contact, and this impulse divided by the one derived from momentum conservation. This gives a factor which the force – time curve can be scaled by to give the correct impulse. In mathematical notation, the correction factor is calculated thusly:

$$ICF = \frac{\int_{contact}^{separation} F_{net} \cdot dt}{m_{impactor} \cdot \left(v_{separation} - v_{contact}\right)}$$